THE ROLE OF HEAT SHOCK PROTEIN 70 IN LASER IRRADIATION AND THERMAL PRECONDITIONING

By

Joshua Thornton Beckham

Dissertation

Submitted to the Faculty of the

Graduate School of Vanderbilt University

In partial fulfillment of the requirements

for the degree of

DOCTOR OF PHILOSOPHY

in

Biomedical Engineering

August, 2008

Nashville, Tennessee

Approved:

Professor E. Duco Jansen

Professor Anita Mahadevan-Jansen

Professor Frederick R. Haselton

Professor Takamune Takahashi

Professor Christopher H. Contag

ACKNOWLEDGEMENTS

First, I would like to thank God for teaching me humility through these past years. Through every lab door is a thousand new challenges -which can seem daunting - but, through patience, perseverance, teamwork and a little faith, each person can make their impact.

I am particularly grateful to my wife, Ashley. With love and patience she has been by my side for all of the frustrations and moments of joy, although less frequent, - when an experiment turned out right. This work would not have been possible without her.

My parents have continually inspired me to great accomplishments and through this dissertation work; I hope that I have made them proud. I would like to thank my sister, Anne, for always being in my corner and my brother, Evan, for being a guiding force in my life.

Dr. Jansen has been a wonderful advisor. I have always been impressed with his capacity to grasp aspects of my research and help me to see them on a different level.

Two people to whom I am very indebted are Dr. and Mrs. Takahashi. They welcomed me into their lab with open arms and treated me as family. Keiko has tirelessly taught me and guided me in even the smallest details of molecular biology. Dr. Takahashi has been a generous mentor to me and could always make sense of the convoluted problems that I presented to him.

I would also like to thank the other members of my committee. Dr. Anita Mahadevan-Jansen always sees the research from a unique perspective and asks the tough questions. Dr. Haselton has been very generous in providing me with cell culture facilities in the beginning of this work and with guidance on the dissertation. I would like to thank Dr. Contag for taking an interest in my work and treating it as more than a formality through the time and input he has given, despite being thousands of miles away.

Although I have only known Dr. Opalenik for this past year, she has given me great guidance in the homestretch to the defense. Dr. Opalenik is the kind of person that every graduate student would want on their side.

TABLE OF CONTENTS

LIST OF TABLES

LIST OF FIGURES

LIST OF FIGURES CONTINUED

LIST OF SYMBOLS

Symbol	Definition	Units
Q	Energy	J
q	Heat Flux	W/m^2
E_o	Irradiance at Surface	W/m^2
E	Fluence	W/m^2
H	Radiant Exposure	J/m^2
W	Radiant Energy Density	J/m^3
S	Rate of Heat Generation	W/m^3
δ	Penetration Depth	m
δ_{eff}	Effective Penetration Depth	m
μ_a	Absorption Coefficient	m^{-1}
μ_s	Scattering Coefficient	m^{-1}
$\mu_{s'}$	Reduced Scattering Coefficient	m^{-1}
μ_{eff}	Effective Attenuation Coefficient	m^{-1}
g	Anisotropy Factor	-
n	Index of Refraction	-
L_v	Latent Heat of Vaporization	J/g
ρ	Density	g/m^3
c	Heat Capacity	J/g K
k	Thermal Conductivity	W/m^2K
α	Thermal Diffusivity	m^2/s
h	Convection Coefficient	W/m^2K
T	Temperature	C, K
τ_p	Laser Pulse Duration	s
τ_{th}	Thermal Time Constant	s
τ_s	Stress Time Constant	s
ω_L	Gaussian Radius	m
R	Universal Gas Constant = 8.314	J/mole K
r	Radial Position	m
z	Depth in Tissue	m
Ω	Arrhenius Damage Integral	-
E_a	Activation Energy	J/mole
A	Frequency Factor	1/s
ε	Emissivity	-
h	Planck's Constant	6.62×10^{-23} J s
c	Speed of Light	m/s
σ	Stefan-Boltzman coefficient	5.67×10^{-8} W/m^2 K^4
λ	Wavelength	m

LIST OF ABBREVIATIONS

Hsp70 - (in italics) gene for heat shock protein 70
HSP70 - (uppercase) protein for heat shock protein 70
Hsc70 - constitutive heat shock protein 70
HSP – heat shock proteins
HSR – heat shock response
HSF1 – heat shock factor 1
HSE – heat shock element
MEF - murine embryonic fibroblast cells
MEF(-/-) - *Hsp70* deficient cells
MEF(+/+) - *Hsp70* competent cells
NIH3T3 - National Institutes of Health murine fibroblast cell line
PS - pre shock
HS - heat shock
PS+HS - preshock with heat shock later
ELISA – enzyme-linked immunosorbent assay
BLI – bioluminescence imaging
CCD – charge coupled device
CTB - Cell Titer Blue© viability dye
FACS – fluorescence activated cell sorting
DMSO – dimethylsulfoxide
Ho:YAG – Holmium:Yttrium Aluminum Garnet
CO_2 – carbon dioxide
17-AAG - 17-(Allylamino)-17-demethoxygeldanamycin
GGA - geranyl geranyl acetone
RIN - RNA integrity number
MTC - multiple testing correction
GEO – gene expression omnibus
MIAME – minimum inrormation for a microarray experiment
CEL – microarray spot intensity file
CHP – microarray probe level file
Mas5 - Micorarray Suite Version 5.0 file
qRT-PCR - quantitative reverse transcriptase polymerase chain reaction
TGF-β – transforming growth factor beta
JNK - C-Jun N-terminal kinase

CHAPTER I

INTRODUCTION

Josh T. Beckham

Department of Biomedical Engineering

Vanderbilt University

Nashville, TN 37235

1.1 Introduction

Lasers have taken on an ever-expanding role in the medical field for diagnostic and therapeutic applications. They are now used to treat a wide variety of disorders and cosmetic conditions, such as: port wine stains, scar revision, wrinkle removal, tattoos, birthmarks, vein disorders, hair removal, cancer, vision correction and photorejuvenation of skin [1-8]. Two of the main benefits of laser in medicine are their ability to heat tissue in a selective manner and their non-contact interface. These traits can lead to more precise therapy with fewer complications.

However, lasers can cause damage peripheral to the target site. In many cases, the physician is faced with a trade-off between using enough energy for effective therapy while staying within the thresholds for damage to the surrounding tissue. When the delivery is not thermally confined, heat can diffuse out of the target site and injure tissue that was not directly ablated or killed by the incident beam. Consequently, there is range of damage that usually induces sub-lethal stresses on the surrounding cells. The detrimental effects of this can be redness, swelling, induction of inflammation from dead cells, and loss of function in the case of neurological interventions [7, 9, 10]. Understanding this zone of damage may lead to better strategies to improve recovery after laser treatments.

Commonly, tissue damage has been quantified by such macroscopically visual results as tissue mass removal, carbonization, and melting, as well as, such microscopic results as coagulation and birefringence. The disadvantages to these types of assessments are that they are all end point characteristics of post mortem tissue and they survey damage that is severe. As a result, relatively little knowledge has been gathered about the

cellular level of sub-lethal damage that comes before these other metrics. In reality, damaged cells undergo a complex reformation of their underlying biochemistry when pathways are activated and suppressed in response to heat damage [11]. The ability to select laser parameters (wavelength, spotsize) and treatment parameters (duration of exposure and energy used) based upon the cellular response, as well as the traditional tissue level outcomes may enhance the efficacy of laser protocols in the future.

Along these lines, we used a cell culture system and a molecular biology approach to study sub-lethal damage. By using cells we were able to reduce the complexity of the response to a more fundamental level which can be compared and contrasted to multi-cellular tissue models later on – such as organotypic raft cultures and murine models [12]. Our molecular approach incorporated two key components to interrogate the character and function of HSP70, which is one of the most well know mediators of thermal stress in cells [13]. First a bioluminescent transgene system was used wherein the luciferase reporter gene is expressed upon activation of the *Hsp70* promoter and light is produced. The changes in light production can be used to infer the level of thermal stress within the cells. This technology allows for the facile determination of changes in the gene of interest as the cell responds to heat stress. The second molecular component that was used in this research was a 'knockout' a cell line. In these cells, the *Hsp70* gene is deleted so that we can determine what functionality is lost in the cell when HSP70 protein is absent. These methods allowed us a unique window into the molecular workings of the cell that we can use to understand and improve thermal responses.

One method by which the thermal response can be improved is pretreatment. This method is simply the application of a stimulus prior to the main insult in order to prepare

the cells or tissue to withstand the subsequent stress. Due to the broad protection from heat shock proteins, they have been the most commonly targeted group of proteins for pretreatment. Currently, methods that pretreat cells to activate these heat shock proteins include: preshock with mild temperature elevation [14, 15], adding exogenous heat shock proteins [16, 17], or administering pharmacological agents [18, 19]. The efficacy of pretreatment has been shown in many different damage mechanisms. For example, protection of cardiac tissue through thermal means prior to ischemic events has implicated the heat shock proteins [20]. One of the main mechanism by which these proteins repair damage is by refolding denatured proteins within the cytosol, but they also have anti-apoptotic function. However, pretreatments actually upregulate a wide variety of stress response pathways that can benefit the cell in different ways [21-23]. Ultimately a better understanding of these molecular pathways can be used to develop pretreatment strategies for protection against laser irradiation.

1.2 Specific Aims

1.2.1 Overall specific aim

The general purpose of these specific aims was to investigate the heat shock response of cells and develop a strategy to increase thermotolerance. We hypothesized that the *Hsp70* response would be a good indicator of thermal damage and that it has a crucial role in the thermal recovery process that can be modulated through pretreatment. Through this research, we assert that effective pretreatment protocols in cells can

eventually be translated to pretreatment protocols to reduce collateral damage from laser treatments in tissue.

1.2.2 Specific Aim 1: *To Characterize the response of Hsp70 to thermal damage*

The first part of this aim examined the transcriptional activation of *Hsp70* in cell culture after water bath and laser heat shock protocols by means of a bioluminescent reporter construct that uses the *Hsp70* promoter to produce luciferase. The onset time, duration and magnitude of *Hsp70* were characterized. The amount of hsp70 transcription correlated well to the amount of damage within the cells after laser injury by cell viability assays. Furthermore, an Arrhenius analysis of *Hsp70* promoter activity was used to assess the threshold of damage for promoter activation and the kinetics of the response.

1.2.3 Specific Aim 2a: *To develop a pretreatment protocol that will alleviate thermal damage in laser irradiated cells*

We explored and optimized preshocking methods with the intent of increasing the endogenous heat shock response (HSR) to prepare the cells for a more damaging secondary heat shock. NIH-3T3 cells were used and survivability after thermal damage was assessed through cell counts, bioluminescence imaging of HSP70 transcription, and viability assays at 48 hrs. The pretreatment was optimized to show that 43^{o} C for 30 minutes with a 4 hour lag time between the pretreatment and severe heat shock was ideal. Pretreatment was tested against Ho:YAG pulsed laser irradiation to show that the response was not specific to the long duration, constant temperature exposures seen in the water bath treatments.

1.2.4 Specific Aim 2b: *To determine if HSP70 is responsible for the thermotolerance provided in pretreatment*

One of the most important questions for this dissertation work to address was whether HSP70 simply correlated to increased thermotolerance or if it was responsible for this resistance. Along these lines, an *Hsp70* deficient cell line was compared to an *Hsp70* containing cell line in our water bath pretreatment experiments. The results showed that HSP70 is primarily responsible for the thermotolerance from pretreatment in these cells. However, a small amount of thermotolerance remained without HSP70.

1.2.5 Specific Aim 3: *To determine what other genes are involved in the thermotolerance provided by pretreatment*

Many pathways in cells have redundant functions to each other. Consequently, microarray analysis was performed on these cells to determine which other genes, besides *Hsp70*, were involved in protecting cells from thermal stress. Also, quantitative RT-PCR experiments demonstrated the thermotolerance at two different time points from pretreatment on the level of mRNA transcription.

1.3 Dissertation Outline

This dissertation consists of three manuscripts that investigate the thermal response of cells to better understand its molecular basis and how to affect beneficial changes to the response. Chapter 1 starts out with an introduction to the purpose of the work and includes the specific aims that were to be accomplished.

In Chapter 2 contains the background information pertaining to this research. Laser –tissue interactions are discussed and the roles of the pertinent molecular pathways are outlined. The particular methods that used in this research are described, including: bioluminescence imaging, pretreatment of cells, and microarrays of gene expression.

Chapter 3 consists of a manuscript that was published in *Photochemistry & Photobiology[24]*. It examines the activation and response of *Hsp70* gene transcription through the use of a bioluminescent reporter gene, *Luc*. Transgenic Hsp70Luc cells were heated with a laser and the activity of the *Hsp70* promoter was assessed in order to understand its role in thermal treatment induced by a pulsed Ho:YAG laser. The changes in reporter activity were compared to actual HSP70 protein levels by ELISA to verify that the bioluminescence was a reliable surrogate marker. Then, the changes in reporter activity were compared to viability assays at 8 hours correlate HSP70 levels to survival after severe laser stress. Lastly, an Arrhenius analysis of the *Hsp70* transcriptional response to water bath heat shock was carried out to help characterize how an inherently complex biological system can be modeled after thermal injury. To our knowledge this was the first time that an Arrhenius analysis has been used to investigate the upregulation of the *Hsp70* promoter in response to a stressor. Traditionally, these types of analyses have been limited to physical phenomenon on the tissue level of damage, such as loss of birefringence or protein denaturation, and not necessarily the biological response.

Chapter 4 pertains to the work that is in submission to *Lasers in Surgery and Medicine*. The main focus of this chapter is upon understanding the role of HSP70 in thermal pretreatment strategies. First, the transgenic cell line Hsp70Luc, that expresses bioluminescence when *Hsp70* is activated, was used to determine the peak of gene

expression. Then viability assays were used to optimize the pretreatment temperature, duration and lag time between the pretreatment and severe heat shock in a water bath. The ability of pretreatment to protect cells against short duration, high temperature thermal stress from a laser irradiation was ascertained using a Ho:YAG pulsed laser. Next, a cell line deficient in *Hsp70* displayed the importance of the HSP70 protein in thermal pretreatment when compared to a control cell line. An extension of the Arrhenius work from Chapter 3 was done wherein the behavior of cell survival with and without HSP70 was characterized. Also, the changes in the Arrhenius values due to pretreatment were observed and found to differ from our hypotheses that we had formed. We believe that this is the first Arrhenius analysis of pretreatment.

Chapter 5 addresses the research in the third paper of this dissertation. For this, a microarray analysis was performed on pretreated cells in order to screen for which genes may be important to the benefit of thermotolerance. The groups of genes upregulated in both HSP70 deficient and HSP70 competent cells were compared by their fold inductions and arranged into their categories of molecular functions to better understand the nature of the response on the molecular level. The genes that showed differential expression between the cell lines were also addressed in order to investigate their importance in replacing HSP70 in the deficient cell line. A select set of genes were analyzed by quantitative RT-PCR experiments which validated the microarray levels of induction. These genes were also used in a qRT-PCR comparison of heat shocked cells deficient in HSP70 that were given either a pretreatment beforehand or not. This data showed the ability of pretreatment to restore the production of mRNA transcripts in these cells after a severe heatshock.

Chapter 6 is a conclusion and it discusses the importance of the work to laser-tissue interactions and which future directions would be best to continue upon the findings herein.

1.4 References

1. Kao, B., et al., *Novel model for evaluation of epidermal preservation and dermal collagen remodeling following photorejuvenation of human skin.* Lasers Surg Med, 2003. **32**(2): p. 115-9.
2. Khatri, K.A., et al., *Comparison of erbium:YAG and carbon dioxide lasers in resurfacing of facial rhytides.* Arch Dermatol, 1999. **135**(4): p. 391-7.
3. Papadavid, E. and A. Katsambas, *Lasers for facial rejuvenation: a review.* Int J Dermatol, 2003. **42**(6): p. 480-7.
4. Ross, E.V., J.R. McKinlay, and R.R. Anderson, *Why does carbon dioxide resurfacing work? A review.* Arch Dermatol, 1999. **135**(4): p. 444-54.
5. Ahcan, U., et al., *Port wine stain treatment with a dual-wavelength Nd:Yag laser and cryogen spray cooling: a pilot study.* Lasers Surg Med, 2004. **34**(2): p. 164-7.
6. Paithankar, D.Y., et al., *Subsurface skin renewal by treatment with a 1450-nm laser in combination with dynamic cooling.* J Biomed Opt, 2003. **8**(3): p. 545-51.
7. Kim, J.M., et al., *Effect of thermal preconditioning before excimer laser photoablation.* J Korean Med Sci, 2004. **19**(3): p. 437-46.
8. Rylander, M.N., et al., *Optimizing heat shock protein expression induced by prostate cancer laser therapy through predictive computational models.* J Biomed Opt, 2006. **11**(4): p. 041113.
9. Kelty, J.D., et al., *Thermal preconditioning and heat-shock protein 72 preserve synaptic transmission during thermal stress.* J Neurosci, 2002. **22**(1): p. RC193.
10. Thomsen, S., *Pathologic Analysis of Photothermal and Photomechanical Effects of Laser-Tissue Interactions.* Photochemsitry and Photobiology, 1990. **53**(6): p. 825-835.
11. Welch, A.J. and M.J.C.v. Gemert, *Optical-thermal response of laser-irradiated tissue*, in *Lasers, photonics, and electro-optics*. 1995, Plenum Press: New York. p. 5.
12. Wilmink, G.J., et al., *Assessing laser-tissue damage with bioluminescent imaging.* J Biomed Opt, 2006. **11**(4): p. 041114.
13. Kim, D., H. Ouyang, and G.C. Li, *Heat shock protein hsp70 accelerates the recovery of heat-shocked mammalian cells through its modulation of heat shock transcription factor HSF1.* Proc Natl Acad Sci U S A, 1995. **92**(6): p. 2126-30.
14. Pespeni, M., M. Hodnett, and J.F. Pittet, *In vivo stress preconditioning.* Methods, 2005. **35**(2): p. 158-64.
15. Wilmink, G., et al., *Molecular Imaging-Assisted Optimization of Hsp70 Expression During Laser Preconditioning for Wound Repair Enhancement.* J Invest Dermatol, 2008. **In Press**.

16. Lasunskaia, E.B., et al., *Accumulation of major stress protein 70kDa protects myeloid and lymphoid cells from death by apoptosis.* Apoptosis, 1997. **2**(2): p. 156-63.
17. Wheeler, D.S., K.E. Dunsmore, and H.R. Wong, *Intracellular delivery of HSP70 using HIV-1 Tat protein transduction domain.* Biochem Biophys Res Commun, 2003. **301**(1): p. 54-9.
18. Guo, F., et al., *Abrogation of heat shock protein 70 induction as a strategy to increase antileukemia activity of heat shock protein 90 inhibitor 17-allylamino-demethoxy geldanamycin.* Cancer Res, 2005. **65**(22): p. 10536-44.
19. Wischmeyer, P.E., *Glutamine: the first clinically relevant pharmacological regulator of heat shock protein expression?* Curr Opin Clin Nutr Metab Care, 2006. **9**(3): p. 201-6.
20. Plumier, J.C. and R.W. Currie, *Heat shock-induced myocardial protection against ischemic injury: a role for Hsp70?* Cell Stress Chaperones, 1996. **1**(1): p. 13-7.
21. Cowan, K.J. and K.B. Storey, *Mitogen-activated protein kinases: new signaling pathways functioning in cellular responses to environmental stress.* J Exp Biol, 2003. **206**(Pt 7): p. 1107-15.
22. Feezor, R.J., et al., *Temporal patterns of gene expression in murine cutaneous burn wound healing.* Physiol Genomics, 2004. **16**(3): p. 341-8.
23. Westerheide, S.D. and R.I. Morimoto, *Heat shock response modulators as therapeutic tools for diseases of protein conformation.* J Biol Chem, 2005. **280**(39): p. 33097-100.
24. Beckham, J.T., et al., *Assessment of cellular response to thermal laser injury through bioluminescence imaging of heat shock protein 70.* Photochem Photobiol, 2004. **79**(1): p. 76-85.

CHAPTER II

BACKGROUND

Josh T. Beckham

Department of Biomedical Engineering

Vanderbilt University

Nashville, TN 37235

2.1 Laser – Tissue Interaction

The selection of proper laser parameters for any given procedure is dependent on a variety of factors. These include the laser's optical properties (wavelength, spotsize, pulse duration, energy, and beam profile) and the tissue's physical and optical properties (heat capacity, thermal conductivity, absorption coefficient, scattering coefficient, anisotropy factor, amount of perfusion). These parameters must be chosen properly in order to optimize efficacy while minimizing unwanted side effects and damage.

2.1.1 Lasers Optical Properties

The concept of laser irradiation was proposed in 1917 by Albert Einstein but the idea did not come to practical fruition until 1958 when Townes developed a microwave precursor to the optical laser [1]. In the 1960's Maiman made the first optical solid state ruby crystal laser [2, 3]. Lasers are now routinely used in a myriad of medical procedures for diagnosis and treatment. LASER stands for Light Amplification through Stimulated Emission of Radiation. The fundamental principle behind the laser process is that atoms which constitute the laser gain medium (e.g. Ho:YAG crystal, or CO_2 gas) are excited into higher energy states by energy pumped in through a source, such as an electric discharge, flashlamp or another laser. When these atoms return to their lower energy state, they release a photon which will then interact with another excited atom in the medium. This new atom is then stimulated to return to its ground state and subsequently releases its own photon which is identical to the first photon in direction, energy, and phase. Eventually, when more atoms are in the higher energy state than the lower energy state then the process of population inversion has occurred and lasing is possible. The

cascade of recruiting more atoms into the process is maintained by two reflecting mirrors that trap the majority of photons within the cavity. Only about 10- 20% of photons escape through the one of these mirrors that is partially transmitting [4].

The emitted light from the laser is unique compared to other forms of electromagnetic radiation. All of the laser's energy is of the same wavelength, collimated, coherent, and polarized. Of these characteristics, the first two are important for thermal tissue interaction. The energy is of the same wavelength (monochromatic) because the energy gap from which each photon is derived is the same. Laser light can be broken into three main sections of the spectrum: Ultra-violet (100-380nm), Visible (380-700nm) and Infra-red (700nm – 1mm). There are many different lasers for each of these spectral bands. For example the ArF (argon fluoride 193 nm) laser and Nitrogen (337nm) are UV lasers, the He:Ne (Helium Neon 632 nm) is in the visible, while the Ho:YAG (Holmium: Yttrium Aluminum Garnett 2.1 μm) and CO_2 (10.6 μm) are in the IR. A photon's energy determines its wavelength through the relationship:

$$E = hc/\lambda \tag{1}$$

where h is Planck's constant (6.62×10^{-23} [Js]), c is the speed of light in [m/s], λ is the wavelength in [m], and E is the energy in [J]. Consequently, a tissue's response to a given laser is simpler to interpret in comparison to other forms of light because of the fact that the laser has only one wavelength with which the tissue can interact. This wavelength specificity is where the laser technology derives much of its benefit for medical applications. Essentially, tissue can be chromatically targeted instead of just physically targeted. Selective thermolysis takes advantage of this, wherein one type of cell absorbs a

given wavelength better than other cells. This absorption leads to destruction of only the targeted cells leaving other tissue relatively undamaged.

Laser light is collimated, which means that the directionality is the same for all of the photons in a laser beam due to the orientation of the laser cavity and mirrors. As a result, the light can more effectively be focused and intensified for use in medical procedures compared to other forms of light.

Most lasers exhibit a Gaussian profile of irradiation across the laser beam,

$$E = E_{r=0} \exp\left(\frac{-2r^2}{\omega_L^2}\right) \tag{2}$$

where the beam has a radius (r) and a Gaussian radius (ω_L) at which the irradiance at r=0 (E_o in [W/m^2]) at the center of the beam has been reduced to $1/e^2$ (13.5%). Within the area encircled by the Gaussian radius, there lies approximately 87% of the integrated power of the laser beam [4].

Lasers can be either continuous wave or pulsed in their energy output. Continuous wave lasers are more straight forward in their behavior and can be manipulated with some predictability because of their uniform energy output. However, pulsed lasers are less tractable since the temporal intensity profile of a pulse is highly variable and often unpredictable. For this study a pulsed Ho:YAG (λ = 2.1 μm, τ_p = 250 μs, Schwartz Electro Optics 1-2-3, Orlando, FL) was used. The Ho:YAG laser has a varying intensity profile during the pulse representing a sharp rise followed by a sharp drop in energy.

Light propagation into tissue depends on the wavelength dependent optical properties of the irradiated sample. The irradiance (E_o) is the measurement of power at the surface with respect to area [W/m^2]. In order to make this value an accurate

representation of the energy entering the tissue the amount of reflected light that is lost at the surface must be taken into account. For a 0^o angle of incidence, as was used in this study, the amount of specularly reflected light is shown by Fresnel's equation,

$$R = ((n_i - n_t)/ (n_i + n_t))^2 \quad (3)$$

Where n_i is the refractive index of the incident medium, air ($n_i = 1.0$) and n_t is the index of refraction for the sample, tissue ($n_t = 1.33$) The air – tissue interface leads to a 2% reflection loss at the surface.

In an absorption dominated case where scattering is minimal, the remaining 98% of light is now governed by Beer's Law to determine its penetration into tissue,

$$E(z) = E_o \exp(-\mu_a z) \quad (4)$$

Where E_o is the irradiance at the surface [W/m^2] and E(z) is the fluence at depth z [m], μ_a is the absorption coefficient [1/m] for the tissue at a given wavelength. The penetration depth (δ) is the inverse of the absorption coefficient. Its value represents the depth to which light will penetrate to an intensity of 1/e (37%) of the original surface intensity, less reflective losses. The tissue and the wavelength selected for irradiation determines the penetration depth.

However, for scattering dominated tissue the anisotropy factor must be included to give an accurate model of light propagation. Scattered photons can be directed in different directions once they hit particles within the tissue. The anisotropy (g) is the angle at which photons are scattered,

$$g = \text{average } (\cos \theta) \quad (5)$$

where θ is the angle of scattering. This value can range from -1 to 1 as θ varies from 0^o (direct forward scatter) to 180^o (direct backward scatter). When the light is scattered in

all directions equally, then g = 0. For most tissue g = 0.9 representing a mostly forward scattering situation. A reduced scattering coefficient is utilized to account for direction of scattering:

$$\mu_s' = (1\text{-}g)\ \mu_s \tag{6}$$

Using this value, an effective attenuation coefficient is obtained that is combined with the absorption coefficient to give a more complete picture of photon interaction in tissue.

$$\mu_{eff} = \sqrt{3\mu_a\left(\mu_a + \mu_s'\right)} \tag{7}$$

This then leads to an effective penetration depth given by,

$$\delta_{eff} = \frac{1}{\sqrt{3\mu_a\left(\mu_a + \mu_s'\right)}} \tag{8}$$

Like other lasers in the infrared, the interaction of the Ho:YAG laser in tissue is an absorption dominated case [4] and scattering can be disregarded. The penetration depth is between 300 – 400 microns [5] with an absorption coefficient of $\mu_a = 2.86\ mm^{-1}$. This allows for a uniform irradiation across the depth of cultured cells in a well plate as a layer of cells is approximately 10-20 microns thick. The amount of light remaining at 10 microns - which is the top of the cell layer above the polystyrene floor of a 96 well plate - is 97%. If the cell layer is 20 microns thick, then the light only reduces to 94%. Consequently, the cells receive a very uniform distribution of light across the layer.

2.1.2 Photothermal Effects of Irradiation on Tissue

Once this light has penetrated into the tissue, photothermal effects begin to take place as the light energy is converted into heat. Molecules within the tissue absorb the

heat and transform it into the kinetic energy that is heat. The rate and amount of energy is placed into the tissue per unit volume is given by the rate of heat generation,

$$S(z) = \mu_a E_o e^{-\mu_a z} \tag{9}$$

Where S is in units of [W/m^3], μ_a is the absorption coefficient [m^{-1}], E_o is the irradiance at the surface in [W/m^2] and (z) represents the axial coordinate.

The way that this heat moves in the tissue is determined by properties such as the tissue's specific heat capacity (c) in [J/g K], thermal conductivity (k) in [W/m K], density [g/m^3], and diffusivity [mm^2/s]. For example, the higher the water content of the tissue, the more capable it is of holding thermal energy without elevating temperatures because of water's higher heat capacity. However, when the thermal buildup continues to rise vaporization can occur as the liquid changes state into a gas. The boiling point for water, which is the primary constituent of most tissue, is 100^o C at standard atmospheric pressure. The energy needed to obtain vaporization is described by,

$$W_{Th} = \rho c\left(T_v - T_i\right) + \rho L_v \tag{10}$$

where, W_{Th} is the threshold radiant energy density [J/m^3], ρ is the density of water [g/m^3], c is the heat capacity [J/kg K], T_v is the temperature of vaporization, T_i is the initial temperature, and L_v is the latent heat of vaporization [J/kg]. Subsequently, the threshold radiant exposure needed at the surface needed to bring about vaporization is,

$$H_{Th} = W_{Th}\delta \tag{11}$$

where, H_{Th} is in units of [J/m^3], W_{Th} is the threshold radiant energy density from above, and δ is the penetration depth of the laser into the tissue in [m]. Once the energy is generated wihtin the tissue it begins to propagate throughout the sample by four different

mechanisms: conduction, convection, perfusion and radiation. Radiative heat flux is described by the equation,

$$q = \sigma\varepsilon\left(T_s^4 - T_a^4\right) \tag{12}$$

where, q = the heat flux [W/m^2], σ is Boltzman's constant = 5.67x 10^{-8} [W/m^2 K^4], ε is the emissivity that is unitless and is a measure of how well a surface radiates energy, T_s is the temperature of the tissue and T_a is the surrounding temperature. Radiation is not prominent for transfer of heat to surrounding tissue.

Convection plays a role when a fluid is present that can circulate the heat away from an area. Consequently, convection is a concern at the surfaces of tissue where heat can be lost to the surrounding air. Convective heat flux is described by the equation,

$$q = h\left(T_S - T_a\right) \tag{13}$$

where, q = the heat flux [W/m^2], h is the convection coefficient [W/m^{2}K^4], and T_s is the temperature of the tissue and T_a is the surrounding temperature.

A special case of convection is presented by perfusion of blood vessels next to the tissues that can carry away heat from the site of generation. Consequently, perfusion is only concern in well perfused tissue. The equation for perfusion is,

$$q = \omega\rho c\left(T_a - T_v\right) \tag{14}$$

where q = the heat flux [W/m^2], ω is the ratio of the volume rate of flow of blood to the amount of tissue that the vessel perfuses [m^3/s], ρ is the density of blood [g/m^3], and c is the heat capacity of blood [J/g K].

Conduction is the primary mode of heat transport in tissue and is driven by a temperature gradient. Fourier's law describes how heat is conducted though the tissue,

$$q = -k\,\frac{\Delta T}{\Delta X} \tag{15}$$

where q = the heat flux [W/m^2], k is the thermal conductivity [W/m^2 K] and the last term is the temperature gradient in the direction of heat flow. When the rate of heat generation and the heat conduction are put together, the general heat transfer equation is,

$$k\nabla^2 T + S = \rho c \frac{\partial T}{\partial t} \tag{16}$$

where, the first term is the temperature gradient in all directions, S is the heat generation, and the right hand side is the change in temperature over time with ρ as density [g/m^3] and c [J/g K] as the heat capacity. The equation describes the build up of heat within the tissue and its distribution over time.

For this study, the primary method of heat transfer is conduction. Convection plays only a small role at the surface of a well plate since air is not a highly efficient medium for transferring heat. Since samples used are cell culture plates, perfusion is not a factor. Also, radiation is not a significant source at the temperatures studied. However, the thermal conductivity and heat capacity of the plastic tissue culture plates do affect how the heat is conducted to the cells.

The rate at which heat from a pulsed laser spreads within the tissue is characterized by a thermal time constant. The time constant's relation to the pulse duration of the laser predicts whether heat will be allowed to be conducted from the site of irradiation to the peripheral tissue before the end of the laser pulse. Thermal confinement allows for a more controlled environment because heat is not allowed to effect surrounding tissue. Thermal confinement occurs when the pulse duration is less than the thermal time constant,

$$\tau_{th} = \delta^2/4\alpha \tag{17}$$

with α = thermal diffusivity in [mm^2/s]. With a few exceptions, thermal confinement is usually desirable for medical laser procedures because there is not enough time during a pulse to create collateral heat damage. For this study we assumed the properties water to represent the tissue culture media with a thermal diffusivity of $\alpha = 0.15$ mm^2/s and a penetration depth of $\delta = 300$ μm, leading to a value for the thermal time constant $\tau_{th} = 0.150$ s. With a pulse duration of 250 μs, the Ho:YAG laser pulse is considerably less than the thermal time constant. Consequently, heat is not able to escape the zone of irradiation during the pulse, but can diffuse out over the course of multiple pulses.

The temperature profile and time at which the tissue is subjected to elevated temperatures is referred to as the thermal history. This history can be categorized into three regions of low temperature (43-100^o C), middle temperature (100-300 ^{o} C) and high temperature (300^o-1000^o C) [6]. The high temperature region is characterized by ablation of tissue, tissue vaporization, carbonization and molecular dissociation. The middle temperatures exhibit water dominated effects as the liquid begins to vaporize. The low temperature region is most relevant to this study and is characterized by deactivation of enzymes, protein unfolding (denaturation), acceleration of metabolism, cell death, cell shrinkage, birefringence loss, membrane rupture, and hyalinization of collagen [6, 7]. These effects are less outwardly visible and the cellular response can be delayed in time as different response proteins are transcribed and translated into their active forms. As a result of the cellular repair mechanisms, some low temperature damage can be reversible. The damaged proteins can be repaired or degraded and replaced with new ones. Compromised membrane structure can be restored with time also. However, visible whitening of the tissue can be a result of heat damage that is irreversible as proteins

coagulate. Coagulation is a result of a more damaging temperature profile to the tissue which affects structural proteins. Structural proteins are more thermally stable than the metabolically oriented proteins that are involved in reversible heat damage. Consequently, coagulation signifies a lethal endpoint for the tissue [8]. Another irreversible change is the birefringence loss that comes about when the regular arrangement of collagen molecules is disrupted. Birefringence is a rotation in the angle of polarization of the tissue. This property can be detected by transmission polarizing microscopy (TPM) [6].

2.1.3 Photomechanical Effects of Irradiation on Tissue

Photomechanical effects can play a major role in laser irradiation damage when relatively short pulse durations are used. The increase in temperature of a tissue subject to laser irradiation leads to increases in pressure due to expansion. Thermoelastic expansion then leads to acoustical waves that propagate through the tissue [9]. Acoustical waves can develop significant mechanical stresses upon the tissue when the laser pulse is considered to be stress confined. Stress confinement occurs when the laser pulse duration, τ_p, is less than the stress time constant, τ_s, where

$$\tau_s = \delta/\sigma \tag{18}$$

where δ = the penetration depth of the laser into the tissue in [m], σ = speed of sound in tissue in [m/s]. When a laser is stress confined, the sample volume does not have enough time to dissipate the pressure. For the goal of non ablative irradiation, stress confinement is undesirable because these pressure waves may tear and rupture tissue. The Ho:YAG laser used in these studies was not stress confined with respect to tissue. We assumed the

properties of water to represent the media with a penetration depth of δ = 300 μm. The speed of sound in water is 1520 m/s. These values give a thermal time constant of τ_s = 1.97 ns. With a pulse duration of 250 μs, the Ho:YAG is greater than the stress time constant. Consequently, for this study significant mechanical stresses upon the cells were not present and only thermal effects played a role in cell damage. Furthermore, mechanical stress considerations for cells in culture are vastly different than for tissues that are held together by connective proteins and different layers of cells.

When the pressure waves created by thermoelastic expansion are reflected from a free interface, such as that of tissue and air, they are transformed into a tensile wave [9]. Since tissue is inherently good at handling compressive stresses but fares poorly in response to tensile stresses, these bipolar waves can be highly destructive. However, these pressure waves can be beneficial in some cases such as, tumor ablation, laser assisted lithotripsy of renal calcifications or in breaking up vascular plaque deposits [6].

When temperatures are near 100^{o}C for water based tissue, ablation of material can arise from the surface layer. Once the vaporization temperature is met, the underlying tissue expands more quickly than the surface layer and enough pressure is created to eject material [10]. As a result of the recoil derived from ejecting material, a monopolar pressure wave is created in the tissue. When tissue is irradiated within a liquid, vaporization bubbles can form within the liquid [11]. These cavitation bubbles increase in size as more heat is applied and then they collapse, creating pressure waves within the tissue.

2.1.4 Arrhenius Integral

The kinetics of several morphological and physiologic responses to thermal damage are exponentially dependent on temperature and linearly dependent on time of exposure [12]. The Arrhenius integral is a rate process for characterizing this tissue damage that works well for low temperature phenomenon, such as coagulation or birefringence loss. The metric for damage (Ω) is commonly a ratio of the concentration of native (undamaged) tissue before thermal exposure (C_0) to the concentration of native tissue at the end of the exposure time (C(t)). The equation for the integral is:

$$\Omega = \ln\left(\frac{C_0}{C(t)}\right) = \int_0^{t_p} A \exp(-E_a / RT)dt \tag{19}$$

where Ω is the tissue damage, A is the frequency factor - i.e. damage rate (1/sec), E_a is the activation energy in [J/mole], T is the temperature of exposure [^{o}K], R is the gas constant at 8.32 [J/mol K] and the integral is over the time of the heat exposure. The Arrhenius integral takes into account the temperature-time history of the sample to characterize the tissue damage. The relationship predicts that for a four degree increase in temperature the exposure time should be reduced by one order of magnitude in order to achieve the same amount of damage. If the time and temperature conditions change in accordance with these parameters, then the damage to the tissue should be the same.

To empirically determine the behavior of a given tissue to heat a threshold of damage is used that gives an easily distinguishable binary result (either damage or undamaged). In tissue, the presence of visible whitening that represents structural protein denaturation is an example of a damage threshold (Ω). Thermal treatment is stopped once this threshold is met. Thus, different temperatures and time points are collected that

represent the same level of damage. From this data, the two unknown parameters (E_a and A) of the Arrhenius equation can be determined for comparison to other damage systems. The activation energy, E_a [J/mol], is the amount of energy necessary to initiate the damage. The more resistant the tissue is to thermal damage, the higher the activation energy will be. The frequency factor, A [1/s], is a measure of the damage rate. A higher frequency factor indicates that the tissue is succumbing to the thermal stress more quickly.

Constant temperature experimental data can be fitted to the Arrhenius integral by means of converting the equation into a linear relationship [13]. The equation becomes,

$$\Omega = A\exp(-E_a / RT)t \tag{23}$$

when the natural log is taken of all terms and the damage parameter is equal to 1, that is when the damage is equal to the user specified end point, then the equation can be linearized into,

$$\ln(t) = -\ln(A) + E_a / RT \tag{23}$$

Plotting the experimental results on a ln(t) versus 1/T graph will produce a slope (Ea/R) and y-intercept (-ln(A)) value from which the activation energy and frequency factor can be derived, respectively.

Although, most commonly applied to tissue, the Arrhenius damage model can be applied to cellular systems as well [7, 13, 14]. In one of the analyses in this study, cell viability at 48 hours after thermal stress was used as the endpoint of damage. A viability assay quantified the amount of metabolically active cells with a fluorescent dye. The heat stress (temperature and duration) that resulted in only 37% of the fluorescence, C(t), relative to untreated controls, C_0, was then used to calculate Ω and the resulting

activation energy and frequency factor at a given temperature. For this case, $\Omega = \ln(100\%/37\%) = 1$.

Alternatively, in the other Arrhenius analysis in this work, a certain level of *Hsp70* gene signaling by the cells in culture was chosen as the endpoint of damage. Instead of using a binary classification with equal damages (Ω), the varying levels of *Hsp70* gene activation across several different exposure times were equalized using a damage parameter adjustment wherein the gene signaling for each sample was normalized to the sample that had the highest *Hsp70* gene level. This approach allowed for the use of many data points because those that were not at threshold could be incorporated into the calculations.

More importantly, by using *Hsp70* activation levels as the damage metric, we were able to better understand the biological response to heat stress. In contrast, classical studies of thermal damage that utilize the Arrhenius integral are investigating physical damage (birefringence loss, collagen denaturation, cell death). These studies do not capture any biological amplification and signaling within the cell. The biological response is of importance because it ultimately affects the clinical outcome brought about by sub-lethal damage. The cells that have not been immediately killed by the thermal stress respond by activating and suppressing molecular pathways that can improve or worsen healing. Ultimately, to better understand which proteins and pathways are crucial to thermotolerance, it is necessary to analyze their contribution to the cellular response.

2.2 Heat Shock Proteins

Heat shock proteins are in a class of proteins called molecular chaperones. Chaperones help newly synthesized or improperly folded proteins to form into their most stable, native conformation [15, 16]. One of the ways they do this is by preventing proteins from aggregating into clusters with nearby proteins. Newly created proteins extend out from ribosomes with their N-terminus exposed to the cytosol. The nascent protein is now vulnerable to becoming bound to a multitude of other proteins in the cytosol, which would prevent proper folding. The chaperones use their substrate binding domains to find linear sections of the nascent protein that are rich in hydrophobic amino acids [17]. The nascent protein is then shielded and able to properly fold without interference.

The method for rescuing mature proteins that have been denatured by heat or chemicals is similar to the chaperones' role in helping form nascent polypeptides [17]. Whenever proteins are heated they begin to unfold from their tertiary and quaternary structures. Consequently, the domains of the heated proteins are no longer functional and the proteins are unable to perform their respective tasks of binding and interacting with other molecules. The presence of these malfolded proteins leads to the upregulation of chaperones which then intervene and allow the proteins to refold into their native state. Heat activated hsp induction depends on temperature, time of exposure and cell type but the triggering factor is the presence of denatured proteins in the cell. Most mammalian cell lines respond to a temperature increase of at least 5-6^{o} C , which is at 42^{o} C if the ambient optimal growth temperature of the cells is at 37^{o} [18].

There are many different proteins in the heat shock family, such as HSP40, HSP60, GroEL, DnaJ, HSP25, HSP110, HSP70, and HSP90, all with varied functions in the cell. However, the HSP70 system is structurally and functionally distinct from most other HSP proteins because it does not have a cylindrical structure within which to house misfolded proteins [17]. These cylindrical proteins envelope whole, unfolded proteins and allow them to fold. In contrast, the HSP70 protein is considered a holding protein that binds small portions of amino acid chains and plays a significant role in protecting newly translated proteins and rescuing mature denatured proteins.

The heat shock protein 70 system is a ubiquitous set of proteins that are found in virtually all organisms. Interestingly, nearly all of the HSP70 proteins found in various species are relatively similar as evidenced by their high amino acid conservation (60-78% in eukaryotes) [19]. The widespread nature and high conservation show that HSP70s are crucial to survival since they have withstood evolutionary change through the years. The HSP family of proteins is constitutively expressed (making up 5% to 10 % of total protein content in the cell) but some forms can also be upregulated (up to 15 % of total cellular content) in the presence of cellular insults [20]. These insults include heat stress, oxidative stress, anoxia, cytokines, viral infection and heavy metals [18, 20]. The HSPs are thought to be involved in response to conditions such as inflammation, cancer, atherosclerosis, and such amyloid diseases as Alzheimer's [20, , 21, 22]. HSP70 has also been shown to block apoptosis by preventing translocation of BAX, an apoptotic signaling protein, to the mitochondria [23]. HSP70 was examined for its part in impaired inflammatory wound healing response of diabetic mice [24]. The HSP70 response was delayed in cutaneous wounds of diabetic mice when compared to nondiabetic controls

and was correlated to a delay in wound healing. Release of HSP70 upon cellular necrosis was investigated as a mechanism for immune response involving signaling to the dendritic cells [25]. Exogenous delivery of HSP70 to the wound bed has been shown to increase the up-regulation of macrophage-mediated phagocytosis to bring about faster wound closure rates in a BALB/cJ mouse model [26]. The cytokine IL-1β has been shown to upregulate *Hsp70* gene in β cells but not in α cells leading to a hypothesis for autoimmune destruction of β cells of the pancreas in insulin-dependent diabetes [27].

The HSP70 has a mass of approximately 70 kilodaltons that contains two domains. The first one is the N-terminal ATP binding domain. The other is the C-terminal substrate binding domain. As ATP attaches to the HSP70 molecule, the substrate binding domain will more rapidly bind and release the substrate [17]. This function of HSP70 is accelerated by HSP40 within the 'foldosome' complex that consists of HSP40, HSP70, HIP, HOP, p23 and HSP90 [17, 28, 29]. HSP40 proteins are dependent upon HSP70 for their ability to help refold heat inactivated firefly luciferase within the cytosol [30]. This result portrays HSP40 as an enhancer of the capacity of HSP70 to refold proteins because the presence of tetracycline induced HSP70 without HSP40 was able to rescue hamster fibroblast cells after thermal stress, however, to a lesser degree than thermally preshocked cells which included the HSP40 protein [29]. Consequently, HSP40 is considered a co-chaperone that works within the 'foldosome' to assist in substrate binding and release with HSP70 and HSP90 for refolding [31, 32]. In parallel, HSP110 is an inducible protein that is responsible for repairing high temperature stress and needs the assistance of another protein, the constitutive HSC70, for refolding [33]. HSP25 is a small heat shock protein that is activated by p38 which is part of the stress

response mechanism of cells [34]. The p38 MAPK pathway is one of the pathways that can be upregulated by heat. HSP25 has anti-apoptotic function that may be important to surviving thermal stress. HSP90 is a constitutively active heat shock protein that has a primary function in the proper folding of signaling molecules such as steroid hormones [28]. The abundance of HSP90 (up to 2% of total cellular content) is a testament to its importance in homeostasis. However, HSP90α isoform is also inducible by thermal stress implying its role in thermotolerance.

There are three heat shock transcription factors (HSF) that drive the signaling for turning on heat shock proteins. Of these, HSF1 is only stress activated and is not implicated in constitutive activation of HSPs [35]. Most HSF1 resides in clusters called stress granules in the cytosol and in a complex with constitutive HSPs until a driving factor such as heat is applied. The HSPs that are present are then recruited to repair the newly heat denatured proteins. This dissociates the HSF1 molecules to translocate to the nucleus, whereupon, they join as trimers and bind to the DNA sections that are called heat shock elements (HSE) to initiate hsp transcription [19, 35-38]. Newly synthesized HSPs then bind to free HSF1s as a feedback inhibition signal to prevent the overproduction of more HSPs.

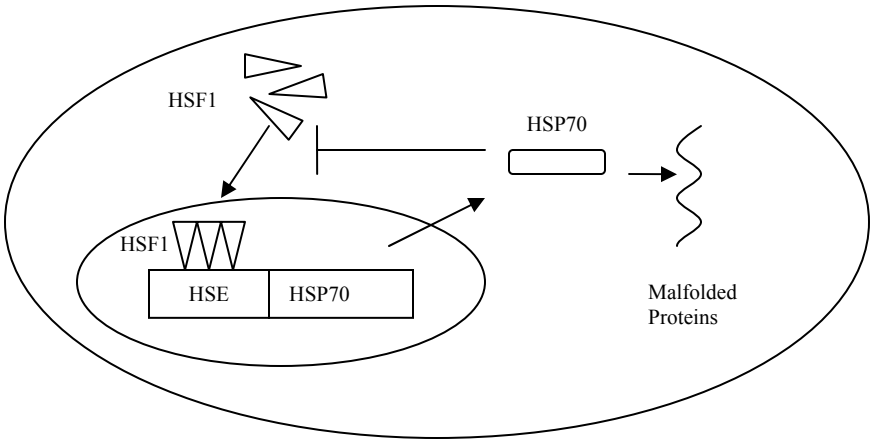

Figure 2.1: Schematic of *Hsp70* response pathways in the cell. When improperly folded proteins are present in the cell, HSPs binds them and is no longer free to bind HSF1. Release by HSP allows HSF1 to trimerize and then translocate to the nucleus and bind the heat shock elements (HSE). This, in turn, promotes the transcription of the *Hsp70* gene to satisfy the demand for more HSP70 protein [18].

2.3 Pretreatment of Cells and Tissues

Most often when a procedure involves high temperatures - such as with ablation or coagulation - damage to tissue that is adjacent the irradiation site is a concern. While a given laser protocol may minimize damage on a macroscopic scale to these collateral sites, there may still be cellular level damage that is not so readily evident. There are currently a few methods which seek to reduce the amount of heat that is getting to peripheral tissue, e.g. cryogen spray cooling, optically transparent (sapphire) cooled blocks, or heat conductive templates [39-42]. However, these are not always effective or are not practical to use (e.g on the deeper side of the target tissue where contact cooling cannot reach).

As an alternative or adjuvant to these heat reduction methods, one strategy to prevent collateral damage from a thermal stress is to pretreat the tissue in some manner at a time before the laser irradiation. The intention is to prepare the tissue for the severe damage by upregulating pathways and proteins with a mild stress. The concept of pretreatment has been applied to non-thermal injury as well. For example, hyperbaric oxygen has been used to ameliorate the damage from wounds and from cerebral hemorrhage [43, 44]. Cardiac tissue has been preconditioned prior to ischemia for the end goal of reducing reperfusion injury to prolong bypass procedure times and improve transplantation outcomes. [45-47].

Cells react to these external pretreatment stimuli by myriad, complex physiological pathways. As a result, a reservoir of repair proteins is present within the cell at the time of the more severe stress. For proteins that are highly inducible, such as HSP70, this strategy is particularly efficacious. Basal levels of the inducible form of HSP70 are very low to non existent and it can take hours to produce the protein in sufficient quantities [48]. However, the stress response pathway is not very discriminating as to which stimuli may upregulate it. For example, anoxia, heavy metals, denaturing agents and thermal stimuli can all activate the heat shock response to stress [10, 49-52]. While many of these different methods have been used to prepare the cells or tissue for the more severe laser stress, the most easily implemented method is to heat the tissue at a low temperature for a duration long enough to induce proteins like the heat shock proteins. The literature cites the most common pretreatment temperatures to be in the range of 42-44^{o} C for a duration of anywhere between 10-60 minutes when done in cell culture [29, 35]. The ideal protocol for pretreatment stress is still being debated

because different pathways are expressed at different temperatures and durations, which can lead to variable effects. The important criterion to consider for a pretreatment protocol is that it will not induce too much cell stress or cell death by itself. The cell would then be less able to cope with the secondary laser stress later on. There also needs to be sufficient time for the cells to recover and respond to the first stress as early time points show reductions in thermotolerance. Alternatively, waiting too long between pretreatment and the severe treatment will allow the cells to return back to homeostasis without any benefit because the HSR is transient in nature.

The stress response has primarily been noted for its role in helping to refold denatured proteins within the cell. However, HSP70 also directly inhibits the apoptotic pathway through interfering with BAX signaling to the mitochondria [53]. The activation of p38 MAPK stress pathway and the JNK apoptosis pathway have been observed in heat stress [34]. These are major signaling modules of the stress response pathway that determines the fate of cells. Another gene upregulated by heat was *Gadd45g [54]*. This gene is known to respond to stress and it inhibits cell growth, acts as a cyclinB1 kinase inhibitor with a role in cell cycle checkpoint arrest, and it induces apoptosis [55, 56]. Another pathway that has been observed to be upregulated in response to thermal stress is the TGF-β [57-59]. There was a correlation between improvement of wound healing and increases in TGF-β. This protein is of particular interest for dermatological applications because it has shown to be responsible for scarless wound healing for fetuses *in utero* [60]. A study of second degree burn wounds in mice show that TGF-β was significantly upregulated at the 2 hour time point along with some of the heat shock proteins [61]. The endpoints of the burn wounds showed no scarring or wound contraction at the 14 day

timepoint in mice. In work in our lab, there was a correlation between increased HSP70 expression from thermal pretreatment with a laser and increased tensile stress of scalpel wounds in mice [62]. These results indicate the promise of thermal preconditioning in clinical applications.

The ability to initiate a heat shock response without inducing any prior damage is an attractive alternative. This can be accomplished through pharmacological agents such as: bimoclomol, and geranyl geranyl acetone (GGA) [63-66]. The mechanism of action for bimoclomol seems to be as a co-inducer of the heat shock response by facilitating the stability of HSF (heat shock factor 1) trimerization in the cell [63, 66]. Alternatively, GGA binds to the HSP70 molecule and frees HSF1 to translocate to the nucleus driving the upregulation of the heat shock response [67]. These strategies may serve to provide more clinically relevant applications as the patient could take the drug at a prescribed time without having to be present for an additional procedure several hours before the actual laser treatment. However, the benefits to thermotolerance by these drugs relative thermal pretreatment have not been fully characterized. Potentially, induction of only one aspect of the cellular stress response may prove to be insufficient in an *in vivo* situation where the complex environment of cells within a tissue relies on many other pathways for successful wound response and prevention [68]. In contrast to pharmacological means, the allure of thermal pretreatment is that it is harnessing the body's natural ability to heal, repair and prevent damage by itself [36]. In many instances in medicine, exogenous agents used to bring about improvements in diseases or conditions can bring about side effects that are unwanted and even intolerable in light of the benefit they might give. For example, immune reactions to these substances can cause inflammation, swelling and

even death [69]. In contrast, pretreatment is a method wherein the resources are already available in the cells.

2.4 Optically Active Reporter Genes

Traditionally, HSP70 levels in cells have been determined by methods such as western blotting and in situ hybridization. However, both of these techniques require that the tissue be sacrificed. They are also rather laborious procedures to carry out in the lab. In contrast, the method used in this study to track HSP70 response is through the use of a reporter gene [48] [70]. The key concept to the use of reporter genes is that genes have promoter sequences. A promoter is the first region of DNA in a gene that essentially acts as an 'on/off' switch to regulate the reading and subsequent transcription of the rest of the gene, which, in turn, makes a protein. For a reporter gene system, the promoter sequence is isolated from the rest of the gene and the DNA sequence of the reporter gene is put in place behind the promoter. The new transgene is transfected back into the cell line. So, now the 'on/off' switch controls a different protein – in this case luciferase. The luciferase protein is easier to monitor than HSP70 because of its light producing capabilities that can be detected with a camera [71, 72]. So, as we track luciferase we are by association tracking *Hsp70* promoter activity, which means that we are tracking the signaling that turns on *Hsp70* in the cells. The *Hsp70* promoters already present in the genome of the cell are not affected by the presence of this new construct. The native promoters continue to produce HSP70 in a normal fashion. Monitoring of the *Hsp70* response in cell culture by means of a reporter gene provides an effective and convenient method of determining cellular response to heat stress after laser irradiation.

2.5 Luciferase-Luciferin Bioluminescence

For millions of years, nature has used bioluminescence as a tool for signaling in such organisms as the jellyfish, firefly and bacteria [73]. The uses of the light signaling are as varied as the different animals from which they have come. Baiting, camouflage, and courtship are examples of the utility of bioluminescence in nature. Recently, however, man has learned how to harness this phenomenon in a synthetic manner and use it for the purpose of scientific advancement as a reporter gene.

Bioluminescence is a unique reaction in which light is produced through a chemical reaction. The origin of this light emission differs from fluorescent and phosphorescent emissions due to the fact that a chemical reaction, rather than the absorption of light, supplies its excitation energy. The luciferase enzyme found in the common North American firefly, *Photinus pyralis*, catalyzes the oxidation reaction of the substrate luciferin in the presence of ATP, Mg^{2+}, and molecular oxygen [74].

$$\text{Luciferase} + \text{Luciferin} + \text{ATP} + O_2 \xrightarrow{Mg^{2+}} \text{Luciferase-Luciferin} + \text{AMP} + PP_i \quad (22)$$

$$\text{Luciferase-Luciferin} + \text{AMP} + O_2 \longrightarrow \text{Oxyluciferin*} + CO_2 + \text{AMP} \quad (23)$$

$$\text{Oxyluciferin*} \longrightarrow \text{Oxyluciferin} + h\nu \quad (24)$$

In this reaction, the oxidation of luciferin forms oxyluciferin in its electronically excited state [75]. Oxyluciferin returns to the ground state while emitting light of energy in joules as determined by $E = h\nu$, where h is Planck's constant at 6.62×10^{-23} J sec and ν is the frequency of light in [1/s]. The light emission is at a peak wavelength of 563 nm with a broad band range of 500-700 nm, at pH equal to or greater than 7 [76]. For each molecule of luciferin oxidized, a single photon is emitted [77]. The quantum yield of this bioluminescent reaction is 0.88, which is the highest known efficiency of any

chemiluminescent reaction [74]. Kinetic studies of the luciferase reaction *in vitro* indicate a peak-intensity reached within seconds following the addition of luciferin. However, the duration of the reaction can be extended with such cofactors as acetyl CoA. In the presence of excess luciferin, the light emitted is proportional to the concentration of luciferase protein [78].

The full luciferase gene (luc) that is derived from the firefly is 2387 base pairs long, which makes a 550 amino acid luciferase protein [73]. The various forms of luciferase are actually quite different from each other and they share very little sequence homology from organism to organism [73]. Because the luciferase is a monomer that does not require any post-translational modifications, it is available as a mature enzyme directly upon translation from its mRNA [79]. Once translated, the protein resides in the cytoplasm and peroxisomes of the cell where it can catalyze the bioluminescent reaction once the luciferin substrate has penetrated the cell membrane.

The luciferase-luciferin system is more advantageous than traditional methods of visualizing cellular response. This technology allows for non-invasive monitoring of biological phenomenon. The cells are left relatively unaffected except for the production of luciferase and addition of luciferin, both of which are non toxic to cells [80]. Furthermore, multiple time points of data can be taken instead of one end point in which the sample is sacrificed, as is the case for Western blots or immunohistochemical analysis. Therefore, the time course of expression can be tracked with one sample which is convenient and also more effective because biological variations that would be present in multiple samples are not a factor. In this system, there is inherently no background noise to compromise signal-to-noise ratios because most cells and organisms do not

naturally produce bioluminescence, except some very low levels of metabolic light [81]. Also, time is saved with the luciferase-luciferin system when compared to other more labor-intensive lab procedures that require many preparation steps before the actual assay is performed. Lastly, no hazardous reagents, such as radioactive isotopes, are needed.

In contrast to fluorescence, bioluminescence has many advantages for this study. The wavelength produced from bioluminescence has effective tissue penetration properties which allows for imaging at depth in live animal tissue. The emission spectrum of luciferase is rather broadband in that it extends from 500-700 nm. The wavelengths above 600 nm are the ones necessary for deep tissue imaging in live animals. According to Rice, et al., at a 1 cm depth the light from a 650 nm source has been attenuated by $\sim 10^2$, but for wavelengths of 550 nm the attenuation is as high as 10^{10} [81]. Bioluminescence also avoids potential bleaching and auto-fluorescence issues that arise in fluorescence measurements. The absence of an excitation source further demonstrates the benefit of the luciferase-luciferin system. Most commonly, excitation wavelengths for fluorescent molecules are in the blue and green portions of the spectrum, which do not penetrate well into tissue. So, getting the light in, as well as out becomes a problem. Penetration depths for fluorescence imaging are on the order of millimeters, while luminescence can image at centimeter depths [81]. Furthermore, the benefit of not having an excitation source means the number of cells to be detected is proportional only to the amount of light emitted and not to the light which would be used for excitation.

The detection of luciferase emission is usually done with a charge coupled device (CCD) camera. The background noise is commonly reduced through thermo-electric cooling to a temperature of $-90^{o}C$ or below. The quantum efficiency is 85% whereas that

of the older technology of intensified CCDs (ICCD) is in the range of 1-10% in the spectrum of interest around 600 nm [81]. Due to the increased sensitivity of a cooled CCD system, as few as 150 cells in culture can be detected. Furthermore, CCDs are more sensitive in the spectral range above 650 nm to which tissue is relatively transparent. As a result, in vivo imaging at depth is more effective. Subcutaneous detection can be as low as 500 cells, and as few as 10^6 cells could be detected at a depth of 2 cm in a mouse model [81].

Consequently, luciferase has been adapted for use in a multitude of applications. Detection of ATP can be achieved by supplying the other reagents in the reaction in abundance so that the ATP is the limiting reagent. Tracking of *E. coli* bacterial pathogens to monitor wound healing has been done with the luciferase system [82]. Another wound healing application is visualization of transgene expression. An MMP-13 promoter fused to the luciferase gene was monitored after cutaneous wound repair to study spatial and temporal characteristics of the MMP-13 promoter in wounds [83]. MMP-13 is a matrix metalloproteinase that plays a role in tissue remodeling in normal states but has been implicated in pathological matrix degradation in cancerous states. The luciferase system has also been able to elucidate the potential for gene therapy. DNA delivery and expression were studied with a viral promoter (HIV) and a luciferase reporter gene in their delivery via cationic liposomes in cell culture and with in vivo models [71]. Luciferase expression could be detected after both topical and systemic delivery of substrate. The progression and spatial characterization of metastasis was examined with the use of luciferase as a cellular tag for cancerous prostate cells [84]. The luciferase method helped to elucidate the fact that these adenocarcinoma cells spread from the

prostate to the lymph but do not travel via the blood. Sadikot, et. al. examined the effects of dexamethasone treatment on nuclear factor NF-κB activation and lung inflammation in transgenic reporter mice expressing *photinus pyralis* luciferase under the control of an NF-κB–dependent promoter. The inflammatory response controlled by NF-κB was able to be detected with an intensified CCD camera after intra peritoneal injection of luciferin [85].

2.6 Gene Expression Analysis (microarray and qRT-PCR)

While the heat shock response is the most well known response to thermal insult, there can be other protective pathways that allow the cell to cope with the stress. [54, 61, 86]. A better understanding of the full scope of genes activated or suppressed by pretreatment methods may allow for more effective optimization of protocols and selection of targets.

Gene expression analysis using cDNA microarrays analysis allows for the parallel investigation of thousands of genes from the same sample. They can represent as snapshot of the cells' response at a given time. From this data much information about the status of the cell and the changes it will make can be inferred.

Microarrays examine gene expression through measuring fluorescent signals of bound cDNA targets. The cDNA is a copy of the RNA with in a cell made using poly-A primers to only replicate message RNA. This mRNA is the expression profile of a given sample's genes [87]. These cDNA targets are then hybridized to matching probes which are bound to a solid substrate, usually glass or silicon. The amount of fluorescence is correlated to how many molecules of target have bound to the probes. As the technology

evolves, microarrays have increased in their density of genes per chip. For this study we used a single color, spotted array from Affymetrix that can scan over 45,000 different probesets corresponding to well known gene transcripts or to EST (expressed sequence tags) that target those of unknown function.

Despite the vast potential of microarrays, there are some downsides. First of all, the amount of data garnered from an experiment can be intractable. Microarray analysis requires technical expertise in statistical methods in order to reduce the data and determine significant findings and trends. Strategies such as multiple testing corrections and p-value determinations across samples are implemented to give more meaningful data. In an effort to standardize the content of microarray data, a standard called MIAME (Minimum Information About a Microarray Experiment) has been adopted. Fortunately, the demand for these arrays has attracted the establishment of specialized core facilities to undertake the work and analysis and to guide the researcher in drawing conclusions.

Microarrays are also only considered a screening method that identifies genes which are potentially involved in the response that is being investigated. They do not give functional or causal information because the data only identifies the presence of mRNA transcripts within the cell. This does not directly correlate to actual protein being made or the functionality of the protein. There are several stages when going from signaling to transcription to translation that can alter the end amount of expression and microarrays do not account for these intermediate steps. Post translational modifications can further complicate this relationship as proteins may not be in an active state until further events take place. These include phosphorylation events, enzymatic cleavage, ubiquitination and dimerization [87].

Furthermore, microarrays are not seen as a truly quantitative measure of gene expression. They are commonly validated with quantitative RT-PCR in order to determine actual levels of mRNA. Also, some microarrays cannot completely account for all of the mRNA. The Affymetrix chips used in this work are only designed to probe the 3' end of the mRNA transcript. Consequently, splice variants and exons not on the 3' end of the gene are not detected as well, which can lead to an underestimation of the contribution by a gene. However, qRT-PCR primers that hit specific targets and exons of interest can be designed to determine these levels accurately. The latest generation of expression arrays is now able to more accurately represent gene levels by probing several target sites throughout a gene transcript. Ultimately, microarrays coupled with functional protein data provide a powerful tool into the response of cells to stimuli such as thermal and laser treatments.

2.7 References

1. Gross, A.J. and T.R. Herrmann, *History of lasers.* World J Urol, 2007. **25**(3): p. 217-20.
2. Niemz, M.H., *Laser-tissue interactions : fundamentals and applications*. 1996, Berlin ; New York: Springer. 297.
3. Maiman, T.H., *Stimulated Optical Radiation in Ruby.* Nature, 1960. **187**(4736): p. pp. 493-494.
4. Welch, A.J., J.H. Torres, and W.-F. Cheong, *Laser Physics and Laser-Tissue Interaction.* Texas Heart Institute Journal, 1989. **16**: p. 141-9.
5. Welch, A.J., et al., *Laser thermal ablation.* Photochem Photobiol, 1991. **53**(6): p. 815-23.
6. Thomsen, S., *Pathologic Analysis of Photothermal and Photomechanical Effects of Laser-Tissue Interactions.* Photochemsitry and Photobiology, 1990. **53**(6): p. 825-835.
7. Rylander, M.N., et al., *Thermally induced injury and heat-shock protein expression in cells and tissues.* Ann N Y Acad Sci, 2005. **1066**: p. 222-42.
8. Welch, A.J. and M.J.C.v. Gemert, *Optical-thermal response of laser-irradiated tissue*, in *Lasers, photonics, and electro-optics*. 1995, Plenum Press: New York. p. 5.

9. Esenaliev, R.O., et al., *Studies of acoustical and shock waves in the pulsed laser ablation of biotissue.* Lasers Surg Med, 1993. **13**(4): p. 470-84.
10. Minowada, G. and W.J. Welch, *Clinical implications of the stress response.* J Clin Invest, 1995. **95**(1): p. 3-12.
11. Jansen, E.D., et al., *Effect of pulse duration on bubble formation and laser-induced pressure waves during holmium laser ablation.* Lasers Surg Med, 1996. **18**(3): p. 278-93.
12. Moritz, A. and F. Henriques, *Studies of thermal injury in the conduction of heat to and through skin and the temperatures attained therein.* Am. J. Pathol., 1947. **23**: p. 531-549.
13. McNally, K.M., et al., *Optical and thermal characterization of albumin protein solders.* Appl Opt, 1999. **38**(31): p. 6661-72.
14. Simanovskii, D.M., et al., *Cellular tolerance to pulsed hyperthermia.* Phys Rev E Stat Nonlin Soft Matter Phys, 2006. **74**(1 Pt 1): p. 011915.
15. Lepock, J.R., *How do cells respond to their thermal environment?* Int J Hyperthermia, 2005. **21**(8): p. 681-7.
16. Baler, R., W. Welch, and R. Voellmy, *Heat shock gene regulation by nascent polypeptides and denatured proteins: hsp70 as a potential autoregulatory factor.* J. Cell Biol., 1992. **117**(6): p. 1151-1159.
17. Frydman, J., *Folding of newly translated proteins in vivo: the role of molecular chaperones.* Annu Rev Biochem, 2001. **70**: p. 603-47.
18. Morimoto, R.I., P.E. Kroeger, and J.J. Cotto, *The transcriptional regulation of heat shock genes: a plethora of heat shock factors and regulatory conditions.* Stress Inducible Cellular Responses, 1996. **77**: p. 139-63.
19. Kiang, J.G. and G.C. Tsokos, *Heat shock protein 70 kDa: molecular biology, biochemistry, and physiology.* Pharmacol Ther, 1998. **80**(2): p. 183-201.
20. Pockley, A.G., *Heat shock proteins, inflammation, and cardiovascular disease.* Circulation, 2002. **105**(8): p. 1012-7.
21. Beckham, J.T., *Molecular Chaperones and the Heat Shock Response: Meeting Notes*. 2002: Cold Spring Harbor Laboratory, NY.
22. Westerheide, S.D. and R.I. Morimoto, *Heat shock response modulators as therapeutic tools for diseases of protein conformation.* J Biol Chem, 2005. **280**(39): p. 33097-100.
23. Mosser, D.D., et al., *Role of the human heat shock protein hsp70 in protection against stress-induced apoptosis.* Mol Cell Biol, 1997. **17**(9): p. 5317-27.
24. McMurtry, A.L., et al., *Expression of HSP70 in healing wounds of diabetic and nondiabetic mice.* J Surg Res, 1999. **86**(1): p. 36-41.
25. Basu, S., et al., *Necrotic but not apoptotic cell death releases heat shock proteins, which deliver a partial maturation signal to dendritic cells and activate the NF-kappa B pathway.* Int Immunol, 2000. **12**(11): p. 1539-46.
26. Kovalchin, J.T., et al., *In vivo delivery of heat shock protein 70 accelerates wound healing by up-regulating macrophage-mediated phagocytosis.* Wound Repair Regen, 2006. **14**(2): p. 129-37.
27. Strandell, E., et al., *Interleukin-1 beta induces the expression of hsp70, heme oxygenase and Mn-SOD in FACS-purified rat islet beta-cells, but not in alpha-cells.* Immunol Lett, 1995. **48**(2): p. 145-8.

28. Duncan, R.F., *Inhibition of Hsp90 function delays and impairs recovery from heat shock.* Febs J, 2005. **272**(20): p. 5244-56.
29. Nollen, E.A., et al., *In vivo chaperone activity of heat shock protein 70 and thermotolerance.* Mol Cell Biol, 1999. **19**(3): p. 2069-79.
30. Michels, A.A., et al., *Hsp70 and Hsp40 chaperone activities in the cytoplasm and the nucleus of mammalian cells.* J Biol Chem, 1997. **272**(52): p. 33283-9.
31. Taylor, D.M., et al., *Characterizing the role of Hsp90 in production of heat shock proteins in motor neurons reveals a suppressive effect of wild-type Hsf1.* Cell Stress Chaperones, 2007. **12**(2): p. 151-62.
32. Uchiyama, Y., et al., *Heat shock protein 40/DjB1 is required for thermotolerance in early phase.* J Biochem, 2006. **140**(6): p. 805-12.
33. Oh, H.J., X. Chen, and J.R. Subjeck, *Hsp110 protects heat-denatured proteins and confers cellular thermoresistance.* J Biol Chem, 1997. **272**(50): p. 31636-40.
34. Cowan, K.J. and K.B. Storey, *Mitogen-activated protein kinases: new signaling pathways functioning in cellular responses to environmental stress.* J Exp Biol, 2003. **206**(Pt 7): p. 1107-15.
35. Huang, L., N.F. Mivechi, and D. Moskophidis, *Insights into regulation and function of the major stress-induced hsp70 molecular chaperone in vivo: analysis of mice with targeted gene disruption of the hsp70.1 or hsp70.3 gene.* Mol Cell Biol, 2001. **21**(24): p. 8575-91.
36. Schett, G., et al., *Enhanced expression of heat shock protein 70 (hsp70) and heat shock factor 1 (HSF1) activation in rheumatoid arthritis synovial tissue. Differential regulation of hsp70 expression and hsf1 activation in synovial fibroblasts by proinflammatory cytokines, shear stress, and antiinflammatory drugs.* J Clin Invest, 1998. **102**(2): p. 302-11.
37. Zhang, Y., et al., *Targeted disruption of hsf1 leads to lack of thermotolerance and defines tissue-specific regulation for stress-inducible Hsp molecular chaperones.* J Cell Biochem, 2002. **86**(2): p. 376-93.
38. Trinklein, N.D., et al., *Transcriptional regulation and binding of heat shock factor 1 and heat shock factor 2 to 32 human heat shock genes during thermal stress and differentiation.* Cell Stress Chaperones, 2004. **9**(1): p. 21-8.
39. Ahcan, U., et al., *Port wine stain treatment with a dual-wavelength Nd:Yag laser and cryogen spray cooling: a pilot study.* Lasers Surg Med, 2004. **34**(2): p. 164-7.
40. Paithankar, D.Y., et al., *Subsurface skin renewal by treatment with a 1450-nm laser in combination with dynamic cooling.* J Biomed Opt, 2003. **8**(3): p. 545-51.
41. Schaffer, C.J., et al., *Comparisons of wound healing among excisional, laser-created, and standard thermal burns in porcine wounds of equal depth.* Wound Repair Regen, 1997. **5**(1): p. 52-61.
42. Robbins, J.B., L. Reinisch, and D.L. Ellis, *Wound healing of 6.45-microm free electron laser skin incisions with heat-conducting templates.* J Biomed Opt, 2003. **8**(4): p. 594-600.
43. Beckham, P.H. *Effect of Hyperbaric Oxygenation on Wound Strength in Dogs: A Preliminary Report*. in *Hyperbaric Oxygenation*. 1964.
44. Qin, Z., et al., *Preconditioning with hyperbaric oxygen attenuates brain edema after experimental intracerebral hemorrhage.* Neurosurg Focus, 2007. **22**(5): p. E13.

45. Gowda, A., et al., *Cardioprotection by local heating: improved myocardial salvage after ischemia and reperfusion.* Ann Thorac Surg, 1998. **65**(5): p. 1241-7.
46. Plumier, J.C. and R.W. Currie, *Heat shock-induced myocardial protection against ischemic injury: a role for Hsp70?* Cell Stress Chaperones, 1996. **1**(1): p. 13-7.
47. Plumier, J.C., et al., *Transgenic mice expressing the human heat shock protein 70 have improved post-ischemic myocardial recovery.* J Clin Invest, 1995. **95**(4): p. 1854-60.
48. OConnell Rodwell, C.E., et al., *A genetic reporter of thermal stress defines physiologic zones over a defined temperature range.* FASEB Journal, 2003. **18**(2).
49. Morris, S.D., et al., *Specific induction of the 70-kD heat stress proteins by the tyrosine kinase inhibitor herbimycin-A protects rat neonatal cardiomyocytes. A new pharmacological route to stress protein expression?* J Clin Invest, 1996. **97**(3): p. 706-12.
50. Souil, E., et al., *Treatment with 815-nm diode laser induces long-lasting expression of 72-kDa heat shock protein in normal rat skin.* Br J Dermatol, 2001. **144**(2): p. 260-6.
51. Topping, A., et al., *Successful reduction in skin damage resulting from exposure to the normal-mode ruby laser in an animal model.* Br J Plast Surg, 2001. **54**(2): p. 144-50.
52. Lee, J.S. and J.S. Seo, *Differential expression of two stress-inducible hsp70 genes by various stressors.* Exp Mol Med, 2002. **34**(2): p. 131-6.
53. Stankiewicz, A.R., et al., *Hsp70 inhibits heat-induced apoptosis upstream of mitochondria by preventing Bax translocation.* J Biol Chem, 2005. **280**(46): p. 38729-39.
54. Dinh, H.K., et al., *Gene expression profiling of the response to thermal injury in human cells.* Physiol Genomics, 2001. **7**(1): p. 3-13.
55. Mak, S.K. and D. Kultz, *Gadd45 proteins induce G2/M arrest and modulate apoptosis in kidney cells exposed to hyperosmotic stress.* J Biol Chem, 2004. **279**(37): p. 39075-84.
56. Vairapandi, M., et al., *GADD45b and GADD45g are cdc2/cyclinB1 kinase inhibitors with a role in S and G2/M cell cycle checkpoints induced by genotoxic stress.* J Cell Physiol, 2002. **192**(3): p. 327-38.
57. Cao, Y., et al., *TGF-beta1 mediates 70-kDa heat shock protein induction due to ultraviolet irradiation in human skin fibroblasts.* Pflugers Arch, 1999. **438**(3): p. 239-44.
58. Wehrhan, F., et al., *Exogenous Modulation of TGF-beta(1) Influences TGF-betaR-III-Associated Vascularization during Wound Healing in Irradiated Tissue.* Strahlenther Onkol, 2004. **180**(8): p. 526-33.
59. Chen, S.J., et al., *The early-immediate gene EGR-1 is induced by transforming growth factor-beta and mediates stimulation of collagen gene expression.* J Biol Chem, 2006. **281**(30): p. 21183-97.
60. Lanning, D.A., et al., *TGF-beta1 alters the healing of cutaneous fetal excisional wounds.* J Pediatr Surg, 1999. **34**(5): p. 695-700.
61. Feezor, R.J., et al., *Temporal patterns of gene expression in murine cutaneous burn wound healing.* Physiol Genomics, 2004. **16**(3): p. 341-8.

62. Wilmink, G., et al., *Molecular Imaging-Assisted Optimization of Hsp70 Expression During Laser Preconditioning for Wound Repair Enhancement.* J Invest Dermatol, 2008. **In Press**.
63. Hargitai, J., et al., *Bimoclomol, a heat shock protein co-inducer, acts by the prolonged activation of heat shock factor-1.* Biochem Biophys Res Commun, 2003. **307**(3): p. 689-95.
64. Nishida, T., et al., *Geranylgeranylacetone induces cyclooxygenase-2 expression in cultured rat gastric epithelial cells through NF-kappaB.* Dig Dis Sci, 2007. **52**(8): p. 1890-6.
65. Suzuki, S., et al., *Geranylgeranylacetone ameliorates ischemic acute renal failure via induction of Hsp70.* Kidney Int, 2005. **67**(6): p. 2210-20.
66. Vigh, L., et al., *Bimoclomol: a nontoxic, hydroxylamine derivative with stress protein-inducing activity and cytoprotective effects.* Nat Med, 1997. **3**(10): p. 1150-4.
67. Otaka, M., et al., *The induction mechanism of the molecular chaperone HSP70 in the gastric mucosa by Geranylgeranylacetone (HSP-inducer).* Biochem Biophys Res Commun, 2007. **353**(2): p. 399-404.
68. Eming, S.A., T. Krieg, and J.M. Davidson, *Inflammation in wound repair: molecular and cellular mechanisms.* J Invest Dermatol, 2007. **127**(3): p. 514-25.
69. Posadas, S.J. and W.J. Pichler, *Delayed drug hypersensitivity reactions - new concepts.* Clin Exp Allergy, 2007. **37**(7): p. 989-99.
70. Baran, J., *Noninvasive monitoring of hsp70 during Ho:YAG laser irradiation*, in *Biomedical Engineering*. 2000, Vanderbilt University: Nashville.
71. Contag, C.H., et al., *Visualizing gene expression in living mammals using a bioluminescent reporter.* Photochem Photobiol, 1997. **66**(4): p. 523-31.
72. Contag, C.H. and M.H. Bachmann, *Advances in in vivo bioluminescence imaging of gene expression.* Annu Rev Biomed Eng, 2002. **4**: p. 235-60.
73. Greer, L.F., 3rd and A.A. Szalay, *Imaging of light emission from the expression of luciferases in living cells and organisms: a review.* Luminescence, 2002. **17**(1): p. 43-74.
74. Gould, S.J. and S. Subramani, *Firefly luciferase as a tool in molecular and cell biology.* Anal Biochem, 1988. **175**(1): p. 5-13.
75. Hastings, J.W., *Chemistries and colors of bioluminescent reactions: a review.* Gene, 1996. **173**(1): p. 5-11.
76. Ugarova, N.N. and L.Y. Brovko, *Protein structure and bioluminescent spectra for firefly bioluminescence.* Luminescence, 2002. **17**: p. 321-330.
77. Nguyen, V.T., M. Morange, and O. Bensaude, *Firefly luciferase luminescence assays using scintillation counters for quantitation in transfected mammalian cells.* Anal Biochem, 1988. **171**(2): p. 404-8.
78. Brasier, A.R., J.E. Tate, and J.F. Habener, *Optimized use of the firefly luciferase assay as a reporter gene in mammalian cell lines.* Biotechniques, 1989. **7**(10): p. 1116-22.
79. Wood, K. ***The Chemistry of Bioluminescent Reporter Assays***. 1998 [cited; Available from: http://www.promega.com/pnotes/65/6921_14/default.html.
80. Bhaumik, S. and S.S. Gambhir, *Optical imaging of Renilla luciferase reporter gene expression in living mice.* Proc Natl Acad Sci U S A, 2002. **99**(1): p. 377-82.

81. Rice, B.W., M.D. Cable, and M.B. Nelson, *In vivo imaging of light-emitting probes.* J Biomed Opt, 2001. **6**(4): p. 432-40.
82. Hamblin, M.R., et al., *Rapid control of wound infections by targeted photodynamic therapy monitored by in vivo bioluminescence imaging.* Photochem Photobiol, 2002. **75**(1): p. 51-7.
83. Wu, N., et al., *Real-time visualization of MMP-13 promoter activity in transgenic mice.* Matrix Biol, 2002. **21**(2): p. 149-61.
84. Rubio, N., M.M. Villacampa, and J. Blanco, *Traffic to lymph nodes of PC-3 prostate tumor cells in nude mice visualized using the luciferase gene as a tumor cell marker.* Lab Invest, 1998. **78**(10): p. 1315-25.
85. Sadikot, R., et al., *High dose dexamethasone accentuates nuclear factor-kB activation in endotoxin-treated mice.* Am J Respir Crit Care Med, 2001. **164**: p. 873-878.
86. Sonna, L.A., et al., *Invited review: Effects of heat and cold stress on mammalian gene expression.* J Appl Physiol, 2002. **92**(4): p. 1725-42.
87. Alberts, B., *Molecular biology of the cell*. 4th ed. 2002, New York: Garland Science. xxxiv, [1548] p.

CHAPTER III

ASSESSMENT OF CELLULAR RESPONSE TO THERMAL LASER INJURY THROUGH BIOLUMINESCENCE IMAGING OF HEAT SHOCK PROTEIN 70

Joshua T. Beckham [1], Mark A. Mackanos[1], Cornelia Crooke[2], Takamune Takahashi[2], Caitlin O'Connell-Rodwell[3], Christopher H. Contag[3], E. Duco Jansen[*1]

[1] Department of Biomedical Engineering, Vanderbilt University, Nashville, TN

[2] Department of Medicine, Vanderbilt University, Nashville, TN

[3] Departments of Pediatrics, Radiology and Microbiology & Immunology, Stanford University, Stanford, CA

Vanderbilt University

Nashville, TN 37235

Portions of this manuscript have been published in:

"Assessment of Cellular Response to Thermal Laser Injury Through Bioluminescence Imaging of Heat Shock Protein 70," *Photochemistry & Photobiology*. 2004; 79(1):76-85.

3.1 Abstract

Assessment of laser-induced tissue damage is not complete without an investigation into the resulting cellular and molecular changes. In the past, tissue damage was quantified by macroscopically visual effects such as tissue mass removal, carbonization, and melting. Microscopically, assessment of tissue damage has typically limited to histological analysis of excised tissue samples. In this research, we used heat shock protein (*Hsp70*) transcription, to track cellular response to laser-induce injury. A stable cell line (NIH 3T3) was generated containing the firefly luciferase (*luc*) reporter gene attached to the heat shock protein promoter (murine hsp70a1). After thermal injury with a pulsed Holmium:YAG laser (λ= 2.1 μm, τ_p = 250 μs, 30 pulses, 3 Hz), luciferase is produced upon hsp70 activation and emits broad spectrum bioluminescence over a range of 500-700 nm with a peak at 563 nm. The onset of bioluminescence can be seen as early as two hours after treatment and usually peaks at 8-12 hours depending on the severity of heat shock. The luminescence was quantified in live cells using bioluminescence imaging. A minimum pulse energy (65 mJ/pulse (total energy 1.95 J; total radiant exposure = 6 J/cm^2)), was needed to activate the hsp70 response and a higher energy (103 mJ/pulse (total energy 3.09 J; total radiant exposure = 9.6 J/cm^2)) was associated with a reduction in hsp70 response and cell death. Bioluminescence levels correlated well with actual hsp70 protein concentrations as determined by ELISA assay. Photon counts were normalized to the percentage of live cells by means of a flow cytometry cell viability assay. Within a relatively small range between a lower activation threshold and an upper threshold that leads to cell death, the hsp70 response followed an Arrhenius relationship when constant temperature water bath and laser experiments were carried out.

3.2 Introduction

Assessment of laser radiation on biological tissue has traditionally been limited to macroscopic effects and histopathological endpoint analysis. The irradiation parameters (wavelength, spot diameter) and treatment parameters (pulse duration and radiant exposure) are essential factors in determining the outcome of the laser procedure. In the past, these parameters have been chosen with limited insight into the lethal and sublethal injury that may occur on a cellular level. A better understanding of the cellular mechanisms, pathways activated, and effects involved will further facilitate the selection of laser parameters which may significantly enhance the treatment provided by laser irradiation by reducing undesirable side effects and by potentially providing new pathways for therapeutic intervention [1]. Moreover such insight may be important in determining maximum exposure levels in numerous diagnostic, spectroscopic and optical imaging procedures where induction of cellular changes by excitation or probing light must be avoided.

3.2.1 Heat Shock proteins

In most scenarios of light-tissue interaction, optical energy is converted to thermal energy and tissues and cells may be reversibly or irreversibly thermally damaged. Biophysical markers such as vacuolization, hyperchromasia, protein denaturation (birefringence loss) are typical signs of thermal damage [2-5]. More subtle thermal effects are not as obviously visible and often are not acutely apparent. Among the most sensitive biological indicators of thermal stress are the heat shock proteins. The heat shock protein 70 system is found in all organisms showing high levels of similarity across species as evidenced by their high amino acid conservation (60-78% in eukaryotes) [6]. The widespread nature and high conservation show that HSP70s are crucial to survival since they have

withstood evolutionary change through time. The HSP family of proteins is constitutively expressed (making up 5% to 10 % of total protein content in the cell) but some forms can also be upregulated (up to 15 % of total cellular content) in the presence of cellular insults [7].

Heat shock protein 70 is in a class of proteins called molecular chaperones that are involved in the cellular response to such stressful conditions as: heat, oxidative stress, anoxia, viral infection and heavy metals [7-11]. Chaperones play a significant role in protecting newly translated proteins and rescuing mature, denatured proteins. Chaperones either envelope or attach to denatured proteins and allow them to refold without interference from adjacent molecules [12]. Heat activated HSP induction depends on temperature, duration of exposure and cell type but in all cases is mediated by the presence of denatured proteins in the cell [13, 14]. The activation of HSP by chemical methods appears to be due to the presence of denatured proteins as well, but the mechanism involved in shear stress activation has yet to be elucidated [15, 16]. Most mammalian cell lines respond to a temperature increase of at least 5-6 ^{o}C, i.e. 42-43 ^{o}C if the ambient optimal growth temperature of the cells is at 37 ^{o}C [13]. Similar trends have been observed in vivo [17]

HSP70 has been shown to have significance in thermotolerance, apoptosis and necrosis in cells. Release of HSP70 upon cellular necrosis was investigated as a mechanism for immune response involving signaling to the dendritic cells via activation of the NF-κB pathway [18]. HSP70 has been noted for preventing cells from entering apoptosis after pro-apoptotic agents, such as etoposide, have been given to cultured cells [19]. Also, HSP70 has been implicated in the role of thermotolerance for cells subjected to severe heat stress (44^{o} C for 40 min) when preinduction of the protein had been achieved by milder heat stress (43^{o} C for 20 min) applied up to 40 minutes prior to second thermal challenge [20]. This resistance

to thermal stress is due to the direct effects of HSP70 reducing damage through helping proteins refold but it may also be due to the ability of HSP70 to simultaneously inhibit the apoptotic pathway through such mechanisms as cytochrome c release and caspase pathway intervention [21, 22]

Traditionally, HSP70 levels in cells have been determined by methods such as Western blotting and *in situ* hybridization. However, both of these techniques are time- and labor intensive procedures and require that the cells by lysed or tissue be excised. Moreover, no dynamic (temporal) information can be obtained from a single sample. In contrast, the method used in this study is more convenient through the use of an optically active reporter gene [23, 24]. The reporter gene system utilizes the promoter sequence of one gene (murine *Hsp70A1*) to act as an 'on/off' switch to control the transcription of a bioluminescent reporter gene – in this case luciferase (*luc*) from firefly (*Photinus pyralis*). Bioluminescence differs from fluorescent and phosphorescent emissions due to the fact that a chemical reaction, rather than the absorption of light, provides its excitation energy. In this respect, bioluminescence provides several advantages over fluorescent markers, such as GFP (green fluorescent protein). First, luciferase, which doesn't require optical excitation and emits broadband (500-700nm) light, allows deep tissue imaging (cm) in contrast to GFP imaging which is limited to ~ 1mm. While in this study with cell cultures we did not need this feature, we plan to carry out future experiments using in vivo (transgenic) models which will take advantage of this. Second, (semi) quantitative data analysis of luciferase induced light emission is known to be superior to fluorescence (GFP) – which is complicated due to uncertainties in excitation light parameters and phenomena such as photobleaching. Third, bioluminescence imaging is inherently superior in tracking dynamic changes owing to the relatively short half-life of the luciferase enzyme in the physiological environment. In contrast, GFP is stable and hence accumulates over time making quantitative imaging of dynamic processes very difficult.

The luciferase enzyme catalyzes the oxidation of the substrate luciferin in the presence of ATP, Mg^{2+}, and molecular oxygen [25]. In this reaction, the oxidation of luciferin forms oxyluciferin in its electronically excited state [26]. Oxyluciferin returns to the ground state while emitting broadband light with an emission spectrum of 500-700 nm and a peak emission wavelength of 563 nm [27]. For each molecule of luciferin oxidized, a single photon is emitted [28]. The quantum yield of this bioluminescent reaction is 0.88, which is the highest known efficiency of any chemiluminescent reaction [28]. Kinetic studies of the luciferase reaction *in vitro* indicate a peak-intensity reached within 0.3 seconds following the addition of luciferin to crude protein extracts from cells that were mixed with Mg+ and ATP [25]. In the presence of excess luciferin and ATP, the light emitted is proportional to the concentration of luciferase protein [29]. Thus, as we track luciferase we are by association tracking hsp70 transcription. The native hsp70 promoters already present in the genome of the cell continue to produce hsp70 in a normal fashion. It is important to note that this promoter- reporter system monitors the transcriptional activation of the *Hsp70* gene and not the actual protein produced.

The observed changes in reporter gene activity can be used to infer the amount of cellular stress caused by the laser irradiation and can be correlated with various laser irradiation protocols. In addition, this method provides the opportunity to document the sequence of responses that precedes cell death or may lead to increase thermotolerance.

3.2.2 Arrhenius Damage Integral

The kinetics of several morphological and physiologic indicators of thermal damage are exponentially dependent on temperature and linearly dependent on time of exposure [30]. The Arrhenius integral describes a rate process for characterizing tissue damage that works well for low temperature phenomena, such as coagulation or birefringence loss:

$$\Omega = \ln\left(\frac{C_0}{C(t)}\right) = \int_0^{t_p} A\exp(-E_a / RT)dt \quad (1)$$

where Ω is the tissue damage [unitless], A is the frequency factor - i.e. damage rate [1/sec], E_a is the activation energy in [J/mole], T is the temperature of exposure [K], R is the gas constant at 8.32 [J/mol] and the integral is over the time of the heat exposure. A detailed description of the Arrhenius formulation and its various identities can be found in [31]. The Arrhenius integral takes into account temperature-time history of the sample to predict tissue damage based on the damage threshold. A precisely defined, reproducible and measurable indicator of the thermal damage is identified by experimental analysis. The threshold of the thermal damage is commonly a ratio of the concentration of native (undamaged) tissue before irradiation exposure (C_0) to the concentration of native tissue at the end of the exposure time (C(t)). For this study, the maximum level of hsp70 production as determined by bioluminescence was chosen as the endpoint of damage.

For a constant temperature exposure, the Arrhenius relationship predicts a linear increase in damage with increasing exposure time. In order to test the linearity of a system, the experimental data can be fitted to the Arrhenius integral by means of converting the equation into a linear relationship [32]. When the damage parameter (Ω) is equal to 1, which is when the damage is equal to the arbitrary end point, the equation becomes:

$$\ln(t) = -\ln(A) + E_a / RT \quad (2)$$

Plotting the experimental results on an ln(t) versus 1/T graph will produce a slope (E_a/R) and y-intercept (-ln(A)) from which the activation energy and frequency factor can be derived, respectively. It should be noted that the original Arrhenius formulation as well as many studies that have used it to analyze tissue damage are predominantly using it to

determine biophysical damage done to tissue (i.e. using direct measurements of protein denaturation by means of scattering increase or birefringence loss) and do not take into account the non-linear amplification of the biological response to biophysical damage. In contrast, our experiments use the biological endpoint of hsp70 transcription as damage indicator. In this study we will examine if and to what extent the Arrhenius relation can be used to describe the expression of heat shock proteins.

3.3 Material & Methods

3.3.1 Cell Culture Conditions

An adherent, murine embryo fibroblast NIH-3T3 cell line (American Type Culture Collection, Manassas, VA) was used in this study. Two DNA plasmids were transfected into these cells; pGL3Basic-hsp70a1luc and a pcDNA3.1(+) vector. The pGL3Basic-hsp70a1luc consisted of a murine *Hsp70* promoter followed by the coding region of a modified firefly luciferase gene (pGL3 from Promega Corp, Madison WI). The modifications include removal of a subcellular localization sequence that directs the luciferase to the peroxisomes to create a cytoplasmic enzyme [33]. The pcDNA3.1(+) vector was a used to provide a drug selection marker, neomycin resistance gene, to enable the generation of a stable cell line. Stable transfectants were selected in 1 mg/ml Geneticin (G418, GIBCO BRL, Gaithersburg, MD). Cells were cultured and heat shocked in Dulbeccos Modified Eagle Medium (DMEM, GIBCO BRL, Gaithersburg, MD) supplemented with 10% Fetal Bovine Serum (FBS, GIBCO BRL, Gaithersburg, MD). For laser experiments the cells were plated in 96-well (i.d. = 6.4 mm) tissue culture plates (Costar, Corning Incorporated, Acton, MA) with 4 x 10^4 cells per well in 100 μl culture medium. The cells were returned to a 37 °C, 5% CO_2 incubator

(Forma Scientific, Marietta, OH) for an overnight incubation of 12 hours leading to a confluent monolayer of cells with about 1 x 10^5 cells per well. Cells were used for experiments only if they had not been passaged more than ten times in order to maintain consistency in the cell line.

3.3.2 Laser Irradiation Experiments

A schematic of the laser exposure setup is shown in Figure 3.1. Cells in 96-well tissue culture plates (in 100 μl of medium) were placed in a modified 37 °C Lab Line incubator (VWR, West Chester, PA), which allowed laser delivery to individual wells through an optical fiber inside the incubator. This modified incubator had neither humidity nor carbon dioxide control. However, the time that the cells were subject to this deprived environment was < 10 minutes and did not produce an hsp70 response higher than control cells that were kept in the incubator. A computer controlled X-Y translation stage (Semprex, Campbell, CA) was used to sequentially position each well of a 96 well plate over the optical fiber. In order to minimize crosstalk from neighboring wells, black walled (but clear bottom) tissue culture plates were used (Fisher Scientific). The high absorbance walls helped to prevent scattered and stray light from the periphery of the laser beam from entering adjacent wells. In addition this minimized crosstalk of bioluminescence during the imaging experiments. A pulsed Holmium:YAG laser (λ= 2.1 μm, τ_p = 250 μs, Schwartz Electro Optics 1-2-3, Orlando, FL) was used in all laser experiments. Laser radiation was coupled into the 600 μm low hydroxide (OH) optical fiber (NA = 0.39) using a 25 mm focal length CaF_2 lens and an SMA connector. The Ho:YAG wavelength has an optical penetration depth in water of approximately 300 μm thus allowing relatively uniform heating over the thickness of the cells (~ 10 μm). The distal end of the fiber was placed under each well, such that the

bottom of the 96 well plate was 3 cm above the tip of the fiber. Due to the divergence of light emitting from the fiber, the Gaussian radius ($1/e^2$) of the beam was determined to be 6.7 mm by translating a pinhole across the beam path. Consequently, at the edge of the well with a 3.2 mm radius, the intensity is 63 % of the initial intensity at the center of the beam spot allowing a more uniform exposure over the radius of each well (see figure 3.1). Consequently, only ~37 % of the pulse energy emitted from the fiber irradiated the surface directly beneath the cells, as determined by integrating the Gaussian profile out to 3.2 mm in radius. The wells used were separated by intervening empty rows in order to reduce collateral heat damage and crosstalk from exposure of adjacent wells. In this scenario, the lateral heat shock from adjacent wells was determined to be negligible (data not shown). Of the light aimed at the bottom of the polystyrene culture plate well 4.5% was lost due to Fresnel reflections. The refraction index mismatch between air (n = 1) and polystyrene (n=1.5) causes a 4% reflection while the index mismatch of the polystyrene to the cells/media (n=1.3) leads to a 0.5% reflection. Another 23% of light is lost due to the absorption of light in the polystyrene that makes up the bottom of the cell culture plate. Beer's law predicts the absorption of light by the polystyrene based on the thickness of the bottom of the plate (d = 0.88 mm) and the measured absorption coefficient of the plate material at the $\lambda = 2.1$ μm wavelength (μ_a =0.29 mm^{-1}). In all, only 27% of light out of the fiber was actually used to irradiate the cells. As a result of these losses, the initial energy coming out of the fiber ranged from 160 mJ/pulse to 460 mJ/pulse, however, the pulse energy reaching the cells was between 43 – 124 mJ/ pulse (total radiant exposure 4.01 J/cm^2 – 11.56 J/cm^2). The laser was set to pulse at 3 Hz for all experiments and an irradiation time of 10 seconds corresponding to 30 pulses was used in most experiments, unless otherwise stated. An external shutter (VMM-T1, Vincent Associates, Rochester, NY) located between the fiber and the laser cavity was

used to control the number of pulses delivered to each well. Following laser exposure the cells were placed back in the incubator and removed only for imaging for about 5 minutes at a time. Un-irradiated control wells are present in each plate as a negative control to compare any given sample's light expression to a basal level.

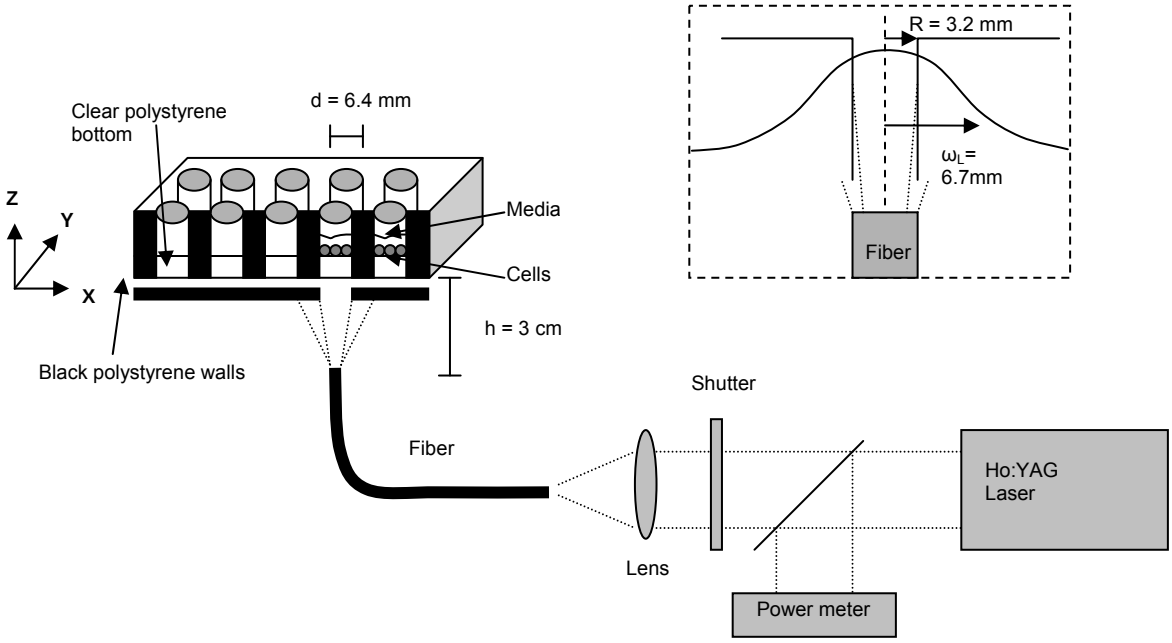

Figure 3.1 Schematic of laser experiment setup. Cells were irradiation via a fiberoptic with a Ho:YAG laser (λ = 2.1 μm, τ_p = 250 μs, 3 Hz). The beamsize at the level of the culture plate was 6.7 mm in radius. Only the center 3.2 mm radius of the beam irradiates the well thus allowing more homogenous exposure over the area of the cells.

3.3.3 Luciferase Imaging

Following heat shock, the substrate needed for the enzymatic reaction of luciferase, firefly potassium salt – i.e. D-Luciferin (4,5-Dihydro-2-[6-hydroxy-2-benzothiazolyl]-4-thiazolecarboxylic acid potassium salt ($C_{11}H_7N_2O_3S_2K$), Biosynth AG, Switzerland), was added in excess to the culture medium in a 20 μl solution of distilled, deionized water to a final concentration of 0.15 mg/ml in each well. The luciferin is taken up by the cells though the cell membrane to interact with luciferase in the cytosol. Luciferase activity was measured

at various time points following heat shock using a liquid nitrogen cooled, back thinned, back illuminated charge coupled device (CCD) camera (EEV 1300x1340, Roper Scientific, Trenton, NJ) operating at –90 ^{o}C. Photon counting images were taken for an integration time of 3 minutes and on-chip binning of 5 x 5 pixels. All images were background subtracted prior to further analysis. The light tight imaging box was at room temperature and cells were kept in an incubator at 37 ^{o}C until they were placed in the box for imaging. Room temperature luciferin was added 5 minutes prior to imaging, while the cells are still in the incubator. Bioluminescence activity starts within seconds after luciferin addition to the media. We image 5 minutes after the substrate is added which allows light emission to be at a constant level. All cells in a 96-well plate were imaged simultaneously for 3 minutes and then placed back in the incubator. Photon counts recorded by the CCD camera are analyzed by defining regions of interest for each cell sample using Metamorph software (Version 4.6r6, Universal Imaging Corporation, Downingtown, PA). The program quantifies the total integrated intensity over the region of interest (corresponding to a single well in the 96 well plate). For all exposure conditions, at least three wells were used. Untreated control wells are present for each plate to compare any given sample's light expression to a basal level. The effect of the pH indicator dye present in the media upon the generation or transmission of bioluminescence was experimentally determined not to be a factor for these experiments as pH shifts were negligible and all samples had equal concentrations of the dye.

3.3.4 Viability Assays and Normalization

In order to determine the percentage of live and dead cells remaining in a sample after irradiation, a Live/Dead cytotoxicity kit L-3224 (Molecular Probes, Eugene, OR) was utilized as an endpoint measurement roughly one hour after a plate had been imaged. As this is an endpoint experiment, the life-dead assay was performed on a plate that was treated

identical to the plate that was continuously imaged. Eight hours after laser exposure this plate was imaged for the last time at which point the cells are trypsinized and spun down into microcentrifuge tubes in groups of three. The cells are then incubated at room temperature with two fluorescent dyes, calcein (staining live cells) and ethidium homodimer (staining dead cells). Percentages of live and dead cells were determined using a flow cytometer (FACSCalibur, Becton Dickinson, Franklin Lakes, NJ). In order to calibrate the flow cytometry procedure, the samples are compared to live controls (untreated cells) and dead controls (70 % ethanol for 10 minutes). A total of 5000 cells are counted per sample in the flow cytometer. While there are on the order of about 100,000 cells per well, this small subset that is analyzed is assumed to be representative of the whole sample population, in particular since the 5,000 cells were obtained as a random sample after trypsinizing and resuspending (by pipet) of the population of cells in a well. Once the ratio of live to dead cells is determined, the photon counts from the bioluminescence experiments for each sample are normalized by dividing the photon counts by the percentage of live cells remaining in the sample at the time of flow cytometry. As a result, the light production per live cell can be compared from sample to sample.

3.3.5 ELISA Assays

In order to validate that our method of luciferase imaging is indeed representative of HSP70 production in cells, an enzyme linked immuno-sorbent assay (ELISA) kit EKS-700 was used to quantify hsp70 levels in samples (Stressgen, Victoria, BC, Canada). Cell preparation for the assay was carried out according to the kit instructions. Color development of the assay is in proportion to the amount of captured HSP70. The intensity of the color is measured in a microplate reader at 450nm (Titertek, Huntsville, AL). HSP70 concentrations from the sample are quantified by interpolating absorbance readings from a standard curve

generated with the calibrated HSP70 protein standard provided. All samples for ELISA analysis were harvested at 8 hours after irradiation since this time point showed good reproducibility of HSP70 production in previous experiments.

3.3.6 Arrhenius Water Bath Experiments

Thermal exposure in a water bath was used to assess the heat shock protein's response in relation to the Arrhenius damage integral under controlled conditions. The benefit of a water bath is that constant temperatures are more attainable than with laser irradiation, due to relatively short heating up and cooling off phases in comparison to the rather long duration of exposure at the water bath temperature. Five different constant temperature water bath experiments were performed (42 - 46^{o} C in 1 ^{o}C increments) each having eight samples at different durations of heat exposure (5, 10, 15, 20, 25, 30, 35, and 40 min) to investigate *Hsp70* response as function of time and temperature. The cells were treated by floating a 96-well cell culture plate on the water bath. Hence the cells growing at the bottom of these wells were exposed to heat but not to the water. Unheated controls were used for comparison. The plates were imaged for bioluminescence 8 hours after the water bath exposure. Photon counts from each experiment were then used as the measure of the damage parameter for the model as represented by Ω. Photon counts were normalized to the percentage of live cells by the flow cytometry assay. Conceptually, in this experiment temperature and exposure duration were the experimental variables whereas Ω is the measured quantity (represented by bioluminescence). Note that this is in contrast to many of the reported studies where temperature and exposure duration are varied to achieve a constant Ω (see for example McNally [32]). Consequently, in order to compare all samples relative to each other, photon count values of each sample were normalized to the maximum photon count found over all experiments, which was 44^{o} C for 40 minutes - this was defined for our experiments as the

arbitrary endpoint for maximum damage (i.e. Ω = 1). In turn, this normalization was taken into account in equation (1) by reformulating the linear Arrhenius integral curves by subtracting from the ln(t) values the natural log of the damage parameter for each sample:

$$\ln(t) - \ln(\Omega) = -\ln(A) + E_a / RT \tag{3}$$

Once the damage for each time/temperature combination is plotted on the ln(t) versus 1/T graph, a linear fit can be applied to the data. The slope and y-intercept were obtained and used to calculate the activation energy (E_a [J/mol]) and frequency factor (A [1/s])). These E_a and A values were averaged for all time sets to render a single activation energy and frequency factor for the whole *Hsp70* temperature-time response in cultured NIH 3T3 cells. Those samples that had more than 10% cell death, as detected by flow cytometry, were excluded from these calculations since these many cells in these samples were severely compromised leading to significant reduction in photon counts relative to the other samples.

Alternatively, the activation energies (E_a), can be determined by using a graph of the damage integral (Ω) versus time [34]. An analysis of the slopes of the curves for different constant temperature settings produced a value for the activation energy for comparison to the previous method used above. However, no natural logarithms are used in this calculation and the best fit lines are forced to intercept the x-axis at zero. The equation is

$$E_a = \frac{R \ln\left\{\frac{m_2}{m_1}\right\}}{\left[\frac{1}{T_1} - \frac{1}{T_2}\right]} \tag{4}$$

the m values represent the slopes for the curves as determined by linear best fits to the data, R = 8.314 J/mole K, T_1 = start temperature, T_2 = end temperature.

3.3.7 Arrhenius Analysis of Laser Experiments

With the water bath experiments, a constant temperature was easy to achieve. However, the pulsed laser-induced the temperature profile is very dynamic. This is discussed in more detail in the discussion. Consequently, a different method was needed to observe if the hsp70 response to laser irradiation follows the Arrhenius relationship. Since the Arrhenius relationship is an integral of temperature and time, the area under the temperature-time curve should be representative of the damage even when non-constant temperatures are used [31]. In order to test the cells' heat shock response adherence to the Arrhenius damage integral in response to laser irradiation, several sample wells were irradiated with various combinations of energies and irradiation times that were empirically determined to result in equal areas under the temperature-time profile curve. We hypothesized that the *Hsp70* response, visualized by bioluminescence emission, would be constant if the exposure temperature-time integral was constant. In order to determine temperature values during laser exposure, a wire thermocouple (Type E, Chromel/Constantin, Omega Engineering Inc, Stamford, CT) was placed in the center of the well at the level of the cells during irradiation and the temperature values were recorded at a rate of 500 Hz using a data acquisition system (Labview, National Instruments, Austin, TX). The exposure temperature-time integral 'area under the curve' was estimated from the temperature-time curves using only temperatures above 38 ^{o}C. The times, pulses, and energies used for the laser experiment were (determined empirically to give a constant area under the temperature-time curve): 10 seconds, 30 pulses, at 108 mJ/pulse (total radiant exposure: 10.2 J/cm^2); 20 seconds, 60 pulses, at 68 mJ/pulse (total radiant exposure 12.7 J/cm^2); 30 seconds, 90 pulses, at 51 mJ/pulse (total radiant exposure 14.3 J/cm^2); 40 seconds, 120 pulses, at 43 mJ/pulse (total radiant exposure 16.04 J/cm^2). All irradiations were at 3 Hz repetition rate. Photon counting images were taken at

10.5 hours after irradiation and the cell viability assays were done with the flow cytometer one hour after imaging.

3.4 Results

3.4.1 Viability Assays

Cell viability was determined at 8 hours after laser-induced heat shock by flow cytometry (Figure 3.2). The onset of cell death is at 76 mJ/pulse (7.09 J/cm^2) with a gradual, consistent rise thereafter. Within the 97 mJ/pulse (9.05 J/cm^2) energy group there was 50% viability. Live control cells, no laser treatment, were handled the same as the irradiated wells, and there was 90% viability in these wells. The cell death control was treated with ethanol 30 minutes prior to flow cytometry, and these wells showed 100% loss of viability.

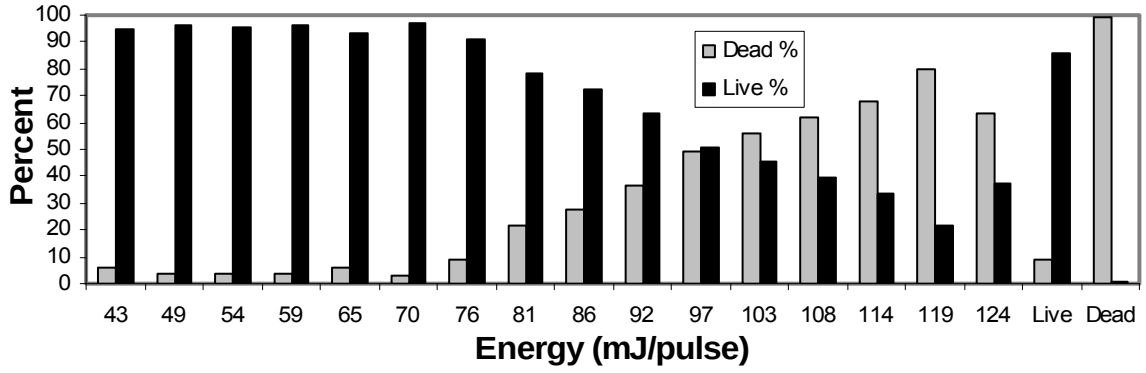

Figure 3.2 Flow cytometry viability assay of hsp-luc cells, 8 hours after exposure to Ho:YAG laser irradiation (3 Hz, 30 pulses, 10 seconds) for varying energies per pulse (43-124 mJ/p), n = 3 wells per sample, 5,000 cells/sample. Live cells detected by calcein. Dead cells detected by ethidium homodimer.

3.4.2 Normalized Photon Counts for 1, 4, 8, and 12 Hours

Figure 3.3 shows the bioluminescence values for cells that were irradiated in a 96 well plate with energies from 43 - 124 mJ/pulse at 3 Hz corresponding to 30 pulses per well (4.01 – 11.56 J/cm^2). The plate was imaged at several time points (1, 4, 8, and 12 hours) after

laser exposure and all photon counts have been normalized to the percentage of live cells (as determined by flow cytometry). The graphs show that there is a lower energy threshold of 65 mJ/p (6.06 J/cm^2) to turn on hsp70 response while there is also an upper energy threshold of 103 mJ/p (9.61 J/cm^2) where the hsp70 response drops off to negligible levels. The maximum expression is at 97 mJ/p (9.05 J/cm^2) at 8 hours. The 12 hour time has a maximum at 92 mJ/p (8.58 J/cm^2) and the 4 hour time has a maximum at 81 mJ/p (7.55 J/cm^2). The maximum induction at 97 mJ/p (9.05 J/cm^2) is 52 times greater than that of the live control.

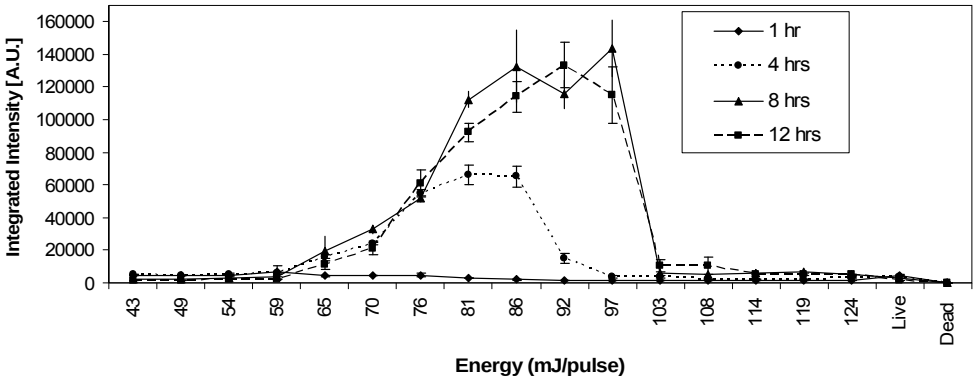

Figure 3.3 Normalized Bioluminescence emission at 1,4,8, and 12 hours acquired by CCD camera after Ho:YAG laser irradiation (3 Hz, 30 pulses, 10 seconds) of hsp-luc cells for varying energies per pulse (43-124 mJ/p). Error bars represent standard deviation of the three wells irradiated per sample. Photon counts were normalized to the percentage of live cells (as determined from Figure 3.2).

3.4.3 Validation with ELISA Assay

After luminescence imaging, samples in which bioluminescence was observed (i.e. pulse energies of 65 – 124 mJ/p), were harvested for ELISA assay eight hours post irradiation. Another, equally irradiated plate was used for flow cytometry to normalize the photon counts. Figure 3.4 shows the correlation between the normalized photon counts and actual hsp70 protein concentrations determined by the ELISA assay. The resulting correlation

coefficient of r^2 = 0.9893 demonstrates that photon counts are directly related to hsp70 protein quantities.

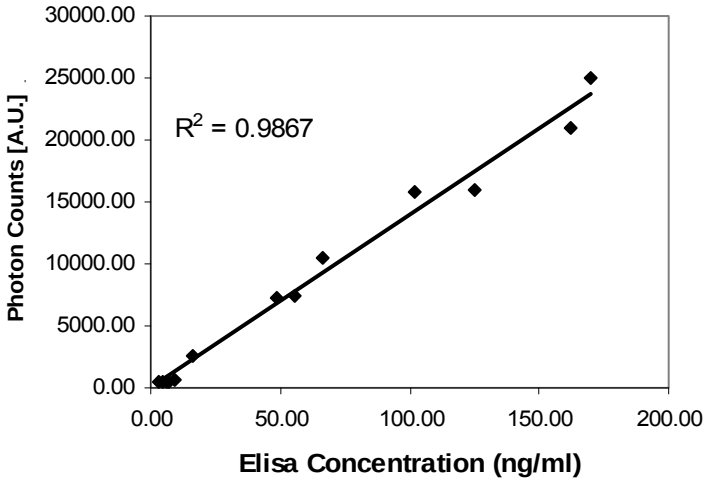

Figure 3.4 Correlation between ELISA protein values and unnormalized photon counts of Ho:YAG laser irradiated hsp-luc cells. Ho:YAG laser irradiation (3 Hz, 30 pulses, 10 seconds) of hsp-luc cells for varying energies per pulse (65-124 mJ/pulse).

3.4.4 Constant Temperature Water Bath

Figure 3.5 shows the hsp70 response to constant temperatures. At the 42^o temperature there is no significant heat shock response even after 40 minutes exposure. For the higher temperatures a rising *HSP70* production trend is seen until an upper threshold is reached where the cells can no longer produce *HSP70*. For each temperature, there are sections that show a linear increase in hsp70 production with increasing exposure time, as would be expected from the Arrhenius integral.

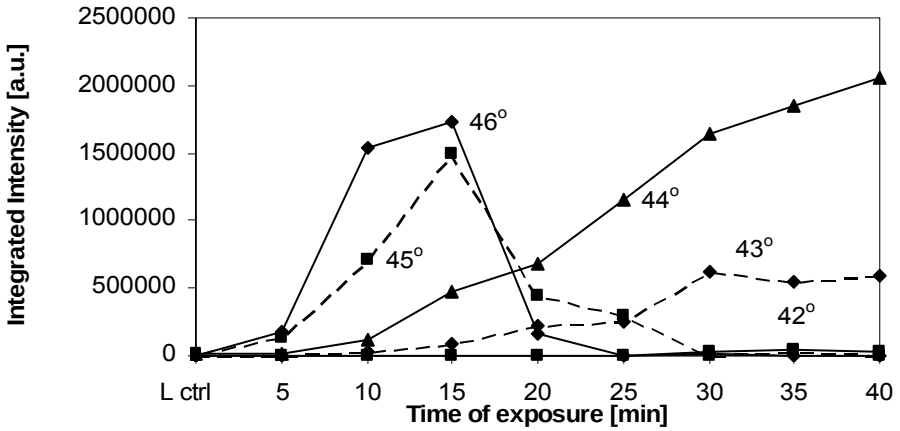

Figure 3.5 Photon counts at 8 hrs after constant temperature water bath experiments for hsp-luc cells at various temperatures (42-46 ^{o}C) and exposure times (5-40 min). Six samples were taken for each data point and normalized to the percentage of live cells by flow cytometry.

3.4.5 Linear Arrhenius Curves and Predicted Damage Values

In Figure 3.6, the data from Figure 3.5 is plotted on an ln(t)-ln(Omega) vs. 1/T scale. Data points from each of the various times (5, 10, 15, 20, 25, 30, 35, and 40 min) at a given temperature (42, 43, 44, 45, and 46^{o}C) are averaged. The error bars represent the standard deviation of the averages for each temperature. A linear best-fit line is fitted through the five averaged temperature data points. From the best fit line, a slope and y-intercept are derived to calculate the activation energy (E_a) = 1.74 E+06 [J/mol], and frequency factor (A) = 7.0 E+282 [1/s] for the system as a whole over the temperature and time ranges studied.

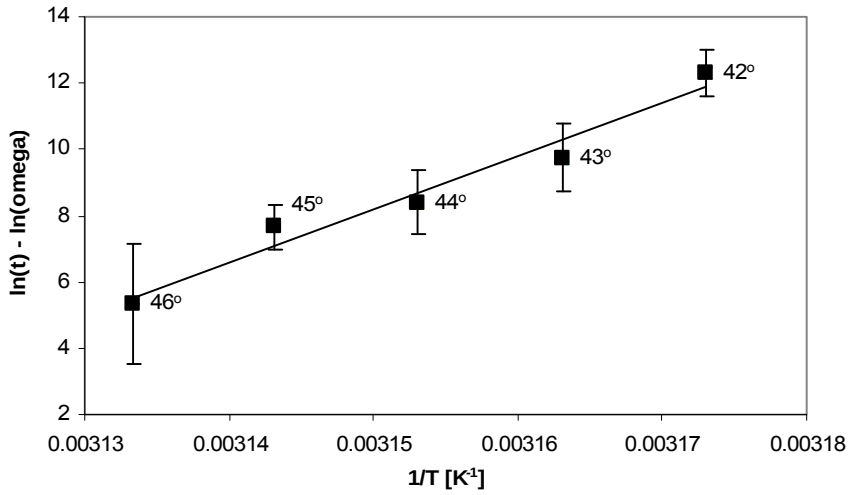

Figure 3.6 Arrhenius plot for constant temperature water bath experiments. Photon counts are plotted for hsp-luc cells. The error bars represent the standard deviation of the averages for each temperature. Six samples were taken for each data point and normalized to the percentage of live cells by flow cytometry.

The slopes of the best-fit lines in Figure 3.7 are used to calculate an E_a value from empirical data. From the ratios of slopes the value for the activation energy was found to be: E_a = 1.06 E+06 [J/mol]. This value is on the same order of magnitude as determined in Figure 3.6. The R^2 values were 0.79, 0.84, 0.91, 0.81, and 0.60 for 46, 45, 44, 43, and 42^o C, respectively.

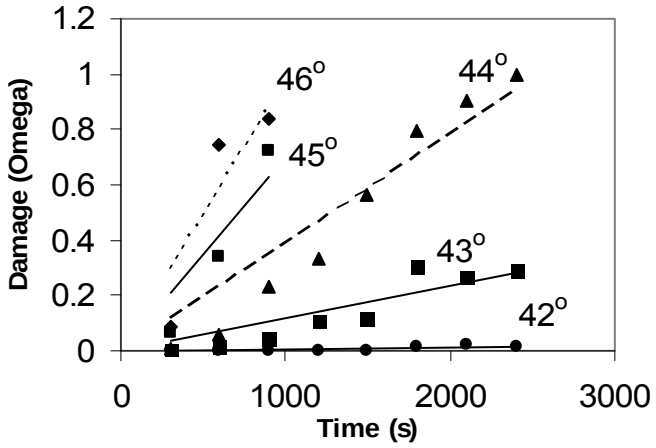

Figure 3.7 Damage parameter (Ω) as function of exposure time for various constant temperature. Note that the maximum hsp70 expression (highest photon counts) was found in the cells exposed to 44 °C for 40 min which was chosen to represent maximum damage (Ω = 1). All other photon count values (and hence damage values) were used relative to this sample. Six samples were taken for each data point. Six samples were taken for each data point and normalized to the percentage of live cells by flow cytometry.

3.4.6 Area Measurements

Figure 3.8 shows the bioluminescence emission from the laser-exposed samples that were irradiated with different energies for different times but in which the integrals of the temperature-time curves for each were kept constant. The temperatures measured represent average, bulk temperature in the well and not the transient maximum temperatures associated with each of the 30 laser pulses. As can be seen, the *Hsp70* responses for the 10, 20, and 30 second exposure times are not statistically significantly different ($p<0.05$). The cells from the 40 second exposure group do not follow this trend. Flow cytometry determined that nearly all cells in this group were dead.

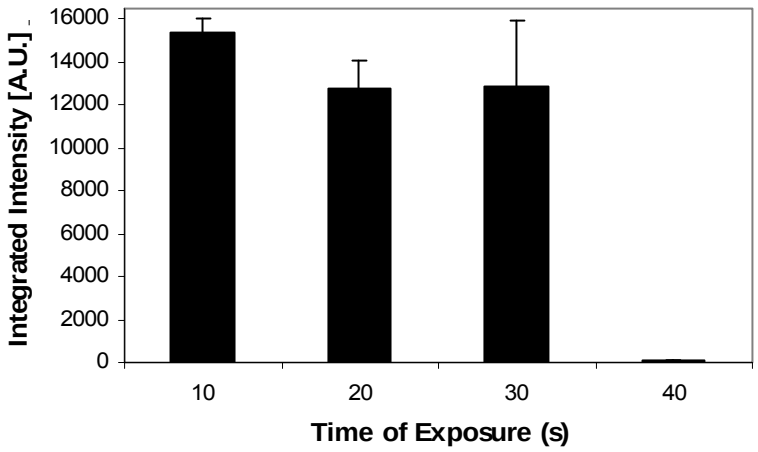

Figure 3.8 Normalized photon counts for area under curve experiment at 10.5 hours after Ho:YAG irradiation in hsp-luc cells. 10 seconds, 30 pulses, at 108 mJ/pulse (total radiant exposure: 10.2 J/cm^2); 20 seconds, 60 pulses, at 68 mJ/pulse (total radiant exposure 12.7 J/cm^2); 30 seconds, 90 pulses, at 51 mJ/pulse (total radiant exposure 14.3 J/cm^2); 40 seconds, 120 pulses, at 43 mJ/pulse (total radiant exposure 16.04 J/cm^2). All irradiations were at 3 Hz repetition rate. Error bars represent standard deviation of the three wells irradiated per sample. Photon counts were normalized to the percentage of live cells by flow cytometry.

3.5 Discussion

In this study we have shown that a stable cell line with the hsp70a1-luc construct was able to provide an effective and convenient method to non-invasively quantify *Hsp70* transcription as function of time after moderate temperature heat shock. Moderate temperature induced damage phenomena in tissue have been difficult to examine with conventional methods of detection such as light microscopy [2]. However, monitoring of transcription using a genetic engineering approach has provided a method sensitive enough to detect the subtle biochemical changes in cells in a rather non-invasive way.

3.5.1 Characterization of *Hsp70* Response

The first aim of this research was to define the *Hsp70* response in the cells. From literature and previous studies, we expected the *Hsp70* response to behave as many other proteins do in that it would be up-regulated after an initial stimulus and then decline after the

signal from the stimulus had stopped in a classic feedback inhibition manner. The presence of denatured proteins (a product of thermal stress) within the cell acts as a stimulus for the transcription of hsp70 [12]. Of the three heat shock transcription factors (HSF) that drive the signaling for hsp70, only HSF1 is stress activated and is not implicated in constitutive activation of hsp70 [17]. Most HSF1 resides in clusters called stress granules and in a complex with hsp70 protein until a driving factor such as heat is applied. HSP70 is then recruited to repair the newly denatured proteins. This frees the HSF1 molecules to translocate to the nucleus, whereupon they join as trimers and bind to the DNA sections known as heat shock elements (HSE) [6, 17]. Once bound to the HSE, they can initiate hsp transcription when activated through phosphorylation [35]. Newly synthesized hsp then binds to free HSF1 as a feedback inhibition signal to prevent the overproduction of HSP70.

When the content of HSP70 protein has exceeded that necessary to repair the damage, the extra hsp70 can bind the transcription factor, HSF1, which then down-regulates HSP70 production. Figure 3.4 shows that there is an increase of hsp70 transcription in response to laser irradiation beginning at an energy of 65 mJ/pulse (6.06 J/cm^2). When the thermocouple temperatures were recorded for this energy, the temperature rise at the end of the 10 s exposure time (30 pulses at 3 Hz) was 8 ^{o}C. This change corresponds to a temperature in the well of 43 ^{o}C over the initial temperature of 35 ^{o}C. This increase is in general agreement with previous literature where heat shock with mild temperatures (39 - 43 ^{o}C) was used to activate the heat shock response [17]. However, the dynamics of the temperature over time for 30 consecutive laser pulses is complicated. First, each individual laser pulse will cause an impulse response temperature increase. For example, a 65 mJ laser pulse (0.202 J/cm^2/p) at the level of the cells (z=0) will cause an instantaneous temperature rise of ~ 1.5 ^{o}C at the level of the cells assuming an absorption coefficient μ_a = 30 cm^{-1}. Prior to the next pulse,

roughly 333 ms later, most of this heat will have diffused to the overlying media since the thermal relaxation time constant of the system is approximately 185 ms. In the remainder of this discussion we will neglect the transient temperature rise and instead focus on the 'baseline temperature', i.e. the cumulative temperature of the media / cells prior to the next laser pulse. This is justified by the fact that the laser pulse induced temperature transients (< 3 ^{o}C per pulse increase at z=0 for the highest pulse energy used) are too short to have a significant effect on thermal damage. We confirmed this experimentally by exposing cells to the same laser parameters but by changing the volume of the media overlying the cells. In this experiment (data not shown) the cells growing on the bottom of the culture well were exposed to the same transient temperature increase but the baseline temperature rise was lower due to the larger volume of media. It was found that hsp70 expression scaled with the baseline temperature. Since each culture well can be reasonably approximated as an insulated system owing to the low thermal conductivity of polystyrene and surrounding air, the baseline temperature of the volume in the well is expected to rise for the 10 s over which the laser pulses are deposited, then fall after the laser is turned off.

In addition to the low energy threshold whereupon the heat shock response is activated, a high energy threshold where the heat shock response is no longer active is seen at 103 mJ/pulse (9.61 J/cm^2). The corresponding measured maximum temperature was 53.9 ^{o}C at the level of the cells (i.e. a baseline temperature rise at the bottom of the well of 18.9 ^{o}C). The latter threshold is most likely due to excessive cellular damage that destroyed the machinery in cells necessary to produce proteins. The production of protein, including hsp70 and luciferase, is dependent on ribosomes and other intracellular structures which can, themselves, be denatured by the heat stress. The viability assays support this (Figure 3.2) as it can be seen that greater than 60% of cells are dead at this point, which is indicative of serious and non-reversible destruction of cellular function, whether through apoptotic or necrotic

pathways. Although the remaining 40% of cells might still be alive, they are so badly damaged that they cannot produce hsp70 as our ELISA assays have shown. One alternative explanation for the lack of luminescence in these cells could be due to compromised mitochondria which would leave the cells without ATP to carry out the reaction. However, O'Connell – Rodwell, et. al. have shown that there still remains a significant level of ATP in these highly compromised cells [23]. The *Hsp70* response to cellular damage is a transient one provided the damage does not lead to cell death. This transient nature is in part due to the fact that some of the damage is reversible, as noted by Thomsen [2]. The pulse energies associated with moderate temperature increases (65 and 70 mJ/p in Figure 3.3) show that the *Hsp70* response increases between 4 and 8 hours after laser exposure but then decreases at 12 hours. The rising and falling trend is indicative of the *Hsp70* having repaired the denatured proteins and the cells no longer needing such quantities of the protein and thus *Hsp70* transcription is down-regulated. It is important to note the low levels of *Hsp70* transcription at one hour. At this time point, there has not been sufficient time for the *Hsp70* gene promoter to receive the signal to activate transcription from HSF1, transcribe the luciferase gene to mRNA, and then translate the functional protein. The delay in response to stimulus is seen at all energies. The earliest sign of *Hsp70* response has first been seen at about two to three hours post heat shock (data not shown). These onset times are consistent with data from Amici, et. al. where mRNA levels of HSP70 were upregulated as early as 90 minutes [14].

The additional delay in transcription of *Hsp70* for high energies is also an important feature of the response. For example, while exposure to relatively low energies (81 mJ/p or 7.55 J/cm^2) results in the maximum *Hsp70* expression at 4 hours, the peak hsp70 expression for higher energies (97 mJ/p or 9.05 J/cm^2) occurs between 8-12 hours after laser exposure. This indicates that at higher energies the cells are so severely compromised that even the

machinery necessary to make the thermally protective protein (hsp70) cannot be readily transcribed at the shorter times. The 92 mJ/p (8.58 J/cm^2) energy shows this well because its 4 hour HSP70 levels are very low and it doesn't start making significant HSP70 until 8 and 12 hours (see Figure 3.3). The fact that the highest hsp70 expression occurs at the energy (97 mJ/p or 9.05 J/cm^2) just below threshold for cell death indicates that the cell has not been able to repair the denatured proteins for this high energy. As a result, the 'on' switch for *Hsp70* transcription is still very high even at laser irradiations that are very damaging to the cells.

3.5.2 Validation of Photon Counts

To quantify the *Hsp70* response, photon counts were normalized to the fraction of cells still alive at a given time point. Cell death represents an extent of cellular damage that no longer offers quantitative information as far as *Hsp70* transcription is concerned. Hence, this normalization allows us to view the intensity of photon counts on a per cell basis for the remaining, living cells. The viability assay shown in Figure 3.2 indicates that at 8 hours post laser exposure nearly 50% of the cells in the 97 mJ/p energy group (9.05 J/cm^2) had died. Below 76 mJ/p (7.09 J/cm^2), there seems to be no lethal cell injury due to irradiation indicated by the fact that the fraction of dead cells is similar to our unexposed controls. Notably, the bioluminescence data in Figure 3.3 shows a lower onset of damage as indicated by *Hsp70* expression (65 mJ/p or 6.06 J/cm^2)). This difference in thresholds for *Hsp70* expression and cell death is intuitive as one would expect for the heat shock response to be activated at exposure levels below those that can cause irreversible damage.

After the initial onset of cell death at 76 mJ/p (7.09 J/cm^2), the viability assay (Figure 3.2) shows an increase in the cell death rate as delivered energy is increased. This trend, however, is not seen in the photon counting graphs. As Figure 3.3 shows, the *Hsp70* response

drops off sharply at 103 mJ/p (9.61 J/cm^2) even though the viability assays show that there are still ~ 45% of live cells present. Hence, the cell viability of irradiated cells does not correlate directly to amount of HSP70 production. We hypothesize that this discrepancy is due to the fact that although these heavily damage cells are still alive at the time of the viability assay, they are so seriously damaged that they are unable to perform protein synthesis, including the synthesis of hsp70. This could also signify that the cells have initiated apoptosis and are destined to die, thereby shutting down new protein synthesis. It is interesting to note that HSP70 not only directly prevents cell death by rescuing denatured proteins but also indirectly blocks cell death by preventing apoptosis signaling [36]. One of the ways in which it does this is by inhibiting the activation of the *SAPK/JNK* pathway that begins an apoptosis signaling cascade [22]. Furthermore, hsp70 has been shown to block *BAX*, a pro-apoptotic molecule, translocation from the mitochondria [22]. Consequently, high levels of HSP70 may actually delay the process of cell death

In order to validate our model of using bioluminescence to quantitatively assess hsp70 transcription, we correlated our bioluminescence data to ELISA assays. The primary purpose of the ELISA experiments was to validate the bioluminescence imaging method as a metric of HSP70 production by correlating photon counts to actual HSP70 production. In addition, the ELISA assay provides some insight in the absolute amounts of HSP70 protein in the cells after irradiation. Figure 3.4 shows the correlation between photon counts and the HSP70 protein concentrations determined using ELISA. A linear fit results in an r^2-value = 0.9867. This signifies that our method which detects *Hsp70* transcription is directly proportional to actual HSP70 protein production.

We conclude that the method of bioluminescence imaging or our genetically engineered cells provides an accurate measure for the production of HSP70 in response to laser-induced heat damage. Moreover this method allows for multiple time points

measurements from the same sample. The ability to examine responses at different times is crucial when there are time variations in the response of the cells. This is a major advantage of the bioluminescence method.

3.5.3 Arrhenius Relationship

The Arrhenius relationship predicts that tissue injury is linearly proportional to time of exposure for a given constant temperature [30]. Several studies have confirmed this relationship in the context of laser-induced heating of tissue. Interestingly, two important questions remain open to date. First, it is unknown to what extent the Arrhenius formulation will hold for very short heating times (less than 1 s) and secondly, the Arrhenius formulation at its core assumes a biophysical process, typically of protein denaturation. The ensuing biological response of gene regulation and cellular signaling to these biophysical damage processes is poorly understood and it is not known if and to what extent the Arrhenius formulation can be applied to the genetic and signaling response. The two primary goals of this study were 1) to determine if hsp70 expression can be used as a sensitive and representative marker for cellular damage in living cells and 2) to determine if and to what extent the hsp70 expression follows the Arrhenius relationship. Figure 3.5 shows that for constant temperature exposures there are portions of each graph that show linear increases in hsp70 response with increasing exposure time. Consequently, the linear relationship between time of exposure and damage predicted by the Arrhenius relationship holds at least over the small temperature range used in this experiment. Thomsen et al. [2] indicated that the lowest threshold for (reversible) thermal damage even for long exposure times is 43 ^{o}C. Our data confirms this as exposure to 42 ^{o}C even for 40 minutes does not induce measurable levels of HSP70 where as for 43 ^{o}C, after 40 minutes hsp70 production has increased by 15-fold.

From these graphs, linear best-fit lines yielded an activation energy (E_a) and frequency factor (A) as the values that describe the Arrhenius behavior of the system. The resulting activation energy and frequency factor are E_a = 1.74 E+06 J/mol A = 7.0 E+282 1/s, respectively. An alternative analysis of the water bath data, described by Welch is shown in Figure 3.7 [34]. The resulting activation energy from this method (1.74 E+6 J/mol) corresponded reasonably well to the values obtained from the fit in Figure 3.6 (1.06 E+6 J/mol). In comparison, McNally, et al. found for the denaturation of liquid protein solders made of albumin, E_a = 3.8 E+05 J/mol and A = 3.2 E+56 1/s [32]. When comparing our data to these published values for these two parameters, it is clear that while the activation energy values are on the same order of magnitude, the frequency factors are dramatically different. However, the processes that are being modeled are fundamentally different. McNally analyzed structural denaturation of proteins (a direct biophysical phenomenon) using visible whitening (increased scattering) as an endpoint for damage. In contrast, we are investigating effects on the biological and physiological level by tracking cell signaling for *Hsp70* expression by monitoring gene transcription in cell culture in response to thermal damage. It is important to recognize that the A and E values for each chosen thermal damage endpoint are unique to that particular endpoint. Therefore, A and E values for tissue whitening, tissue birefringence loss, skin reddening, *Hsp70* expression, etc. are expected to be different because they are different phenomena produced by different mechanisms with different dynamics. Cell signaling is also a much more sensitive phenomenon to temperature changes than tissue whitening; moreover, the transcription of *Hsp70* in response to cellular stress is subject to a variety of complex enhancing and inhibiting pathways causing presumably significant but unpredictable signal gain. We hypothesize that this latter phenomena of biological gain is responsible for the dramatic difference in frequency factor. Nevertheless,

our data shows that within a relatively narrow window between a lower threshold of *Hsp70* induction and an upper threshold for cell death, the Arrhenius relationship appears to hold.

The experiments in which we exposed the cells to varying laser parameters, keeping the area under the temperature-time curve constant confirmed that the resulting HSP70 production is indeed constant provided the cells do not die. This is shown in Figure 3.8 which shows no statistically significant difference ($p<0.05$) between the first three samples. The last sample (40 s exposure) had no living cells left as indicated by the viability assay. Again, this suggests that within a narrow window between the lower threshold for *Hsp70* induction and an upper threshold for cell death, the expression of *Hsp70* in response to laser-induced thermal damage does follow the Arrhenius relationship.

3.5.4 Clinical Implications

The HSP family has been researched for its role in a vast array of pathways and responses. The HSP proteins are thought to be involved in response to conditions such as inflammation, cancer, atherosclerosis, and amyloid diseases such as Alzheimer's [7]. HSP70 was examined for its part in impaired inflammatory wound healing response of diabetic mice [9]. The *Hsp70* response was delayed in cutaneous wounds of diabetic mice when compared to nondiabetic controls and was correlated to a delay in wound healing. Also, *Hsp70* upregulation was noted with accelerated wound healing in laser assisted skin closure by means of a 815 nm diode laser [11]. *Hsp70* upregulation after 810 nm diode laser irradiation was observed in the chorioretinal layers of the rabbit eye for transpupillary thermotherapy to treat small choroidal melanomas [10]. The subthreshold doses of the infrared light did not affect tissue architecture but were able to upregulate *Hsp70*.

Hsp70 expression in response to laser-irradiation of biological tissue is of potential importance. As shown in this study, it is one of the most sensitive markers of thermal

alteration of living cells. Therapeutically, *Hsp70* expression may be used as marker for (collateral) thermal damage, it may affect wound healing, angiogenesis, apoptosis and other cellular pathways involved in the normal physiological and pathological processes. Several clinical procedures can be expected to have significant contributions of *Hsp70* expression (interstitial hyperthermia) or are relying primarily on the expression of hsp70 for its therapeutic effect. For example, in transpupillary thermotherapy (TTT) direct laser heating of small selected choroidal melanomas, alone or in conjunction with radiotherapy has been used for several years [37, 38]. Recently, this therapeutic procedure has been evaluated for the treatment of subfoveal occult choroidal neovessels of age-related macular degeneration (AMD) in pilot studies [39-41]. In this context hsp production has been suggested to play a role in the decreased exudation from the choroidal neovessels [42]. It has been hypothesized that synthesis and overexpression of HSP70 as a cell-protective agent may drive damaged cells to preferentially die via apoptotic rather than necrotic pathways thus limiting inflammation, release of cytokines and potentially resulting in more rapid healing with a superior cosmetic result [11, 43]. Typically, these approaches use relatively long exposures (> 1 min) at low power levels. An approach for reducing the exposure times (but maintaining the same biological effect by increasing power levels - i.e. temperatures) would be advantageous in a clinical setting [10]. Our data suggests that laser dosimetry for procedures relying on hsp70 induction may be based on the Arrhenius integral provided the threshold for inducing cell death is not exceeded.

3.6 Conclusions

We have shown a novel method of assessing in a non-invasive fashion, moderate levels of thermal damage as indicated by the expression of *Hsp70* using a bioluminescent reporter gene. Bioluminescence was shown to correlate with HSP70 protein levels. Our data

in water bath experiments shows that within a relatively narrow window between a lower threshold of *Hsp70* induction and an upper threshold for cell death, the Arrhenius relationship appears to hold true for these cells. Activation energy values were in general agreement with published values while frequency factor values were much higher, presumably due to various biological amplification processes leading to the detected bioluminescence. Irradiation for a fixed duration with a pulsed Ho:YAG laser showed a lower threshold for *Hsp70* induction and an upper threshold leading to cell death. Notably, higher exposures below the threshold for cell death caused a delay in *Hsp70* upregulation which moved the peak of expression from 2-4 hours to 8-12 hours. Within a limited range the laser-exposed cell damage as indicated by *Hsp70* induction was shown to follow the Arrhenius relationship. In conclusion, our data suggests that laser dosimetry aimed at avoiding collateral thermal damage or for procedures relying on *Hsp70* induction may be based on the Arrhenius integral provided the threshold for inducing cell death is not exceeded.

3.7 Acknowledgements

This work was supported a Whitaker Foundation Research Grant, Whitaker Foundation Special Opportunity Award, The Vanderbilt In Vivo Imaging Center (VIVID) NIH P20 CA86283, and AFOSR award No. F49620-01-1-0429.

3.8 References

1. Welch, A.J., et al., *Laser thermal ablation.* Photochem Photobiol, 1991. **53**(6): p. 815-23.
2. Thomsen, S., *Pathologic Analysis of Photothermal and Photomechanical Effects of Laser-Tissue Interactions.* Photochemsitry and Photobiology, 1990. **53**(6): p. 825-835.

3. Thomsen, S.L., *Identification of lethal thermal injury at the time of photothermal treatment*, in *Laser-Induced Interstitial Thermotherapy*, G.J. Mueller and A. Roggan, Editors. 1995, SPIE Publishers: Bellingham, WA. p. 459-467.
4. Thomsen, S.L. *Mapping of thermal injury in biologic tissues using quantitative pathologic techniques*. in *Thermal Treatment of Tissue with Image Guidance*. 1999: SPIE.
5. Thomsen, S.L. *Qualitative and quantitative pathology of clinically relevant thermal lesions*. in *Matching the Energy Source to the Clinical Need*. 1999: SPIE.
6. Kiang, J.G. and G.C. Tsokos, *Heat shock protein 70 kDa: molecular biology, biochemistry, and physiology.* Pharmacol Ther, 1998. **80**(2): p. 183-201.
7. Pockley, A.G., *Heat shock proteins, inflammation, and cardiovascular disease.* Circulation, 2002. **105**(8): p. 1012-7.
8. Morimoto, R.I., P.E. Kroeger, and J.J. Cotto, *The transcriptional regulation of heat shock genes: a plethora of heat shock factors and regulatory conditions.* Stress Inducible Cellular Responses, 1996. **77**: p. 139-63.
9. McMurtry, A.L., et al., *Expression of HSP70 in healing wounds of diabetic and nondiabetic mice.* J Surg Res, 1999. **86**(1): p. 36-41.
10. Desmettre, T., C.A. Maurage, and S. Mordon, *Heat shock protein hyperexpression on chorioretinal layers after transpupillary thermotherapy.* Invest Ophthalmol Vis Sci, 2001. **42**(12): p. 2976-80.
11. Capon, A., et al., *Laser assisted skin closure (LASC) by using a 815-nm diode-laser system accelerates and improves wound healing.* Lasers Surg Med, 2001. **28**(2): p. 168-75.
12. Frydman, J., *Folding of newly translated proteins in vivo: the role of molecular chaperones.* Annu Rev Biochem, 2001. **70**: p. 603-47.
13. Morimoto, R.I., P.E. Kroeger, and J.J. Cotto, *The transcriptional regulation of heat shock genes: a plethora of heat shock factors and regulatory conditions.* Exs, 1996. **77**: p. 139-63.
14. Amici, C., et al., *Antiproliferative prostaglandins activate heat shock transcription factor.* Proc Natl Acad Sci U S A, 1992. **89**(14): p. 6227-31.
15. Schett, G., et al., *Enhanced expression of heat shock protein 70 (hsp70) and heat shock factor 1 (HSF1) activation in rheumatoid arthritis synovial tissue. Differential regulation of hsp70 expression and hsf1 activation in synovial fibroblasts by proinflammatory cytokines, shear stress, and antiinflammatory drugs.* J Clin Invest, 1998. **102**(2): p. 302-11.
16. Salminen, W.F., Jr., R. Voellmy, and S.M. Roberts, *Protection against hepatotoxicity by a single dose of amphetamine: the potential role of heat shock protein induction.* Toxicol Appl Pharmacol, 1997. **147**(2): p. 247-58.
17. Huang, L., N.F. Mivechi, and D. Moskophidis, *Insights into regulation and function of the major stress-induced hsp70 molecular chaperone in vivo: analysis of mice with targeted gene disruption of the hsp70.1 or hsp70.3 gene.* Mol Cell Biol, 2001. **21**(24): p. 8575-91.
18. Basu, S., et al., *Necrotic but not apoptotic cell death releases heat shock proteins, which deliver a partial maturation signal to dendritic cells and activate the NF-kappa B pathway.* Int Immunol, 2000. **12**(11): p. 1539-46.
19. Samali, A. and T.G. Cotter, *Heat shock proteins increase resistance to apoptosis.* Exp Cell Res, 1996. **223**(1): p. 163-70.

20. Zhang, Y., et al., *Targeted disruption of hsf1 leads to lack of thermotolerance and defines tissue-specific regulation for stress-inducible Hsp molecular chaperones.* J Cell Biochem, 2002. **86**(2): p. 376-93.
21. Samali, A. and S. Orrhenius, *Heat shock proteins: regulators of stress response and apoptosis.* Cell Stress Chaperones, 1998. **3**: p. 228-236.
22. Mosser, D.D., et al., *Role of the human heat shock protein hsp70 in protection against stress-induced apoptosis.* Mol Cell Biol, 1997. **17**(9): p. 5317-27.
23. OConnell Rodwell, C.E., *A genetic reporter of thermal stress defines physiologic zones over a defined temperature range.* FASEB Journal, 2003(In press).
24. Beckham, J.T., et al. *Bioluminescence imaging as a marker for cellular Hsp70 response to thermal laser injury*. in *SPIE Laser-Tissue Interaction XIV*. 2003. San Jose, CA.
25. Gould, S.J. and S. Subramani, *Firefly luciferase as a tool in molecular and cell biology.* Anal Biochem, 1988. **175**(1): p. 5-13.
26. Hastings, J.W., *Chemistries and colors of bioluminescent reactions: a review.* Gene, 1996. **173**(1): p. 5-11.
27. Rice, B.W., M.D. Cable, and M.B. Nelson, *In vivo imaging of light-emitting probes.* J Biomed Opt, 2001. **6**(4): p. 432-40.
28. Nguyen, V.T., M. Morange, and O. Bensaude, *Firefly luciferase luminescence assays using scintillation counters for quantitation in transfected mammalian cells.* Anal Biochem, 1988. **171**(2): p. 404-8.
29. Brasier, A.R., J.E. Tate, and J.F. Habener, *Optimized use of the firefly luciferase assay as a reporter gene in mammalian cell lines.* Biotechniques, 1989. **7**(10): p. 1116-22.
30. Moritz, A. and F. Henriques, *Studies of thermal injury in the conduction of heat to and through skin and the temperatures attained therein.* Am. J. Pathol., 1947. **23**: p. 531-549.
31. Welch, A.J. and M.J.C.v. Gemert, *Optical-thermal response of laser-irradiated tissue.* Lasers, photonics, and electro-optics, 1995: p. 561-603.
32. McNally, K., *Optical and thermal characterization of albumin protein solders.* Applied Optics, 1999. **38**(31): p. 6661-6672.
33. Wood, K. *The Chemistry of Bioluminescent Reporter Assays*. 1998 [cited; Available from: http://www.promega.com/pnotes/65/6921_14/default.html.
34. Welch, A.J. and M.J.C.v. Gemert, *Optical-thermal response of laser-irradiated tissue*. Lasers, photonics, and electro-optics. 1995, New York: Plenum Press. xxvi, 925.
35. Kim, D., H. Ouyang, and G.C. Li, *Heat shock protein hsp70 accelerates the recovery of heat-shocked mammalian cells through its modulation of heat shock transcription factor HSF1.* Proc Natl Acad Sci U S A, 1995. **92**(6): p. 2126-30.
36. Garrido, C., et al., *Heat shock proteins: endogenous modulators of apoptotic cell death.* Biochem Biophys Res Commun, 2001. **286**(3): p. 433-42.
37. Shields, C. and J. Shields, *Transpupillary thermotherapy for choroidal melanoma.* Curr Opin Ophthalmol, 1999. **10**: p. 197-203.
38. Overgaard, J. and M. Overgaard, *Hyperthermia as an adjuvant to radiotherapy in the treatment of malignant melanoma.* Int J Hyperthermia, 1987. **3**(6): p. 483-501.
39. Petrone, S., et al., *Transpupillary thermotherapy for subfoveal choroidal neovascularization in age-related macular degeneration.* Invest Ophthalmol Vis Sci, 2000. **41**((4),S320Abstract nr 1689).

40. Ip, M., A. Kroll, and E. Reichel, *Transpupillary thermotherapy.* Semin Ophthalmol, 1999. **14**(1): p. 11-8.
41. Reichel, E., et al., *Transpupillary thermotherapy of occult subfoveal choroidal neovascularization in patients with age-related macular degeneration.* Ophthalmology, 1999. **106**(10): p. 1908-14.
42. Mainster, M.A. and E. Reichel, *Transpupillary thermotherapy for age-related macular degeneration: long-pulse photocoagulation, apoptosis, and heat shock proteins.* Ophthalmic Surg Lasers, 2000. **31**(5): p. 359-73.
43. Souil, E., et al., *Treatment with 815-nm diode laser induces long-lasting expression of 72-kDa heat shock protein in normal rat skin.* Br J Dermatol, 2001. **144**(2): p. 260-6.

CHAPTER IV

ROLE OF HSP70 IN CELLULAR THERMOTOLERANCE

Josh T. Beckham[1], Gerald J. Wilmink[1], Mark A. Mackanos[3], Keiko Takahashi[2], Chris H. Contag[3], Takamune Takahashi[2], E. Duco Jansen[1]

[1] Department of Biomedical Engineering, Vanderbilt University, Nashville, TN
[2] Department of Medicine, Vanderbilt University, Nashville, TN
[3] Departments of Pediatrics, Radiology and Microbiology & Immunology, Stanford University, Stanford, CA

Vanderbilt University
Nashville, TN 37235

Portions of this manuscript have been submitted for publication to:
American Society for Lasers In Medicine and Surgery (ASLMS)

4.1 Abstract

Background and Objective: Thermal pretreatment has been shown to condition tissue to a more severe secondary heat stress. In this research we examined the particular contribution of heat shock protein 70 (HSP70) in thermal preconditioning.

Study Design/Materials and Methods: For optimization of preshock exposures, a bioluminescent *Hsp70*-luciferase reporter system in NIH3T3 cells tracked the activation of the *Hsp70* gene. Cells in 96 well plates were pretreated in a 43^{o} C water bath for 30 min, followed 4 hrs later with a severe heat shock at 45^{o} C for 50 min. Bioluminescence was measured at 2, 4, 6, 8, and 10 hrs after preshock only (PS) and at 4 hours after preshock with heatshock (PS+HS). Viability was assessed 48 hrs later with a fluorescent viability dye. Preshock induced thermotolerance was then evaluated in hsp70-containing Murine Embryo Fibroblast (+/+) cells and hsp70-deficient MEF cells (-/-) through an Arrhenius damage model across varying temperatures (44.5 - 46^{o} C).

Results: A time gap of 4 hours between preconditioning and the thermal insult was shown to be the most effective for thermotolerance with statistical confidence of $p<0.05$. The benefit of preshocking was largely abrogated in *Hsp70*-deficient cells. The Arrhenius data showed that preshocking leads to increases in the activation energies, E_a, and increases in frequency factors, A. The frequency factor increase was significantly greater in *Hsp70*-deficient cells.

Conclusion: The data shows that HSP70 contributes significantly to cellular thermotolerance but there are other pathways that provide residual thermotolerance in cells deficient in *Hsp70*.

4.2 Introduction

Cells have the ability to resist thermal stress when they have been exposed to a prior, sublethal exposure. This has been referred to as 'induction of thermotolerance' or 'thermal preconditioning' [1-5]. Most often the temperature of mild pretreatment lies within the range of 42-45^{o} C and induces reversible damage which involves a denaturation of labile proteins, acceleration of metabolism through the mitochondria and activation of anti-apoptotic pathways [6, 7]. Alternativley, shorter duration, higher temperature protocols have been used to achive thermal preconditioning [2, 8, 9] . Potentially, the ability to affect these biological responses to heat may lead to better clinical outcomes for laser surgical applications.

Currently, there are several methods to pre-treat cells: preshock with mild temperature elevation [10], adding exogenous heat shock proteins [11], or administering pharmacological agents [12-14]. Of particular interest, are the small molecule drugs like geranyl geranyl acetone (GGA) or arimoclomol that upregulate the heat shock response (HSR) by interacting with heat shock factor 1 (HSF1) and act as co-inducers of the heat shock proteins, augmenting the effect of mild thermal shock [15-17]. These strategies can serve to increase cellular survival proteins above basal levels and activate protective molecular pathways prior to a more damaging secondary heat shock a few hours later [18, 19].

At the forefront of this response lie the heat shock proteins (HSP). HSPs are a vital set of chaperone proteins that respond to thermal stress by assisting heat-denatured proteins in the cytosol to refold into their native, functional conformations, thereby restoring the homeostasis of the cell environment [20]. In particular, HSP70 represents

the most highly inducible HSP after thermal stress in mice [21]. The fact that this protein maintains a highly conserved amino acid sequence across almost all organisms attests to its importance to cell survival [22]. HSP70 has been implicated in a plethora of diseases and functions within the body, such as: Alzheimers, ALS, wound healing, and immune signaling [13, 23-26].

In tandem to the role of HSP70 in protein refolding, there are several mechanisms by which it can rescue cells from thermal insult. HSP70 has been implicated in directing severely denatured proteins for degradation through the proteasomal pathway [27, 28] and HSP70 intervenes in cell death by downregulating apoptotic signaling within the cell through its interaction with BAX, a pro-apoptotic signaling protein [7, 29]. However, the reliance of these mechanisms upon other proteins is not fully understood. HSP90, HSP110, HSP25 and HSP40 have also been reported to contribute to thermotolerance [30-34]. HSP90 and HSP40 are known to work in conjunction with HSP70 to refold proteins. While HSP40 only acts as a co-chaperone that enhances the ATP cycling of HSP70, HSP90 can also fold proteins on its own [35, 36].

While our past work [37, 38] has focused on characterizing the transcriptional activation of *Hsp70* after a single thermal injury, this study investigated the importance of HSP70 for pretreatment protocols in advance of a more severe, secondary heat shock. To determine the specific role of HSP70, we utilized an *Hsp70* deficient MEF cell line (a generous gift of Dr. Clayton Hunt at Washington University) [39]. The cell line is deficient in both isoforms of *Hsp70*: *Hspa1a* and *Hspa1b*. These isoforms are identical in their functions and thought to be redundant except for the lack of *Hspa1a* expression in murine liver tissue and differential upregulation in embryonic development [21, 27, 40].

However, in these murine embryonic cells the introduced *Hspa1b* gene was shown to express its protein in a similar fashion to wild type cells through Western blotting in our previous work [41].

While hsp70 has been shown to correlate to successful preconditioning in murine models using scalpel wounds, the causal relationship has not been fully established [42]. It was our hypothesis that the absence of HSP70 would diminish the benefit of pretreatment but it was unknown to what degree or what the time and temperature dependence would be to this perturbation of the natural cellular response.

4.2.1 Arrhenius Integral

The kinetics of several morphological and physiologic responses to thermal damage are exponentially dependent on temperature and linearly dependent on time of exposure [43]. The Arrhenius integral describes a rate process for characterizing tissue damage that works well for low temperature phenomena, such as coagulation or birefringence loss:

$$\Omega = \ln\left(\frac{C_0}{C(t)}\right) = \int_0^{t_p} A \exp(-E_a / RT)dt \qquad (1)$$

where Ω is a unitless metric that quantifies damage, A is the frequency factor - i.e. damage rate [1/sec], Ea is the activation energy in [J/mole], T is the temperature of exposure [K], R is the gas constant at 8.32 [J/mol K] and the integral is over the time of the heat exposure. Although, most commonly applied to tissue characteristics, the Arrhenius damage model can be applied to cellular systems as well [44-46]. The Arrhenius integral takes into account temperature-time history of the sample to predict damage based on the damage threshold. A precisely defined, reproducible and measurable indicator of the thermal damage is identified by experimental analysis. The

threshold of the thermal damage is commonly a ratio of the concentration of native (undamaged) tissue before irradiation exposure (C_0) to the concentration of native tissue at the end of the exposure time (C(t)). For this study, cell viability at 48 hours after thermal stress was used as the endpoint of damage. A viability assay quantified the amount of metabolically active cells with a fluorescent dye. The heat stress that resulted in only 37% of the fluorescence, C(t), relative to untreated controls, C_0, was then used to calculate Ω and the resulting activation energy and frequency factor at a given temperature. For our case, Ω = ln (100%/37%) = 1.

For a constant temperature exposure, the Arrhenius relationship predicts a linear increase in damage with increasing exposure time. In order to test the linearity of a system, the experimental data can be fitted to the Arrhenius integral by means of converting the equation into a linear relationship [44, 46]. When the damage parameter (Ω) is equal to 1, which is when the damage is equal to the arbitrary end point that we chose to be 37% cell viability relative to controls , the equation becomes:

$$\ln(t) = -\ln(A) + E_a / RT \qquad (2)$$

Plotting the experimental results on an ln(t) versus 1/T graph will produce a slope (E_a/R) and y-intercept (-ln(A)) from which the activation energy and frequency factor can be derived, respectively.

In this study we contrasted the Arrhenius damage rate of control cells to that of cells deficient in hsp70. We also wanted to investigate how well the Arrhenius model holds in the case of biphasic heating with our pretreatment protocol. It was our hypothesis that preshocking the cells would increase the activation energy (E_a) and lower the frequency factor (A) for both cell types. However, the changes in the hsp70 deficient

cells were anticipated to be of a lesser magnitude. We expected an increase in the activation energy (E_a) because the preconditioning protocol would increase the threshold at which damage would begin in cells. Furthermore, since the frequency factor (A) is time dependent [1/sec], we anticipated that preconditioning would lower the rate of damage accumulation and this would be manifested as a decrease in the frequency factor.

In this study we set out to determine if pretreatment could rescue cells from a severe heat exposure at a later time point and which parameters brought about the best survival. We used a novel luciferase reporter construct to correlate the expression of *Hsp70* to the preshock behavior. We then ascertained the causal relationship between the benefit of preshock and the presence of HSP70 by using the *Hsp70* knockout cells. Application of the Arrhenius model to the cells' response allowed us to further characterize the importance of HSP70 in repair and prevention of thermal damage. Ultimately, identification of key protein targets such as these may allow for more effective and specific pretreatment protocols for laser irradiation, and other thermally-based therapeutic modalities in the clinic.

4.3 Materials & Methods

4.3.1 Cell Culture

Adherent MEF(-/-), murine embryonic fibroblast, cells made deficient in *Hsp70* through homologous recombination of a region encompassing both isoforms of the murine *Hsp70* gene – *Hspa1a* and *Hspa1b* – were a generous gift of Dr. Clayton Hunt at Washington University [21]. The resulting knockout cells had a Neomycin resistance fragment inserted in place of the *Hsp70* genes. Subsequently, from the knockout cells, a rescue cell line - denoted as MEF(+/+) - had the hspa1b gene reintroduced. These were

used as control cells as their growth characteristics were shown to more appropriately match the knockout cells than a wild type strain of MEF cells (data not shown).

The Hsp70L*uc* cells used in this study were an adherent NIH3T3 murine fibroblast derived cell line stably transfected with two DNA plasmids; pGL3Basic-Hsp70a1luc and a pcDNA3.1(+) vector [37, 47]. The pGL3Basic-Hsp70a1luc was used as a means to assay *Hsp70* promoter activityas it consisted of a firefly, *Photinus pyralis,* luciferase reporter gene (*luc*), inserted downstream of the murine heat shock protein 70 promoter sequence. The luciferase reporter gene is expressed upon activation of the promoter (i.e., by utilizing an external stimulus such as heat), and in the presence of its substrate, luciferin, and various co-factors, emits broadband (500-700 nm) light with a peak wavelength at 563 nm. The observed changes in reporter gene activity can be used to infer the amount of cellular stress caused by the thermal treatment. We have previously shown that bioluminescence levels correlate to the amount of actual HSP70 protein within the cell up until a threshold of thermal damage when the cellular translation machinery has been compromised [37, 38, 47] .

Cells were maintained in a 5% CO_2 incubator (Fisher Scientific) in DMEM (Invitrogen, Carlsbad, CA) supplemented with 10% fetal calf serum (ATCC, Manassas, VA) with 2µl/ml of Normocin (Invivogen, San Diego, CA). For experiments, each 96 well plate was covered with a gas permeable membrane (# 2928-0100, USA Scientific, Ocala, FL) to prevent evaporation of the media and to seal the wells during water bath experiments.

4.3.2 Water Bath Heat Treatment

Cells were plated at a density of $3x10^3$ cells/100 µl of media in removable 8-well strips from a 96 well plate (Corning, Lowell, MA). Only the six middle wells were used so as to reduce edge effects. As depicted in Figure 4.1, at 20 hours after seeding, some samples were pretreated with a mild heat shock of 43^o C for 30 minutes – that was shown to be the optimal duration - in an electronically controlled, constant temperature water bath that was accurate to within +/- 0.1^o C (Fisher Scientific). Temperatures were verified with a separate digital thermometer. The individual 8-well strips were placed in a foam floating device for the water bath exposures. After preshock, a range of severe heat shocks (5-50min at 44.5, 45, 45.5, 46^o C) were administered. Lag times are defined as the waiting period between the preshock (PS) and the more severe heat shock (HS). During the lag time cells were allowed to recover in the incubator. The lag times varied amongst 2, 4, 6, 8, and 10 hrs.

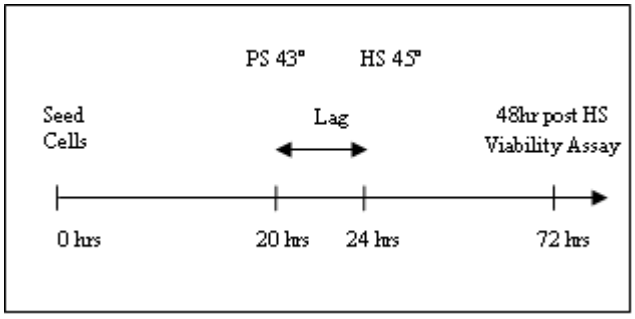

Figure 4.1 Timeline diagram for the water bath heat shock experiments in cell culture. Lag time is the interval between the end of the preshock (PS) and the middle of the heatshock (HS). Time after seeding (t = 0 hrs) is listed on the bottom.

4.3.3 Bioluminescence Imaging

Bioluminescence imaging of the *Hsp70* promoter–luciferase reporter activity in the NIH3T3 Hsp70luc cells was carried out in preshock optimization experiments. The light output of cells was measured at various time points following heat shock using an IVIS 100 bioluminescence imaging system (Xenogen/Caliper Life Science, Alameda, CA). Prior to imaging, the substrate needed for the enzymatic reaction of luciferase, D-Luciferin (4,5-Dihydro-2-[6-hydroxy-2-benzothiazolyl]-4-thiazolecarboxylic acid potassium salt ($C_{11}H_7N_2O_3S_2K$), Biosynth AG, Switzerland), was added in a 20 µl solution of distilled, deionized water at a final concentration of 0.375 mg/ml in the well with media. The cells were placed in an incubator at 37^o C for 3 minutes until they were moved to the light tight imaging box which had a heated stage. Photon counting images were taken for an integration time of 1 minute and a low binning for maximum resolution. The photon flux, in units of [photons/sec/cm^2/sr], from the CCD camera was averaged from six identically treated wells and used as a measure of *Hsp70* expression. Untreated control wells showed no bioluminescence.

4.3.4 Western Blotting

A Western blot assay was used to determine the actual levels of HSP70 protein content within the MEF(+/+) cells at different times after thermal stress since these cells lacked a reporter protein to track expression levels. MEF(+/+) cells were either preshocked only (PS), heat shocked only (HS) or preshocked and heat shocked (PS+HS) in individual 8 well strips. At 2, 4, 6, 8, 12, and 24 hours after treatment, two sets of wells for each condition were pooled and harvested with 150ul of 1xSDS detergent to denature

the proteins. Total protein was quantified using the Micro BCA Protein Assay kit (Pierce, Rockford, IL) in a Synergy HT microplate reader. Ten μg of total protein from each sample was loaded in a 7.5% SDS-PAGE gel, run for 1.5 hrs at 100V, transferred to PVDF membrane (Hybond-P, GE Healthcare, Piscataway, NJ) for 1 hr, and then blocked in 5% milk overnight. Membranes were then incubated for 1 hr with 1:1000 murine anti-hsp70 (SPA-810 Assay Designs, Ann Arbor, MI). After washing, membranes were incubated with 1:3000 secondary antibody, anti-mouse IgG conjugated to Horseradish Peroxidase (NA931, GE Healthcare). Membranes were then incubated in ECL and exposed to radiographic film (Hyperfilm, GE).

4.3.5 Viability Assays

Viability at 24 and 48 hours post heat shocking (HS) was measured by adding 20 μl of Cell Titer Blue (Promega, Madison, WI) reagent to 100ul of cell culture media per well. The assay measures the number of viable cells within the well since dead cells are unable to reduce the non fluorescent reagent resazurin into the fluorescent product resorufin. The fluorescence emission was quantified on the Synergy HT microplate reader (BioTek, Winooski, VT) at 560/590 nm (excitation/emission) at a sensitivity setting of 35 after a 1 hour incubation at 37^{o} C. The baseline fluorescence of wells containing media only was subtracted from each sample and then all intensities were normalized to the fluorescence of untreated controls on the same plate.

4.3.6 Laser Irradiation Experiments

Laser irradiation was used in order to determine if water bath preconditioning could protect cells against a shorter duration, higher temperature stress. With the aim of eventually translating this work to more clinically relevant parameters, a shorter water bath pretreatment at 43^{o} C for 15 min was used. In our optimization experiment of the pretreatment protocol (data not shown), we found a 15 minute duration at 43^{o} C only lowered the viability by 4.6% after a 60 minute severe stress at 45^{o} C. For irradiation experiments, cells in standard 96-well tissue culture plates were placed in a modified 37 °C Lab Line incubator (VWR, West Chester, PA), which allowed laser delivery to individual wells through an optical fiber inside the incubator using similar methods as our previous work [37]. Briefly, Pulsed Holmium:YAG laser (λ= 2.1 μm, τ_p = 250 μs, Schwartz Electro Optics 1-2-3, Orlando, FL) irradiation was coupled into the 600 μm low hydroxide (OH) optical fiber (NA = 0.39) using a 25 mm focal length CaF_2 lens and an SMA connector. The Ho:YAG wavelength has an optical penetration depth in water of approximately 300 μm thus allowing relatively uniform heating over the thickness of the cells (~ 10 μm) that were adhered to the bottom of the plate. The distance between the distal end of the fiber and the bottom of the 96 well plate was 3 cm. As a result of reflection at the plate surface, masking losses due to the black-walled plates, and absorption in the polystyrene, the pulse energy reaching the cells was between 97 – 119 mJ/ pulse (total radiant exposure over all pulses: 9 J/cm^2 – 11 J/cm^2 for the 6.4mm diameter well size). The laser was set to pulse at 3 Hz for 10 seconds for a total of 30 pulses. . Following laser exposure the cells were placed back in the incubator until being imaged.

4.3.7 Arrhenius Analysis

From each viability assay for the water bath preshock with heatshock (PS+HS) condition or the heat shock alone (HS), the exposure duration resulting in 37% viability relative to untreated controls at 48hrs was interpolated from a linear region of the data for each temperature (44.5, 45, 45.5, 46^{o} C), see Fig. 6. These exposure durations represented the arbitrary endpoint for damage (i.e. $\Omega = 1$). Since all of the exposure durations corresponded to the same level of damage, they could then be plotted on an Arrhenius graph of 1/T vs. Ln(t) [sec] to produce linear fits for the determination of the frequency factor, A [1/sec], and activation energy, E_a [Joules/mole]. From Equation 2. above, the activation energy is then determined by the relation: E_a = slope * R. The frequency factor is calculated through: A = - exp (-b), where b is the y-intercept.

4.4 Results

All experiments, except for the Western blot, were done in at least triplicate. Experiments were carried out on separate days and results averaged.

4.4.1 Optimization of Preshocking Time

In order to optimize the preshock protocol to provide maximum thermotolerance the time dependent behavior of *Hsp70* induction after thermal stress was monitored and quantified. We had previously concluded that the optimal duration of preshock was 30 minutes when exposed to a 43^{o} C water bath (data not shown), but the time at which that preshock was to be delivered still needed to be determined. Fig. 4.2 shows the temporal expression profile of hsp70 transcription after PS alone in Hsp70luc cells. The profile is

transient in nature and peaks around 6-8 hrs. This trend indicates that a classical feedback inhibition mechanism is taking place after the cells have recovered. Untreated controls cells do not bioluminesce because hsp70 transcription is not active at basal, unstressed conditions. To account for the inherent biological variation, the photon levels in Figure 4.2 were normalized to the peak value for each day, which was at the 6 hour time point after preshock (PS). The error bars represent the standard error of the mean. Since the data for each sample was normalized to its peak value at 6 hrs, the 6hr data point shows no error bars.

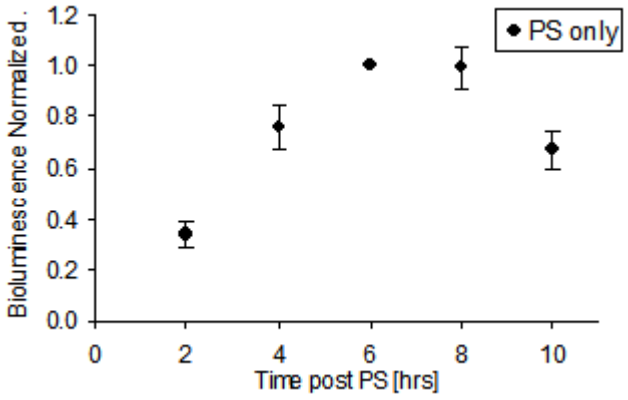

Figure 4.2 Quantification of bioluminescence as a surrogate marker for hsp70 transcription through in NIH3T3 Hsp70luc cells after preshock alone. Bioluminescence was imaged at 2,4,6,8 and 10 hrs after water bath preshock treatment of 43^{o} for 30 minutes. Each data point is normalized to the bioluminescence peak at the 6 hr time point. Error bars are the Standard Error of the Mean.

The data in Fig. 4.3 was used to optimize the lag time between PS and HS by determining which would provide the most thermotolerance, as measured through the quantity of viable cells. Fig. 4.3 shows the fluorescence from the viability assay in Hsp70luc cells at 48 hours after thermal treatment. The 4hr lag between PS and HS produced the most effective thermotolerance resulting in viability of 73% relative to control cells that were only preshocked. The benefit was shown to be statistically significant with a $p < 0.05$, as compared to the other data points using a student's *t*-test. The fluorescence values are normalized relative to samples that had been preshocked only. This PS Only treatment showed similar viability to untreated controls in other experiments (data not shown).

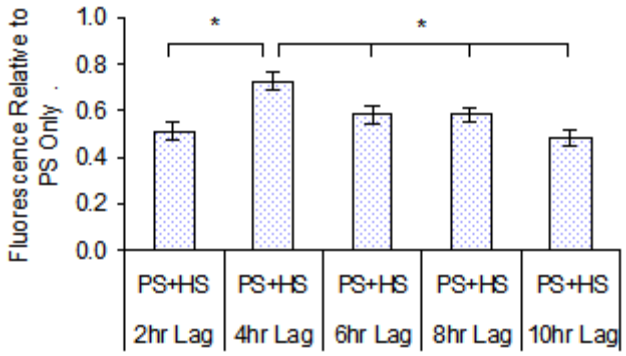

Figure 4.3 Viability assay of NIH3T3 Hsp70Luc cells after both preshock (PS) and severe heatshock (HS). Cells were preshocked at 43^{o} for 30 min then recovered for varying lag times of 2, 4, 6, 8, and 10 hrs before a severe heat treatment of 45^{o} for 50 minutes. Viability was assessed through fluorescent quantification of Cell Titer Blue dye at 48 hrs after the HS exposure. Each point is normalized to the fluorescence of a 30 minute PS only sample at 48hrs. Error bars are the Standard Error of the Mean. * represents statistically significant difference ($p < 0.05$) relative to the 4hr lag point.

4.4.2 Thermal Pretreatment Rescues NIH3T3 Hsp70Luc Cells From Laser Irradiation

The laser irradiation experiment in Fig. 4 was carried out in order to test that preshocking cells in a water bath would also protect against short duration, high

temperature exposures that are common in laser applications. The data shows that a mild pretreatment (43° C for 15 min) at 4 hours before laser exposure increased cell viability relative to unheated controls at the 24hr time point. We chose this shorter PS exposure to assess a more clinically feasible time duration. In unpublished data, we test the PS treatment and determine that 30 minutes was optimal, but a 15 minute duration yielded only a 4.6% decrease in viability and was, therefore, acceptable.

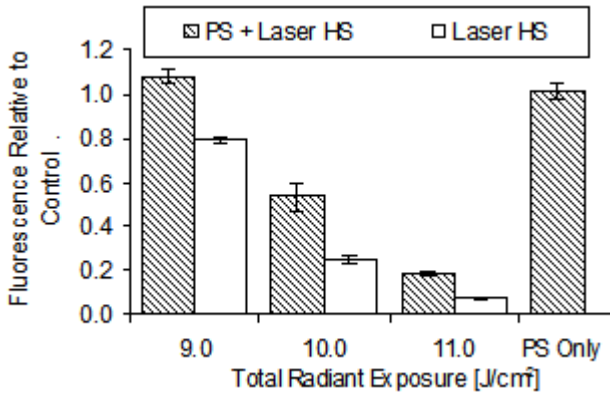

Figure 4.4 Viability assay 24hrs after Ho:YAG laser irradiation in NIH3T3 Hsp70Luc cells. Laser irradiation alone (open bars) or with Preshock (shaded bars) in a 43° C water bath for 15 minutes was applied to cells in a 96 well plate and viability was assessed with Cell Titer Blue fluorescence at 24hrs and normalized to unheated control cells. Infrared Ho:YAG irradiation was pulsed at 3 Hz for 10 seconds through a fiber with a cumulative radiant exposure varying from 9 – 11 J/cm^2 at the interface between the cells and the plastic surface of the wells. Error bars are the Standard Error of the Mean.

The cells exhibited an increase in viability after preshocking at all three laser exposures (9 J/cm^2, 10 J/cm^2, and 11 J/cm^2) by varying the energy out of the fiber, but the middle energy showed the greatest difference between the preshocked and non-preshocked cells. At the lowest radiant exposure, the preshock resulted in cell viability above that of untreated controls, suggesting a stimulatory role of the mild thermal pretreatment. In previous work we measured the average temperature in the well to reach

50^{o} C for the total radiant exposure of 9 J/cm^2 for the 10 second laser treatment. Preshocked only cells (PS Only) show that the pretreatment protocol was not damaging to the cells since this data set produced the same amount of fluorescence in the viability assays as untreated controls (data not shown).

4.4.3 HSP70 Protein Levels in MEF(+/+) Cells

In order to use the MEF(+/+) rescue cells as a control cell line to the *Hsp70* knockout cells MEF(-/-), it was necessary to verify the presence of hsp70 and to track the protein's expression pattern. The Western blot in Figure 4.5 displays the HSP70 production in MEF(+/+) cells after PS and PS+HS treatments. The lag time for optimal thermotolerance was determined to be 4 hours in these cells, similar to the Hsp70luc cells (data not shown).

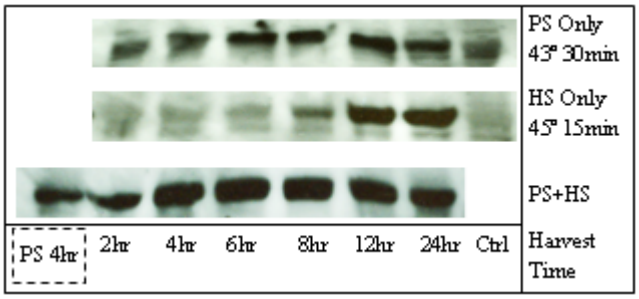

Figure 4.5 Western blot of hsp70 expression in MEF(+/+) cells after water bath thermal treatment. Cells were either preshocked only (top), heatshocked only (middle) or preshocked and heatshocked (bottom) in individual 8 well strips and harvested with 1xSDS at 2, 4, 6, 8, 12 and 24 hrs afterwards. Harvest time refers to the time after HS HS. Total protein was pooled and quantified using MicroBCA assay and then 10µg was loaded onto SDS-PAGE and blotted with antibody against hsp70, then with anti-mouse IgG conjugated to HRP and subsequently visualized with ECL. The dashed box represents a Preshock only (PS) sample harvested at 4hrs after preshock used for direct comparison to the other samples in the bottom row which are PS+HS.

In the top panel of Fig. 4.5, protein levels steadily increased and then peaked at 6-8 hrs after a single, mild preshock of 43^{o} C for 30 minutes (PS Only). This expression profile of protein from these MEF(+/+) cells can be compared to Fig. 4.2 which shows the hsp70 transcription profile in Hsp70luc cells. While the expressions for both assays peak around 6-8 hrs after heating, the MEF(+/+) cells still show high levels of protein up to 12 hrs before declining (Fig 5, Panel A), suggesting a slight difference in the expression of HSP70 between the two cell lines or that the gene transcription as measured by bioluminescence does not correlate directly to actual protein content at this time point. Dinh, et. al. showed this phenomenon in human cells where a 55^{o} C 3 second thermal stress was applied and then mRNA and protein were measured [48]. The levels of mRNA were a 10 fold increase at 4 and 8 hours after heat shock but dropped off by 24 hrs. However, the HSP70 protein amount was low at 4 hrs, 10 fold increase at 8 hrs and then 35 fold increase at 24 hrs. This data demonstrates that while the signal for HSP70 translation (the mRNA transcripts) was turned off, the protein was still within the cell to provide protection. In previous work we have shown a direct correlation between the bioluminescence and actual HSP70 content as measured by ELISA assays at 8 hrs after heating [37]. However, this is a time point that is early enough to still have the transcription and translation matching each other and is consistent with the Dinh study.

In the middle panel, the MEF (+/+) cells showed no hsp70 production at early time points (2, 4, 6, and 8hrs) after the single, severe 45^{o} C heat shock of 15 minutes (HS Only). Only at after 12 hrs do we see levels of hsp70 that were comparable to PS Only in the top panel. In the bottom panel of Fig 4.5, a mild 43^{o} C preshock combined with severe 45^{o} C heat shock (PS+HS) restored the cells' capacity to make hsp70 at the earlier time

points. It is important to note that the harvest times for the bottom panel are after the second HS of 45^{o} C, not the preceding PS of 43^{o} C. The top and middle panels were harvested at the indicated times after their respective, single heat shocks.

The dashed box in the bottom panel represents a PS Only sample harvested at 4hrs after PS loaded on the same gel as the PS+HS samples for direct comparison. MEF(-/-) *Hsp70* deficient cells showed no immunoblotting with anti-HSP70 (data not shown).

4.4.4 *Hsp70* Deficient Cells Show Compromised Thermotolerance after Preshock

In order to determine the importance of the HSP70 protein in thermal pretreatment, we used an *Hsp70* deficient cell line and compared it to a cell line which had *Hsp70*. Figure 4.6 shows the response of MEF(-/-) and MEF(+/+) cells to a severe heat shock with and without preshock as measured through fluorescence viability assays. The MEF(+/+) cells show a robust increase in survival after pretreatment at 43^{o} C for 30 minutes at 4 hours prior to the severe heat treatment at 45, 45.5 or 46^{o} C, as can be seen by the separation between the two linear best fit lines (PS+HS vs. HS Only) on the graph. The survival is represented as an increase in the tolerable exposure time for any given amount of cell survival on the y-axis, in essence, a shift of the line to the right. The dashed line is given as a reference and shows the 37% viability relative to untreated controls.

As the temperature of the secondary heatshock is increased from 45 to 46^{o} C, the tolerated exposure times decrease for both the preshocked and non-preshocked conditions. This is evident by the two lines on the graphs getting closer together. The

MEF(-/-) cells at 46^{o} C show almost no benefit to preshock and the PS+HS line actually has less viability than HS alone in the lowest exposure durations.

It is relevant to note that the HS Only linear best fit lines are relatively similar in slope and location between MEF(+/+) and MEF(-/-) cells for any given temperature (i.e. 45,45.5 and 46^{o}C). However, only when PS is added to the HS do the PS+HS lines vary greatly between MEF(+/+) to the MEF(-/-) samples, implying significant thermotolerance was induced in the MEF(+/+) cells after preshock, but not in MEF(-/-) cells.

4.4.5 Arrhenius Analysis After Preshock

An Arrhenius analysis of the water bath preshock and heatshock data was carried out to quantify the damage response of the MEF(+/+) and MEF(-/-) cells. For this experiment, water bath heat treatment was used in order to acquire steady state heating profiles necessary for the Arrhenius analysis.

The data from Figure 4.6 was used to make the plots in Fig 4.7. The intersection of the HS Only and PS+HS lines with the 37% viability line were taken from each temperature from Fig 6 - 44.5, 45, and 46^{o}C - plus an additional temperature of 44.5^{o} C (that is not displayed) and applied to a linear fit to make the lines in Fig 4.7. The resulting activation energies (E_a) in [J/mol] and frequency factors (A) in [1/s] are listed in Table 1 where E_a = slope * R and A = exp (-b).

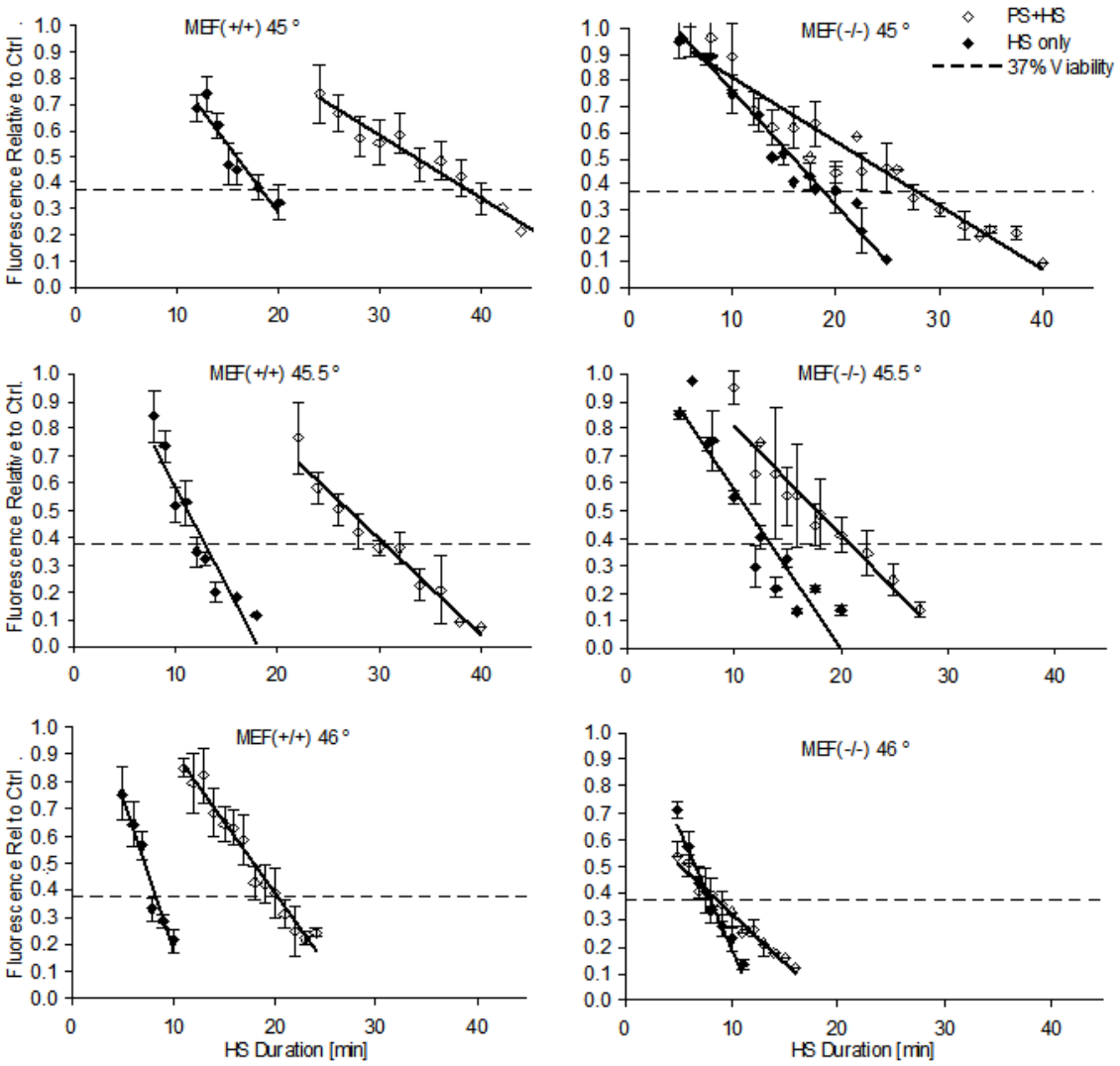

Figure 4.6 Viability assays at 48hrs for water bath heat shocked MEF(+/+) and MEF(-/-) cells. Samples were either heat shocked (HS) alone (closed symbols) at 45, 45.5, and 46^{o} C (Top, Middle, and Bottom, respectively) for varying durations or treated with preshock (PS) of 43^{o} C for 30 minutes at 4 hours prior to HS (open symbols). Cells were allowed to recover for 48hrs and then imaged with Cell Titer Blue fluorescent viability assay with a 1 hour incubation. Solid lines are the linear best fits to the data. The dashed line represents 37% fluorescence intensity relative to untreated controls. Error bars are the Standard Error of the Mean

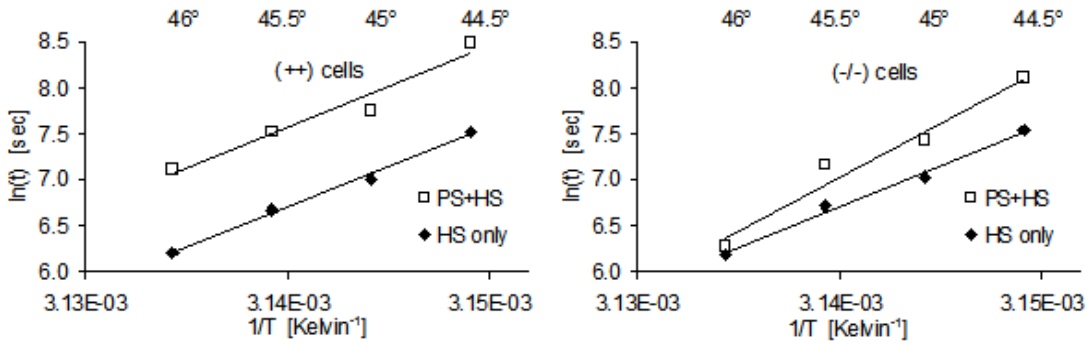

Figure 4.7 Arrhenius analysis of water bath heat shocked MEF(+/+) and MEF(-/-) cells. From the heat shocked only at 45°C (closed symbols) and preshocked at 43°C with heatshock (open symbols) data, the heat shock duration at which cells exhibited 37% fluorescence relative to controls at the 48hr time point was interpolated and plotted as log of exposure time (t) versus 1/T. Four different temperatures were used 44.5, 45, 45.5, and 46°. Best fit lines were then applied to calculate the activation energy (E_a) and frequency factor (A) from the slope and y-intercept. The Celsius conversions of the temperatures are noted on the top.

It can be seen that the activation energy increases slightly from HS only to PS+HS in the MEF(+/+) cells (Table 4.1). However, there is a greater increase in this number for the MEF(-/-) cells. For the case of the frequency factor, the MEF(+/+) cells show a small increase when the cells are preshocked. In contrast, the MEF(-/-) cells show a very drastic increase of several orders of magnitude after preshock.

Table 4.1 Experimentally determined values of activation energy (E_a) and frequency factor (A) from Arrhenius analysis of water bath heat shocked MEF(+/+) and MEF(-/-) cells. The slope and y-intercept of linear best fit lines in Fig 7 were used to calculate the values across four temperatures: 44.5, 45, 45.5, and 46°.

		E_a = slope*R Activation Energy [J/mol]	A = exp (-b) Frequency Factor [1/s]
MEF(+/+)	HS	7.1E+05	4.9E+113
	PS+HS	7.3E+05	6.9E+116
MEF(-/-)	HS	7.3E+05	1.9E+117
	PS+HS	9.8E+05	3.7E+157

4.5 Discussion

The overall goal of this project was to characterize the role of hsp70 protein in thermotolerance to cells. The three different cell lines that we used allowed us to track the activity of hsp70 in a facile manner, and then observe the cellular response when hsp70 is chronically absent. Ideally, this work will provide guidance for more effective pretreatment options to improve laser and thermally-based therapies.

4.5.1 Optimization of Preshock through HSP70 levels

Based on the protein folding properties of HSP70, it could be logically assumed that maximum HSP70 protein levels would correspond to the most protective effect for the cells. Using the luciferase reporter gene as a surrogate measure of actual HSP70 protein allowed us to test this assumption because we could compare the peak expression to the lag time that gave the best viability. The data in Figure 4.2 and Figure 4.3 are shown in order to demonstrate the correlation between bioluminescence levels of *Hsp70* transcription and the viability of cells 48 hrs later.

Fig. 4.2 shows the bioluminescence for the PS Only condition, which is representative of the HSP70 protein levels within the cell. The peak expression occurs between 6-8hrs after PS. However, from Fig. 4.3, it can be seen that the most survival is present in the samples that had the 4 hour time lag between the PS and HS treatments. This data implies that the time of maximal HSP70 expression after PS is not necessarily the best lag time between the pretreatment and the thermal insult. We saw this same phenomenon with the MEF(+/+) cells wherein the HSP70 protein expression peaked at 6-

8 hours but the optimal time according to viability studies was at the same 4 hour time point as the Hsp70Luc cells used in the bioluminescence assays (data not shown).

The most likely explanation for this discrepancy between the peak of HSP70 transcription and actual viability may be the presence of other heat shock response proteins at this earlier time point. While HSP70 may not peak until 6 hours, the thermotolerance of the cells could be highest at 4 hour lag because of the increase of other proteins like HSP90 and HSP40 that interact with and facilitate the function of HSP70. Alternatively, the difference between the peak of HSP70 protein and viability may be due to an overproduction of HSP70. While there may be enough HSP70 protein in the cell to reduce the damage from the heat stress at 4 ours, the cell may continue making protein if the transcriptional signal is still on up through the 6-8 hour time point.

4.5.2 Preshocking Protects Cells From Laser Irradiation

Ultimately, an aim of this work is to lay a foundation for improved laser wound healing and efficacy of therapeutic endpoints. Consequently, we wanted to see if the preshocking protocol that we used with the water bath would translate to protecting against laser irradiation where the exposure times are on the order of seconds versus minutes. The temperature profile from a pulsed laser is more complicated than that from a simple water bath heating. The Ho:YAG is pulsed at 3 Hz at with a pulse duration of 250 μsec. This creates a spike profile of temperature transients. These high local temperatures on small time scales could elicit fundamentally distinct damage responses from the cells that may be a different mechanism than what our pretreatment is able to ameliorate. Nevertheless, the graph in Fig. 4.4 shows successful preconditioning to laser

exposures across a range of energies. Survival was almost doubled for the 10 and 11 J/cm^2 total radiant exposures conditions when pretreatment was applied. In previous work, we used a thermocouple to measure the baseline temperature during the 10 second irradiation to be around 50^o C for 9 J/cm^2 [37].

One example where pretreatment may benefit clinical outcome from laser irradiation is before the use of Er:YAG and CO_2 lasers for skin tightening and resurfacing. The application works by ablating the top surface of the skin and then shrinking collagen fibrils within the dermis [49]. Preconditioning – through thermal or chemical means - may allow for more energy to be supplied by the laser to shrink the collagen but still allow the cells within to remain viable. This strategy may reduce side effects, such as, erythema and swelling while maintaining the effectiveness of the procedure. Furthermore, in applications like port wine stain, tattoo and hair removal procedures, a pretreatment might be able to minimize damage to non-target tissue similar to how surface cooling devices protect the superficial tissue while allowing the deeper dermal tissue to be heated.

4.5.3 HSP70 Is Necessary For Full Thermotolerance

After determining the correlation of *Hsp70* expression to increased survival in the pretreated Hsp70luc cells, we wanted to determine the causality between the effectiveness of preshock and the HSP70 protein. We accomplished this by removing hsp70 from the thermal response with the *Hsp70* knockout cells, MEF(-/-). In order to utilize the *Hsp70* deficient MEF(-/-) cells, we first needed to characterize the hsp70 response of the *Hsp70* competent cell line, MEF(+/+). While this cell line shows less

HSP70 production than a wild type line, its temporal expression trends are the same (data not shown). When comparing the HSP70 protein content after PS in these MEF(+/+) cells (Fig. 4.5, top panel) to the transcription of *Hsp70* in the Hsp70luc cells through bioluminescence in Fig. 4.2, it can be seen that the trends are similar but they peak around 6-8 hrs after the thermal treatment before declining.

The Western blot image in Fig. 4.5 also shows that pretreatment can facilitate HSP70 protein production after severe HS. The severe HS of 45^{o} C for 15 min (Fig. 4.5 middle panel) shows a delay in HSP70 synthesis that is negated when a PS is delivered beforehand (Fig 4.5 bottom panel). Without PS, the insult by the HS is thought to so badly damage the cells that the machinery necessary for transcription and translation of the heat shock response proteins is, itself, compromised until later time points. The pretreatment is able to prepare the cell for this injury by increasing these proteins beforehand so that they do not have to be made after the severe thermal insult.

The lack of HSP70 protein within the cell correlates to a significant reduction in thermotolerance, which can be seen in Fig. 4.6 with the MEF(-/-) cells that were pretreated (PS+HS) as opposed to the MEF(+/+) cells. Similar thermotolerance deficiency has been noted in individual knockouts of the *Hsp70.1* and *Hsp70.3* proteins under different temperature and time conditions [27].

In contrast to the preshocked samples, the viability data for the HS Only sample are relatively similar between MEF(+/+) and MEF(-/-) cells. This result suggests that the inducible gene is not really giving any benefit to the MEF(+/+) cells because it is not present under the basal condition (i.e. at the time right before the severe heat shock insult), as can be seen in the Western blots of Fig. 4.5. The HSP70 protein needs some

time to be upregulated and is best suited for conditioning cells to a secondary insult as opposed to protecting it from an initial one.

The data in Fig. 4.6 also suggests that HSP70 is of particular importance to providing effective thermotolerance at higher temperatures. In MEF(+/+) cells, the increase in exposure duration necessary to reduce viability to 37% of untreated controls – as displayed by the separation between the HS Only and the PS+HS lines in Fig. 4.6- was 120% for 45^{o} C, 134% for 45.5^{o} C, and 144% for 46^{o} C. For the MEF(-/-) cells the increases necessary were 50% for 45^{o} C, 55% for 45.5^{o} C, and only 8% for 46^{o} C. The increasing, then decreasing trend as temperatures rise in the MEF(-/-) cells shows that preshock is unable to maintain proportional survival without HSP70. Coupled with the contrasting behavior of the MEF(+/+) cells where there is actually an increasing thermotolerance trend as temperature rises, this data alludes to the increasing significance of HSP70 at high temperatures wherein the cell can still be rescued through the HSR. We speculate that the functionality of HSP70 is of particular importance for a state of severe protein denaturation within the cells but at lower temperatures the other heat shock response proteins (e.g. HSP90, HSP40, HSC70, HSP60, HSP27) are able to repair the damage on their own. There are two mechanisms of HSP70 that may explain its unique role in severe damage seen at higher temperatures. First, it has been implicated in ubiquitination to signal damaged proteins that are beyond repair to be degraded [27]. Therefore, if these denatured components are allowed to accumulate in the MEF(-/-) cell, this may explain the higher levels of cell death in Fig. 4.6 at 46^{o} C compared to 45.5^{o} C and 45^{o} C. Secondly, the direct anti-apoptotic mechanism of hsp70 through suppression of BAX translocation to the mitochondrion may lead to disproportionately high levels of

cell death in the MEF(-/-) cells [7, 29] If this role of hsp70 extends to even higher temperatures than 46^{o} C, then it may be especially important in pretreating strategies for laser irradiated tissue because of the high peak temperatures seen. However, there is a limit to the extent of damage that a protein can repair due to its expression characteristics and its molecular interactions. When temperatures are high enough and durations long enough, no mechanism will be able to repair the damage and the cells will become necrotic.

4.5.4 Role of HSP70 in the Arrhenius Response

The purpose of the Arrhenius analysis was to determine if the Arrhenius model would still apply to the cells' thermal response under two unique circumstances: when preshock was applied and when hsp70 was missing. In order to see if the activation energies (E_a) and frequency factors (A) that from the MEF(-/-) and MEF(+/+) cell lines were consistent with the literature, we compared them to those found by Rylander, et. al.[50]. We only used the HS Only samples for comparison because Rylander did not have PS data. The values for activation energies in Table 4.1 (E_a = 7.1 – 9.8 x10^5 J/mol) are higher than those obtained by Rylander, et. al. for viability of bovine aortic endothelial cells at 48hrs: (E_a = 3.7x10^5 J/mol). This discrepancy implies that our cell system needed a higher threshold of energy before the damage process was initiated. Given that skin cells (fibroblasts) are likely to be more resistant to environmental dynamics, such as, temperature, compared to endothelial cells, this result is not unexpected. Also the two frequency factors obtained in our experiments for the HS Only condition (A = 4.9 x10^{113} and 1.9 x10^{117}1/s) are markedly different from those reported

by Rylander, et. al. ($A = 5.9x10^{58}$ 1/s). However, the cells and protocols are different. In Rylander's study the temperature spanned from 44 - 50^{o} C, whereas we used a narrower window of 44.5 - 46^{o} C. The end point measurements are also different; we used a metabolic activity assay with the Cell Titer Blue as opposed to hemocytometer cell counts.

In comparing the thermal response of HSP70-containing versus HSP70-deficient cells, it can be seen that the activation energy increases slightly for the MEF(-/-) cells under the HS Only condition in Table 4.1. This change implies that the MEF(-/-) cells needed more energy to initiate the damage process. This is counterintuitive as the absence of a protein involved in cellular repair, HSP70, would be expected to lower the threshold for damage. Nevertheless, this may be a function of both cell types being completely devoid of even basal levels of HSP70. Essentially, the MEF(+/+) and MEF(-/-) cells exhibit the same damage threshold after a single thermal injury because the gene is missing in (-/-) and in the (+/+) cells it takes a few hours before the protein can be synthesized as there is little to no basal activity. The small magnitude of the change in activation energies supports this claim because it may not be significantly different between the two cell lines.

It would be expected for the frequency factor to increase for the HS Only condition when HSP70 is missing. Presumably, the lack of this repair protein would allow the damage rate to proceed at a faster pace. As can be seen in Table 4.1, the frequency factor is indeed higher for the MEF(-/-) cells ($1.9x10^{117}$) relative to the MEF(+/+) cells ($4.9x10^{113}$).

Turning to the preshocked samples for the Arrhenius analysis, our hypothesis was that preshocking will increase the activation energy (E_a) and lower the frequency factor (A) in any given cell type. We found that in our MEF(+/+) cells, the activation energy showed no statistical difference, as seen in Table 4.1 (7.1×10^5 for HS Only and 7.3×10^5 for PS+HS). The similarity can be seen graphically since the activation energy is determined by the slope of the lines. In comparison, when the MEF(-/-) cells' activation energies are calculated, they show an increase, as predicted (7.3×10^5 for HS Only and 9.8×10^5 for PS+HS). An increase means that there needs to be more energy present (as either temperature or exposure duration) to bring about the same amount of damage. If follows that preconditioning tissue to withstand damage would necessitate a higher activation energy. It is interesting that this increase is drastically evident in the MEF(-/-) cells and barely so in the MEF(+/+) cells. This may be a function of the limitations of the Arrhenius equation to model biphasic heating protocols when severe damage is present. Furthermore, the Arrhenius analysis was originally developed to model physical processes, such as protein denaturation; however, the endpoints of viability in these experiments incorporate a greater complexity due to the biological signaling. While the presence of denatured proteins is the physical result of thermal damage, the various cellular pathways of response to this stimulus in repairing itself or undergoing apoptosis determine the endpoint.

In our hypothesis, we also surmised that the frequency factor, A, would be lowered after pretreatment because the rate of damage would be slowed. However, as can be seen in Table 4.1, the MEF(+/+) cells showed a modest increase (4.9×10^{113} for HS

Only and 6.9 $x10^{116}$ for PS+HS) while the MEF(-/-) cells showed an even greater rise in the frequency factor (1.9 $x10^{117}$ for HS Only and 3.7 $x10^{157}$ for PS+HS).

4.5.5 Clinical Implications

Ultimately, we anticipate that this research may translate to the clinical arena by fostering strategies for the augmentation of the heat shock responsive proteins before laser injury to facilitate wound healing. Laser procedures that stand to benefit form pretreatment would include port wine stain, tattoo and hair removal wherein the surrounding tissue would be more capable of surviving the thermal stress. Also, it is plausible that applying these mild thermal treatments after the fact may be beneficial for injuries that are not planned. Trauma wounds, such as, burns or lacerations, may prove to benefit from augmentation of the HSR proteins and pathways if treatment can be applied within a short time frame afterwards.

In contrast to thermal injury as the mechanism of severe injury, the benefits of pretreatment may also apply to non-thermal wounds. There is evidence that some other proteins can be induced by thermal stress and that these increases correlate with better wound healing. Of note is TGF-beta, which has been implicated in scarless wound healing [9, 51, 52]. Work has been done in our lab on murine models that shows a correlation between HSP70 levels from diode laser pretreatment and increased tensile strength of full thickness incisional skin wounds [42].

The benefits of pretreatment may also apply to non-thermal wounds. There is evidence that thermal treatments can increase the levels of TGF-βeta, a protein involved in scarless wound repair, and bring about better healing outcomes [9, 51, 52]. Work has

been done in our lab on murine models that shows a correlation between HSP70 levels from diode laser pretreatment and increased tensile strength of full thickness incisional skin wounds [42]. Ultimately, a better understanding of the molecular level response to pretreatment will allow for guidance of strategies that might be used in the clinic. We are further investigating the molecular pathways through microarray, real time RT-PCR, and protein based methods that may elucidate which one can not only mitigate the initial damage but that may also accelerate the wound healing process after the injury.

4.6 Conclusions

Herein, we have shown that hsp70 is vitally important for thermotolerance in cell culture. The hsp70 response was tracked through bioluminescence imaging and the viability assessed through fluorescence assays in order to ascertain the best pretreatment parameters for a severe heat shock of 45^{o} C in a water bath. The pretreatment protocol also proved to be effective against the high temperature, short time exposures associated with laser irradiation. The response to heat and pretreatment was applied to the Arrhenius model to examine the changes in the frequency factors and activation energies associated with this bi-phasic heating.

4.7 Acknowledgements

The hsp70 deficient MEF cells and the rescue MEF cells were a contribution from Dr. Clayton Hunt's lab at Washington University. Dr. Prasad Shastri in the Department of Biomedical Engineering generously offered the use of the Synergy Biotek

Fluorescence plate reader. Anton Matafanov provided assistance with the Western blots and Caitlin O'Connell-Rodwell developed the hsp70luc plasmid.

This work was funded through an ASLMS Research Grant and the DOD/AFOSR award No. F49620-01-1-4029.

4.8 References

1. Kelty, J.D., et al., *Thermal preconditioning and heat-shock protein 72 preserve synaptic transmission during thermal stress.* J Neurosci, 2002. **22**(1): p. RC193.
2. Kim, J.M., et al., *Effect of thermal preconditioning before excimer laser photoablation.* J Korean Med Sci, 2004. **19**(3): p. 437-46.
3. Gowda, A., et al., *Cardioprotection by local heating: improved myocardial salvage after ischemia and reperfusion.* Ann Thorac Surg, 1998. **65**(5): p. 1241-7.
4. Sonna, L.A., et al., *Invited review: Effects of heat and cold stress on mammalian gene expression.* J Appl Physiol, 2002. **92**(4): p. 1725-42.
5. Ritossa, F., *A new puffing pattern induced by temperature shock and DNP in Drosophila.* Experientia, 1962. **18**: p. 571-573.
6. Pearce, J. and S. Thomsen, *Optical-thermal response of laser-irradiated tissue*, in *Lasers, photonics, and electro-optics*. 1995, Plenum Press: New York. p. 561-603.
7. Stankiewicz, A.R., et al., *Hsp70 inhibits heat-induced apoptosis upstream of mitochondria by preventing Bax translocation.* J Biol Chem, 2005. **280**(46): p. 38729-39.
8. Bowman, P.D., et al., *Survival of human epidermal keratinocytes after short-duration high temperature: synthesis of HSP70 and IL-8.* Am J Physiol, 1997. **272**(6 Pt 1): p. C1988-94.
9. Capon, A. and S. Mordon, *Can thermal lasers promote skin wound healing?* Am J Clin Dermatol, 2003. **4**(1): p. 1-12.
10. Pespeni, M., M. Hodnett, and J.F. Pittet, *In vivo stress preconditioning.* Methods, 2005. **35**(2): p. 158-64.
11. Lasunskaia, E.B., et al., *Accumulation of major stress protein 70kDa protects myeloid and lymphoid cells from death by apoptosis.* Apoptosis, 1997. **2**(2): p. 156-63.
12. Guo, F., et al., *Abrogation of heat shock protein 70 induction as a strategy to increase antileukemia activity of heat shock protein 90 inhibitor 17-allylamino-demethoxy geldanamycin.* Cancer Res, 2005. **65**(22): p. 10536-44.
13. Westerheide, S.D. and R.I. Morimoto, *Heat shock response modulators as therapeutic tools for diseases of protein conformation.* J Biol Chem, 2005. **280**(39): p. 33097-100.
14. Wischmeyer, P.E., *Glutamine: the first clinically relevant pharmacological regulator of heat shock protein expression?* Curr Opin Clin Nutr Metab Care, 2006. **9**(3): p. 201-6.

15. Kieran, D., et al., *Treatment with arimoclomol, a coinducer of heat shock proteins, delays disease progression in ALS mice.* Nat Med, 2004. **10**(4): p. 402-5.
16. Otaka, M., et al., *The induction mechanism of the molecular chaperone HSP70 in the gastric mucosa by Geranylgeranylacetone (HSP-inducer).* Biochem Biophys Res Commun, 2007. **353**(2): p. 399-404.
17. Vigh, L., et al., *Bimoclomol: a nontoxic, hydroxylamine derivative with stress protein-inducing activity and cytoprotective effects.* Nat Med, 1997. **3**(10): p. 1150-4.
18. Capon, A., et al., *Laser assisted skin closure (LASC) by using a 815-nm diode-laser system accelerates and improves wound healing.* Lasers Surg Med, 2001. **28**(2): p. 168-75.
19. Souil, E., et al., *Treatment with 815-nm diode laser induces long-lasting expression of 72-kDa heat shock protein in normal rat skin.* Br J Dermatol, 2001. **144**(2): p. 260-6.
20. Morimoto, R.I., P.E. Kroeger, and J.J. Cotto, *The transcriptional regulation of heat shock genes: a plethora of heat shock factors and regulatory conditions.* Stress Inducible Cellular Responses, 1996. **77**: p. 139-63.
21. Hunt, C.R., et al., *Genomic instability and enhanced radiosensitivity in Hsp70.1- and Hsp70.3-deficient mice.* Mol Cell Biol, 2004. **24**(2): p. 899-911.
22. Frydman, J., *Folding of newly translated proteins in vivo: the role of molecular chaperones.* Annu Rev Biochem, 2001. **70**: p. 603-47.
23. Belmadani, A., et al., *Inhibition of amyloid-beta-induced neurotoxicity and apoptosis by moderate ethanol preconditioning.* Neuroreport, 2004. **15**(13): p. 2093-6.
24. Kovalchin, J.T., et al., *In vivo delivery of heat shock protein 70 accelerates wound healing by up-regulating macrophage-mediated phagocytosis.* Wound Repair Regen, 2006. **14**(2): p. 129-37.
25. Moseley, P., *Stress proteins and the immune response.* Immunopharmacology, 2000. **48**(3): p. 299-302.
26. Pockley, A.G., *Heat shock proteins, inflammation, and cardiovascular disease.* Circulation, 2002. **105**(8): p. 1012-7.
27. Huang, L., N.F. Mivechi, and D. Moskophidis, *Insights into regulation and function of the major stress-induced hsp70 molecular chaperone in vivo: analysis of mice with targeted gene disruption of the hsp70.1 or hsp70.3 gene.* Mol Cell Biol, 2001. **21**(24): p. 8575-91.
28. Pirkkala, L., P. Nykanen, and L. Sistonen, *Roles of the heat shock transcription factors in regulation of the heat shock response and beyond.* Faseb J, 2001. **15**(7): p. 1118-31.
29. Steel, G.J., et al., *Coordinated activation of Hsp70 chaperones.* Science, 2004. **303**(5654): p. 98-101.
30. Duncan, R.F., *Inhibition of Hsp90 function delays and impairs recovery from heat shock.* Febs J, 2005. **272**(20): p. 5244-56.
31. Michels, A.A., et al., *Hsp70 and Hsp40 chaperone activities in the cytoplasm and the nucleus of mammalian cells.* J Biol Chem, 1997. **272**(52): p. 33283-9.
32. Oh, H.J., X. Chen, and J.R. Subjeck, *Hsp110 protects heat-denatured proteins and confers cellular thermoresistance.* J Biol Chem, 1997. **272**(50): p. 31636-40.

33. Uchiyama, Y., et al., *Heat shock protein 40/DjB1 is required for thermotolerance in early phase.* J Biochem, 2006. **140**(6): p. 805-12.
34. Kampinga, H.H., et al., *Overexpression of the cochaperone CHIP enhances Hsp70-dependent folding activity in mammalian cells.* Mol Cell Biol, 2003. **23**(14): p. 4948-58.
35. Nollen, E.A., et al., *In vivo chaperone activity of heat shock protein 70 and thermotolerance.* Mol Cell Biol, 1999. **19**(3): p. 2069-79.
36. Zhao, Y.G., et al., *Hsp90 phosphorylation is linked to its chaperoning function. Assembly of the reovirus cell attachment protein.* J Biol Chem, 2001. **276**(35): p. 32822-7.
37. Beckham, J.T., et al., *Assessment of cellular response to thermal laser injury through bioluminescence imaging of heat shock protein 70.* Photochem Photobiol, 2004. **79**(1): p. 76-85.
38. Wilmink, G.J., et al., *Assessing laser-tissue damage with bioluminescent imaging.* J Biomed Opt, 2006. **11**(4): p. 041114.
39. Hunt, C. and S. Calderwood, *Characterization and sequence of a mouse hsp70 gene and its expression in mouse cell lines.* Gene, 1990. **87**(2): p. 199-204.
40. Pandita, T.K., et al., *Regulation of telomere movement by telomere chromatin structure.* Cell Mol Life Sci, 2007. **64**(2): p. 131-8.
41. Beckham, J., et al., *Role of HSP70 In Cellular Thermotolerance.* In Submission.
42. Wilmink, G., et al., *Molecular Imaging-Assisted Optimization of Hsp70 Expression During Laser Preconditioning for Wound Repair Enhancement.* J Invest Dermatol, 2008. **In Press**.
43. Moritz, A. and F. Henriques, *Studies of thermal injury in the conduction of heat to and through skin and the temperatures attained therein.* Am. J. Pathol., 1947. **23**: p. 531-549.
44. McNally, K.M., et al., *Optical and thermal characterization of albumin protein solders.* Appl Opt, 1999. **38**(31): p. 6661-72.
45. Rylander, M.N., et al., *Thermally induced injury and heat-shock protein expression in cells and tissues.* Ann N Y Acad Sci, 2005. **1066**: p. 222-42.
46. Simanovskii, D.M., et al., *Cellular tolerance to pulsed hyperthermia.* Phys Rev E Stat Nonlin Soft Matter Phys, 2006. **74**(1 Pt 1): p. 011915.
47. OConnell Rodwell, C.E., et al., *A genetic reporter of thermal stress defines physiologic zones over a defined temperature range.* FASEB Journal, 2003. **18**(2).
48. Dinh, H.K., et al., *Gene expression profiling of the response to thermal injury in human cells.* Physiol Genomics, 2001. **7**(1): p. 3-13.
49. Ross, E.V., J.R. McKinlay, and R.R. Anderson, *Why does carbon dioxide resurfacing work? A review.* Arch Dermatol, 1999. **135**(4): p. 444-54.
50. Rylander, M.N., et al., *Correlation of HSP70 expression and cell viability following thermal stimulation of bovine aortic endothelial cells.* J Biomech Eng, 2005. **127**(5): p. 751-7.
51. Cao, Y., et al., *TGF-beta1 mediates 70-kDa heat shock protein induction due to ultraviolet irradiation in human skin fibroblasts.* Pflugers Arch, 1999. **438**(3): p. 239-44.

52. Wehrhan, F., et al., *Exogenous Modulation of TGF-beta(1) Influences TGF-betaR-III-Associated Vascularization during Wound Healing in Irradiated Tissue.* Strahlenther Onkol, 2004. **180**(8): p. 526-33.

CHAPTER V

MICROARRAY ANALYSIS OF CELLULAR THERMOTOLERANCE

Josh T. Beckham[1], Gerald J. Wilmink[1], Susan R. Opalenik[2], Mark A. Mackanos[4], Alex A Abraham[1], Keiko Takahashi[3], Chris H. Contag[4], Takamune Takahashi[3], E. Duco Jansen[1]

[1] Department of Biomedical Engineering, Vanderbilt University, Nashville, TN

[2] Department of Pathology, Vanderbilt University, Nashville, TN

[3] Department of Medicine, Vanderbilt University, Nashville, TN

[4] Departments of Pediatrics, Radiology and Microbiology & Immunology, Stanford University, Stanford, CA

Vanderbilt University

Nashville, TN 37235

5.1 Abstract

Background and Objectives: Previously, we have shown that a 43^{o}C pretreatment can provide thermotolerance to a later, more severe thermal stress at 45^{o}C. Using cells that lack the *Hsp70* gene, we also showed that there is still some thermotolerance when HSP70 protein is missing. The purpose of this study was to determine which genes play a role in thermotolerance and specifically to understand which pathways may be responsible in the absence of HSP70.

Study Design/Materials and Methods: Murine Embryonic Fibroblast cells with and without *Hsp70* (MEF(+/+) and MEF(-/-), respectively) were exposed to a mild heat shock of 43^{o} C for 30 minutes in a constant temperature water bath. After 3 hours of recovery, RNA was harvested from three heated samples sets alongside three untreated controls using a MicroRNeasy kit with DNAse treatment. RNA quality was verified by Agilent Bioanalyzer. The RNA was then converted to cDNA and hybridized to Affymetrix gene expression DNA microarrays. The genes that showed 2-fold change (up or down) relative to unheated controls were filtered by *t*-test for significance at a threshold of $p < 0.05$ using Genespring software. Data was verified by RT-PCR. Genes were then categorized based upon their ontology. **Results**: While many genes were similarly upregulated the main difference between cell types was the increase in transcription factors and nucleic acid binding proteins. Several members of the heat shock protein family (*Hsp70*, *Hsp40*, *Hsp110*, *Hsp25)* were upregulated greater than 2-fold, however, *Hsp90* only increased by 50% under these conditions despite its role in thermotolerance. **Conclusions**: The data herein provides a framework for investigating those genetic pathways that are of interest to pretreatment studies of laser irradiation and, in particular, highlights those genes that may be of importance in the absence of one of the most effective thermotolerance genes, *Hsp70*.

5.2 Introduction

Unwanted thermal damage to tissue that is adjacent to a target site can arise from many different clinical applications such as radiofrequency ablation of tumors, and laser irradiation in dermal cosmetic procedures (e.g. skin resurfacing, hair removal, tattoo removal, port wine stain treatment) [1-4]. Clinicians are faced with a balance of using enough energy for therapeutic efficacy while still staying within a margin of safety to minimize collateral damage. Proteins within the cell that have been denatured by thermal stress are rendered non-functional and ultimately toxic [5]. The ability to mitigate this damage in advance through thermal preconditioning may lead to more desirable outcomes in reducing redness, swelling, blistering and dyspigmentation [6, 7]. Essentially a mild thermal stress applied to the tissue several hours before induces several different proteins and pathways that repair and prevent thermal damage. The most well understood of these thermally sensitive pathways is the heat shock response (HSR) which is made up of heat shock proteins and molecular chaperones which work together to refold denatured proteins or direct them to degradation through the proteasomal pathway [8]

One of the proteins of this response, HSP70, is of particular importance to thermotolerance [9, 10]. Not only does HSP70 protein help to refold denatured proteins, but it also directly inhibits the apoptotic pathway through interfering with BAX signaling to the mitochondria [11]. In our previous study using an HSP70 knockout cell line compared to cell that had the protein, we observed that HSP70 is not the sole mediator of thermotolerance after water bath heating [12, 13]. The differential survival data between these two cell lines show that HSP70 accounts for the majority of thermotolerance. However, there remains a small but still significant increase in survival after pretreatment in the HSP70 deficient MEF (-/-) cells. Consequently, there must exist other pathways and proteins that are able to confer

thermotolerance in the absence of HSP70. The presence of such a pathway would not be surprising since the cell has many redundant systems in place.

In order to better understand the mechanisms responsible for increased cellular survival due to thermal preconditioning; we utilized an expression level approach through cDNA microarray analysis. This technology provides a method to screen thousands of genes that may play a functional role in thermotolerance. The gene list can then be narrowed down to ones showing significant changes in expression. These changes can then be more accurately quantified by selecting a few of interest for quantitative RT-PCR. Potentially, analyzing the genes that show the most changes will allow for more targeted research to be carried out on pathways that could be activated or suppressed to enhance laser-tissue interaction outcomes in the clinic.

5.3 Material & Methods

5.3.1 Cell Culture

Adherent MEF(-/-), murine embryonic fibroblast, cells made deficient in *Hsp70* through homologous recombination of a region encompassing both isoforms of the murine *Hsp70* gene – *Hspa1a* and *Hspa1b* – were a generous gift from Dr. Clayton Hunt at Washington University [14]. The resulting knockout cells had a neomycin resistance fragment inserted in place of the *Hsp70* genes. A rescue cell line - denoted as MEF(+/+) – was generated from the knockout cells through re-introduction of the *Hspa1b* gene through stable transfection of the *Hsp70* promoter with the *Hspa1b* coding sequence. These were used as control cells as their growth characteristics were shown to more appropriately match the knockout cells than a wild type strain of MEF cells (data not shown). These isoforms of HSP70 protein only differ by one amino acid and are thought to be redundant in their

functions except for the lack of *Hspa1a* expression in murine liver tissue and differential upregulation in embryonic development [9, 14, 15]. However, in these murine embryonic cells the introduced *Hspa1b* gene was shown to express its protein in a similar fashion to wild type cells through Western blotting in our previous work [13].

Cells were maintained in a 5% CO_2 incubator (Fisher Scientific) in DMEM (Invitrogen, Carlsbad, CA) supplemented with 10% fetal calf serum (ATCC, Manassas, VA) with 2μl/ml of Normocin (Invivogen, San Diego, CA). For experiments, each 96 well plate was covered with a gas permeable membrane (# 2928-0100, USA Scientific, Ocala, FL) to reduce evaporation of the media and to seal the wells during water bath experiments.

5.3.2 Water Bath Heat Treatment

Prior to thermal treatment, cells were plated at a density of $3x10^3$ cells/100 μl of media in removable 8-well strips from a 96 well plate – 6.4 mm diameter, 0.32 cm^2 surface area (Corning, Lowell, MA). Only the six middle wells in each strip were used so as to reduce edge effects of variable heating around the sides due to the structure of the plate. At 20 hours after seeding, a portion of the samples were pretreated with a mild heat shock of 43^{o}C for 30 minutes in an electronically controlled, constant temperature water bath that was accurate to within +/- 0.1^{o}C (Fisher Scientific). Temperatures were verified with a separate digital thermometer. The 43^{o}C temperature was chosen because it showed strong induction of *Hsp70* without reductions in cell growth. The individual 8-well strips were placed in a foam floating device for the water bath exposures. After preshock, a range of severe heat shocks (5-50 min at 45^{o}C) were administered. The lag time - as defined as the waiting period between the preshock (PS) and the more severe heat shock (HS) - was 4 hours, during which cells were allowed to recover in the incubator at 37^{o}C.

5.3.3 Viability Assays

As an endpoint for the efficacy of thermotolerance, viability at 24 and 48 hours after the severe heat shock (HS) was measured by adding 20 µl of Cell Titer Blue (Promega, Madison, WI) reagent to 100µl of cell culture media per well, as per the manufacturer's specifications. The fluorescence emission was quantified on the Synergy HT microplate reader (BioTek, Winooski, VT) at 560/590 nm (excitation/emission) after a 1 hour incubation at 37^{o}C. The baseline fluorescence of wells containing only media without the dye was subtracted from each sample. All intensities were normalized to the fluorescence of untreated controls on the same plate.

5.3.4 RNA Isolation and Quality Control

For the microarray and real time RT-PCR experiments, cells only received a pretreatment at 43^{o}C for 30 minutes but no severe heat shock. At 3 hours after thermal treatment, cell lysates from 144 individual wells were pooled and total RNA was harvested. Approximately 4-6 µg of RNA was isolated with the RNeasy Micro Kit (Qiagen, Valencia, CA) along with on column DNAse treatment (Qiagen). Sample lysis buffer in the RNeasy Kit was used without adding β-mercaptoethanol in order to reduce background noise on the microarrays.

RNA integrity was assessed by the VMSR (Vanderbilt Microarray Shared Resource) using Agilent's Bioanalyzer microfluidic assay (Agilent Technologies, Palo Alto CA). Spectrophotometric and fluorometric methods were combined to quantify protein and nucleic acids present. Samples that had RIN (RNA integrity number) values above 8.0, ribosomal RNA Ratios [28s / 18s] near 1.9, and 260/280 nm and 260/230 nm absorbance ratios from the spectrophotometer near 2.0 were considered acceptable.

5.3.5 Microarray Experiments

For screening of genes upregulated by the thermal stress, microarrays for 3 biological replicates for each condition (PS and Ctrl) were tested for the MEF(-/-) cells while only 2 biological replicates were used for the MEF(+/+) cells. Only two replicates were used on the MEF(+/+) cells because many of the same genes were upregulated as in the MEF(-/-). Furthermore, the MEF(+/+) data was of consistent quality between the array sets. Microarrays were hybridized and analyzed through the VMSR Core Facility, as per standard protocols (http://array.mc.vanderbilt.edu/).

After quality control, biotinylated complementary RNA was hybridized to an Affymetrix GeneChip Mouse Genome 430 2.0 Array containing 45,000 sets of 11 to 25-mer oligomers, representing 39,000 mouse transcripts (34,000 are annotated as well-defined genes).

GeneChips were scanned using GeneChip Scanner 3000 7G Plus 2 and GeneChip Operating System (GCOS, Affymetrix, Santa Clara, CA). Raw signal intensity values of fluorescence were used to grid images for each gene spot and generate files for further analysis. The microarray data has been uploaded as .CEL and .CHP files according to MIAME standards to the GEO (Gene Expression Omnibus) databank for universal access at geo@ncbi.nlm.nih.gov under the series record (GSE11120).

CEL files (raw Affymetrix data) were imported in GeneSpring 7.3 (Agilent Technologies) and transformed by Mas5 analysis to show normalized signal intensity values. The genes that showed 2-fold change (up or down) in 2 of the 3 samples, MEF(-/-) and 1 of 2 samples, MEF(+/+), were filtered by student's *t*-test for significance at a threshold of $p < 0.05$. Fold inductions were represented as the average of heated samples over the median of the unheated control values for each gene. For the MEF(-/-) genes a Benjamini Hochberg MTC (multiple testing correction) was used prior to the *t*-test analysis. However, the MTC

was not done on the MEF(+/+) genes because the lower replicate numbers would only yield 4 genes when a MTC is added to reduce false positives. Without the MTC, over 200 genes were returned with a confidence of $p < 0.05$. The downside to removing the MTC is that the false discovery rate is 39%. However, our analysis focused on the most highly upregulated genes which have inherently less probability of being false positives than lower expressing genes.

Gene ontology was analyzed with WebGestalt using the annotations from Genespring and the NCBI Entrez Gene website [16]. A spreadsheet was created for groups of genes representing proteins with specific molecular functions (e.g., transcriptional factors), biological process (e.g. signal transduction) or pathway (e.g., TGF-beta signaling). The 'molecular functions' is a broad categorization scheme for genes that show a similar function within the cell. Pathways are more specific category that signifies direct interactions between the gene products that carry out a process in the cell. On the other hand, genes in the same molecular function category do not have to have a direct interaction with other genes in the group.

5.3.6 Quantitative RT-PCR

In order to validate the expression levels of those genes of interest indentified by microarray, quantitative RT-PCR (reverse transcriptase polymerase chain reaction) analysis was performed. Two μg of each sample was reverse transcribed into single stranded cDNA with a high capacity cDNA archive kit using random primers according to manufacturer's instructions (Applied Biosystems, Foster City, CA). cDNAs were used as template in singleplex PCR reactions using Sybr Green (Sigma, St. Louis, MO) as the detection dye for double stranded cDNA. The housekeeping gene, *Gapdh*, was selected as the endogenous control because, under heat shock conditions, it had the smallest intra-sample variability.

Table 5.1 shows the primers that were designed using Beacon® Design software. These were selected based on their known involvement in the heat shock response or because they were of interest for future study. The optimal annealing temperatures were determined through melt curve analysis and reaction efficiencies with a standard dilution curve. The dynamic range of each primer was also determined. All primers except *Egr1* were designed to be intron spanning in the coding sequence of the gene to reduce detection of residual genomic DNA. A reaction containing RNA only was run to confirm the absence of genomic DNA within RNA samples prior to reverse transcription.

Table 5.1 qRT-PCR primers and conditions. Forward and reverse primer sequences used for SybrGreen analysis of genes expression at the listed annealing temperatures and fluorescence capture after the given melt temperatures to reduce non-specific signal.

Gene Target	Forward	Reverse	Annealing Temp	Capture Temp
Hspa1b	ATCGAGGAGGTGGATTAGAGGC	ACCTTGACAGTAATCGGTGCCC	60 °C	80° C
Atf3	AGTCACCAAGTCTGAGGCGG	CTCCAGTTTCTCTGACTCTTTCTGC	60	80
Hsp110	CTGTGTCATCTCAGTCCCATCCTT	GCAACAGCCGTCATGTCATTC	60	80
Egr1	GACCACCTTACCACCCACATCC	TGCCTCTTGCGTTCATCACTCC	60	80
Hspb1	ACAGTGAAGACCAAGGAAGGC	TGAAGCACCGAGAGATGTAGC	60	80
Dnajb4	AGTTTGGCGAAGAAGGCTTGAAG	ACCTCCACCCATCCGTCTCC	60	80
Dnajb1	CGAACAACATTCCAGCAGACATC	CCAGAGTAGGGACATTCACAGTG	60	80
Gadd45g	GCCCAGCATCACCCTTCCC	GCCACTCCAGAGCCAGCAG	60	80
Gapdh	GCCTTCCGTGTTCCTACCC	GCCTGCTTCACCACCTTCTTG	60	80
Dnaja4	GGTGGTGGAGGACGGATGAC	ACCGATGCCTTCACATTTCTCAC	60	78
Fos	CGCAGAGCATCGGCAGAAG	GCAGCCATCTTATTCCGTTCCC	64.5	80

Each PCR reaction contained 5 µL of cDNA template (20 ng RNA equivalent), 10 µL 2X Sybr Green JumpStart *Taq* Ready Mix (Sigma), 1.2 µL of both forward and reverse primers (300 nM final concentration) and 2.6 µL of water for a total volume of 20 µl in each well of a 96 well PCR plate. The cycling PCR reactions were performed in the iCycler, iQ real-time PCR system (Bio-Rad) and consisted of a hot start at 94^{o} C for 2 min, then 40

cycles of (60°C for 30 sec, 72°C for 30 sec, 80°C for 10 sec). One primer set, *Fos*, required an annealing temperature of 64.5°C.

Fluorescence of the double stranded products was captured during the last cycle after a 10 second hold at either 80°C or 78°C to melt out non-specific primer dimers and to reduce background fluorescence. Relative quantitation of mRNA levels was assessed using the $2^{-\Delta\Delta Ct}$ (Livak) method described in the Bio-Rad Real Time Application Guide [17]. The expression was normalized to the housekeeping gene *Gapdh* by subtracting the C_T values from those of the gene of interest for each sample (ΔC_T). Then the ΔCt values of the unheated controls were subtracted from the ΔC_T values of the pretreated samples ($\Delta\Delta C_T$) and the negative of this value was then raised to the second power rendering a fold induction compared to control.

The range for each fold change from the qRT-PCR experiments represents the fold change with the standard deviation either added or subtracted, as expressed as: $2^{(-\Delta\Delta Ct \pm St.\ Dev.)}$ as described in User Bulletin No. 2 ABI PRISM 7700 Sequence Detection System [18].

5.4 Results

5.4.1 HSP70 Rescues MEF Cells From Heat Stress

As noted in our previous work, *Hsp70* deficient cells are able to gain thermotolerance through a pretreatment protocol. Figure 5.1 shows that when a mild pretreatment (PS) of 43°C for 30 minutes is given 4 hours prior to a more severe heat shock (HS) at 45°C, there is an increase in survival at the 48 hour post heating time compared to samples that were not pretreated. This survival advantage is markedly evident in the rescue cells (+/+) that have *Hsp70* in them since the survival assay measures the number of viable cells within the well because only live cells are able to reduce the non-fluorescent reagent resazurin into the

fluorescent product resorufin. However, despite the absence of both isoforms of the inducible *Hsp70* gene in the MEF(-/-) cells, they are still able to show an increase in survival due to pretreatment. Consequently, there are other proteins and pathways within these cells that permit some degree of heat tolerance through pretreatment.

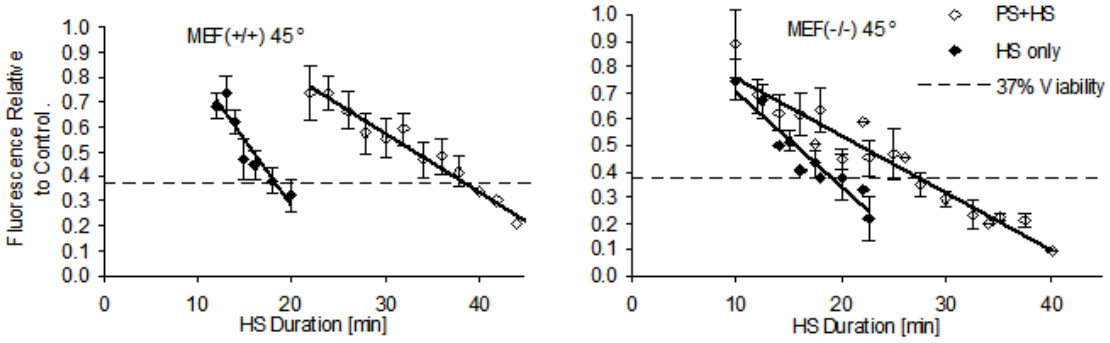

Figure 5.1 Viability assays at 48 hrs for 45°C heat shocked MEF(+/+) and MEF(-/-) cells. Samples were either heat shocked (HS) alone (closed symbols) at 45° C for varying durations (10-50 minutes) or treated with preshock (PS) of 43° C for 30 minutes at 4 hours prior to HS (open symbols). Cells were allowed to recover for 48 hrs and then imaged with Cell Titer Blue fluorescent viability assay with a 1 hour incubation. Solid lines are the linear best fits to the data. The dashed line represents 37% fluorescence intensity relative to untreated controls. Error bars are the Standard Error of the Mean.

5.4.2 Genes with Highest Fold Change in MEF(-/-) and MEF(+/+) cells

In order to screen for those genes that may be differentially expressed in the *Hsp70* containing (+/+) cells relative to the *Hsp70* deficient (-/-) cells, a microarray analysis was conducted on samples that were pretreated. An online program was used to create a Venn diagram in Figure 5.2 that shows the grouping between genes that were upregulated only in MEF(-/-) cells, only in MEF(+/+) or in both cell types [19]. In order to make the list for each cell line, all of the probesets on the microarray which showed a $\geq$ 2-fold change (either upregulated or downregulated relative to control) in signal intensity after filtering with a

student's *t*-test at p≤ 0.05 were included. In MEF(-/-) cells the genes had to show 2-fold change in 2 of the 3 pretreated samples while in the MEF(+/+) cells, that had fewer arrays, the requirement was only a 2 fold change in 1 of the 2 pretreated conditions. Consequently, due to these less stringent requirements, the MEF(+/+) arrays produced a list of 156 genes compared to 135 in the MEF(-/-) cells after *t*-test. The genes with 2.5 fold-change or greater from each cell type were then taken from these lists and analyzed using the Venn diagram. The diagram in Figure 5.2 shows that there are 32 genes that showed changes in both cell types. There are 35 genes upregulated exclusively in MEF(-/-) cells and 19 that are unique to MEF(+/+) cells.

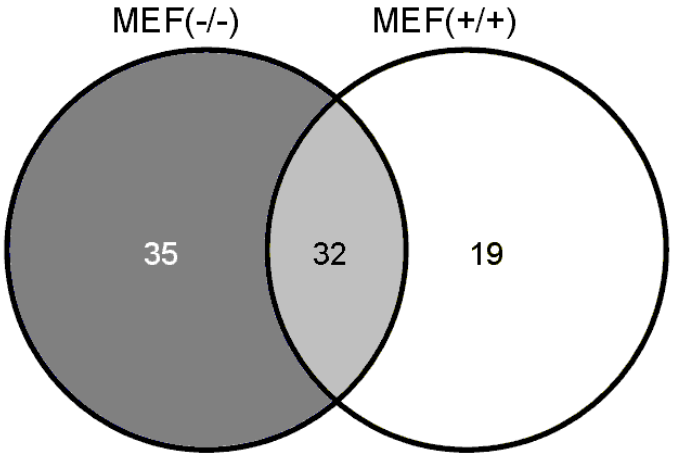

Figure 5.2 Venn diagram representing grouping of genes with at least 2.5 fold-change after thermal pretreatment. The number of commonly expressed genes are in the middle (32) and genes only expressed in MEF(-/-) cells are on the left (35 genes). Those only expressed in MEF(+/+) cells are on the right (19 genes). Genes were filtered by a student's *t*-test for a significance value of p≤ 0.05.

The twenty most highly expressed genes for each cell type relative to untreated controls are shown in Table 5.2 with their values for fold change. Neither of the lists includes downregulated genes since the magnitude of their fold change was below the 2-fold change

filter that we set (which corresponds to either 2 fold change for an increase or a 0.5 change for a decrease).

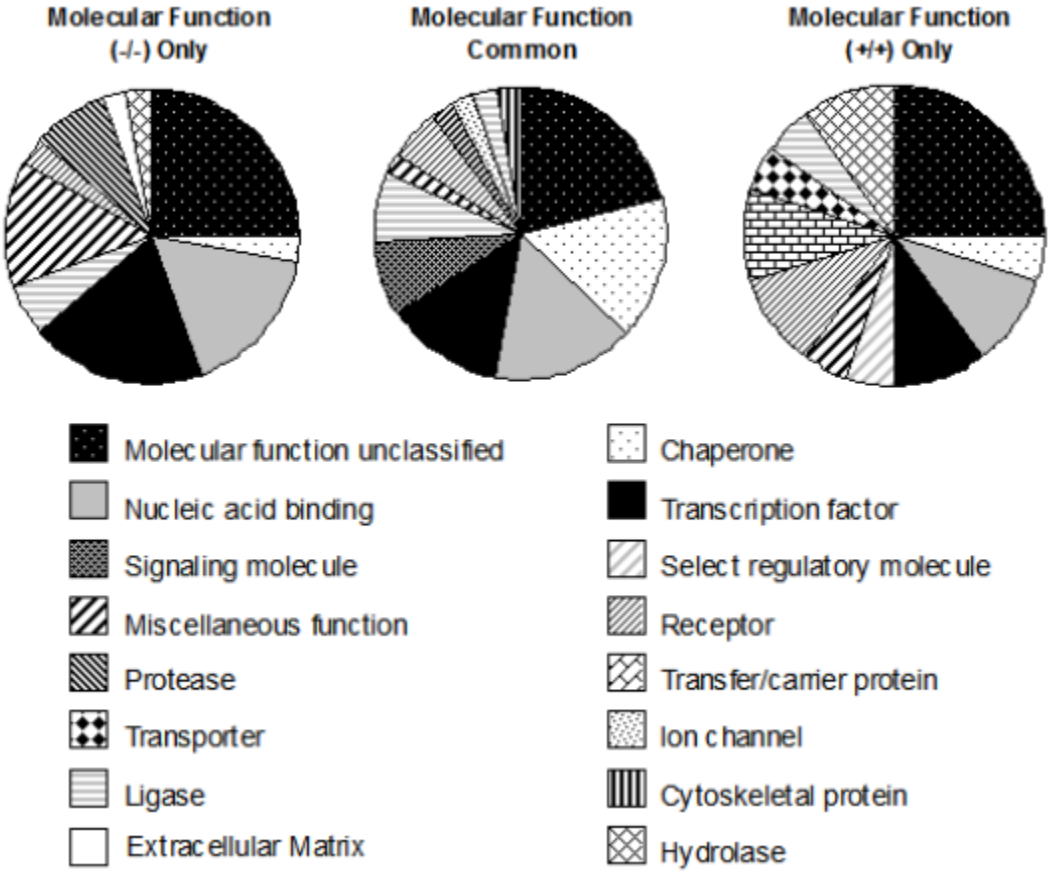

Figure 5.3 Diagrams of molecular functions of the common and differential genes with at least 2.5 fold-change in MEF(-/-) and MEF(+/+) cells after thermal pretreatment. Genes were filtered by a student's *t*-test for a significance value of $p \leq 0.05$. The genes from each cell type were compared by Venn diagram analysis then separated into three lists and sorted by molecular functions using Panther©.

It can be seen that there is an unexpected signal for *Hspa1b* in the MEF(-/-) cells. However, this is an artifact of detection because while these cells are deficient in the *Hspa1a* and *Hspa1b* genes, they have a neomycin resistance gene inserted in place of the two heat shock genes. This substitution retains a small piece of the 3' end of the heat shock gene intact. Consequently, since the Affymetrix Mouse 430 2.0 microarray targets the 3' end of the mRNA transcript, this last piece is being detected as *Hspa1b* signal. We have confirmed

through our qRT-PCR results and Western blot analysis that HSP70 protein is not present. The qRT-PCR primers target the mRNA in a different location and, as expected, show no signal in the MEF(-/-) cells.

For the MEF(+/+) cells, the most highly induced gene is *Hspa1b* at 99.5 fold change increase. This finding is consistent with literature in that *Hsp70* tends to be the most highly upregulated gene in cell culture after thermal stresses [14]. However, the actual value may not be consistent with a true wild type cell line. These cells have the *Hspa1b* gene reintroduced into the location where the original deletion of both *Hspa1a* and *Hspa1b* resided. Consequently, the levels of transcription may be altered. However, Western blot studies show that protein levels of HSP70 after heat shock are similar in trends to wild type cells (data not shown).

Table 5.2 List of most highly changed genes after preshock treatment relative to unheated controls in MEF(-/-) cells and then MEF(+/+) cells with fold change and p-value of significance across the group of arrays. For a select set of genes, qRT-PCR fold change relative to *Gapdh* was determined by the comparative C_T method for quantitative validation of the microarray values. The range for the qRT-PCR was obtained using the standard deviation : Range = $2^{(-\Delta\Delta Ct \pm \text{St. Dev.})}$. N.D. = not determined.

MEF(-/-) Cells		Microarray		qRT-PCR	qRT-PCR
Symbol	Description	Fold Change	p-value	Fold Change	Range
*Hspa1b**	heat shock protein 1B (hsp70)	214.0*	0.0080	undetected	-
Atf3	activating transcription factor 3	25.9	0.0136	63.5	30 - 132
P2rx7	purinergic receptor P2X, ligand-gated ion channel, 7	17.6	0.0183		
Lor	loricrin	12.7	0.0190		
Dnaja4	DnaJ (Hsp40) homolog, subfamily A, member 4	10.3	0.0453	17.8	11- 28
Cpn1	carboxypeptidase N, polypeptide 1	7.1	0.0123		
Egr1	early growth response 1	7.0	0.0499	13.1	4.6 - 37.2
Sprr1a	small proline-rich protein 1A	6.2	0.0295		
Dnajb1	DnaJ (Hsp40) homolog, subfamily B, member 1	6.0	0.0154	12.0	6.3 - 22.9
Gadd45g	growth arrest DNA-damage-inducible 45 gamma	5.8	0.0250	4.5	2.6 - 7.6
Mansc1	MANSC domain containing 1	5.6	0.0278		
2310014L17Rik	RIKEN cDNA 2310014L17 gene	5.4	0.0279		
Zfand2a	zinc finger, AN1-type domain 2A	5.0	0.0061		
1200016B10Rik	RIKEN cDNA 1200016B10 gene	4.9	0.0227		
Clu	clusterin	4.9	0.0375		
Fos	FBJ osteosarcoma oncogene	4.8	0.0280	6.2	2.6 - 14.6
Hsp110	heat shock protein 110	4.8	0.0251	6.8	3.1 - 15.1
Txnip	thioredoxin interacting protein	4.7	0.0115		
Hspb1	heat shock protein 1 (hsp25)	4.6	0.0433	16.0	9.8 - 26.0
Pgf	placental growth factor	4.5	0.0154		
Fosb	FBJ osteosarcoma oncogene B	4.4	0.0154		
Dnajb4	DnaJ (Hsp40) homolog, subfamily B, member 4	4.1	0.0425	4.7	2.8 - 7.9
Gapdh	glyceraldehyde-3-phosphate dehydrogenase			1.0	0.7 - 1.4

* Hspa1b: represents artifact detection from 3' end of substituted Neomycin gene by microarray primer in hspa1b MEF(-/-) cells

MEF (+/+) Cells	Description	Microarray	p-value	q-RT-PCR	Range
Hspa1b	heat shock protein 1B (hsp70)	99.5	0.0067	1290.2	416 - 3997
Atf3	activating transcription factor 3	33.1	0.0067	41.1	17 - 100
P2rx7	purinergic receptor P2X, ligand-gated ion channel, 7	23.4	0.0084		
Lor	loricrin	13.8	0.0055		
Dnaja4	DnaJ (Hsp40) homolog, subfamily A, member 4	8.6	0.0093	9.0	5.1 - 16.2
Fosb	FBJ osteosarcoma oncogene B	6.5	0.0091		
Dnajb1	DnaJ (Hsp40) homolog, subfamily B, member 1	6.0	0.0011	5.1	2.1 - 12.1
Rgs2	regulator of G-protein signaling 2	4.9	0.0252		
Hsp110	heat shock protein 110	4.9	0.0092	6.3	3.5 - 11.6
Sox9	SRY-box containing gene 9	4.8	0.0466		
Zfand2a	zinc finger, AN1-type domain 2A	4.6	0.0285		
Dnajb4	DnaJ (Hsp40) homolog, subfamily B, member 4	4.6	0.0048	6.5	3.9 - 10.9
BC032204	cDNA sequence BC032204(Fermt3)	4.4	0.0254		
Pgf	placental growth factor	4.2	0.0170		
Hspb1	heat shock protein 1 (hsp25)	4.2	0.0298	10.8	6.9 - 16.9
39698	MKIAA4020 protein	3.8	0.0263		
1200016B10Rik	RIKEN cDNA 1200016B10 gene	3.8	0.0356		
Ampd1	adenosine monophosphate deaminase 1 (isoform M)	3.7	0.0210		
Apol2	apolipoprotein L, 2	3.7	0.0086		
Bcl2l11	BCL2-like 11 (apoptosis facilitator)	3.7	0.0255		
Gadd45	growth arrest DNA-damage-inducible 45 gamma	2.9	0.0472	1.2	0.6 - 2.2
Egr1	early growth response 1	2.5	N.D.	3.4	1.8 - 6.3
Fos	FBJ osteosarcoma oncogene	2.0	N.D.	1.2	0.6 - 2.2
Gapdh	glyceraldehyde-3-phosphate dehydrogenase			1.0	0.6 - 1.7

5.4.3 Genes Displaying Differential Expression in MEF(-/-) Relative to MEF(+/+)

Table 5.3A and 5.3B shows the genes that have differential expression between the two cell lines. Consequently, this table highlights differences in expression instead of similar expression – as is seen in Table 5.2. In Table 5.3A the genes with higher expression in MEF(-/-) cells than in MEF(+/+) cells after preshock are shown. To obtain the ratio shown in the left most column, the fold change data from the microarrays (PS divided by Ctrl) for the MEF(-/-) cells was divided by the fold changes in MEF(+/+) cells (either up or down regulated). Essentially, those genes with a high value for the ratio are predominantly expressed in the MEF(-/-) heated condition (Table 5.3A), whereas, those with a low ratio are expressed in the MEF(+/+) cells (Table 5.3B). The list here differs from Table 5.2 because it incorporates genes that are expressed at high levels in one cell type but not in another, while the lists in Table 5.2 have many common elements. The most differently expressed gene is *Hsp70*. However, it is not on the list in Table 5.3A because there was no expression of this gene in the *Hsp70* deficient cells and, therefore, a ratio could not be calculated.

The ratios of three of the genes (*Egr1*, *Fos*, *and Gadd45g*) were also in the set on which we performed qRT-PCR. Consequently, the data in parentheses in Table 5.3a from qRT-PCR validates the ratios from the microarray data.

Figure 5.4 shows a chart of the various molecular functions of the genes from Table 5.3a and 5.3b. The 15 genes with the highest ratio (Table 5.3A) and the 15 genes with the lowest ratio (Table 5.3B) between MEF(-/-) and MEF(+/+) were analyzed using Panther© software to group the molecular functions of each gene together [20]. The number of gene for a given function relative to the total number of genes in the list is then represented in Figure 5.4 as a portion of the pie chart. In Figure 5.4, it can be seen that transcription factors, nucleic acid binding, and kinases have more genes expressed in the list of genes with differential expression between MEF(-/-) cells to MEF(+/+) cells. On the other hand, genes for receptors

and signaling molecules represent the functions more highly expressed in the MEF(+/+) cells which may indicate that the cell is preparing to send and receive intercellular and intracellular messages in order to communicate about further, impending heat stress.

Table 5.3 Lists of genes with the most differential expression between MEF(-/-) and MEF(+/+) cells after thermal pretreatment from microarray experiments. A ratio was calculated as the fold change in (-/-) cells divided by the fold change in (+/+) cells. (3A) Genes more highly expressed in MEF(-/-), i.e. high ratio. (3B) Genes more highly expressed in MEF(+/+), i.e. low ratio.

Table 3A

Ratio	Fold Change				
- - / + +	PS/Ctrl	PS/Ctrl			
Microarray (qRT-PCR)	-/-	+/+	Symbol	Description	Biological Process
2.86 (3.86)	7.2	2.5	*Egr1*	early growth response 1	transcription, T cell differentiation
2.71	0.7	0.3	*Magi2*	membrane associated guanylate kinase	signal transduction
2.69	2.7	1.0	*Egr2*	early growth response 2	transcription
2.46 (5.32)	4.8	2.0	*Fos*	FBJ osteosarcoma oncogene	cell cycle, regulation of transcription, DNA-dependent
2.30	3.3	1.4	*Hemt1*	hematopoietic cell transcript 1	
2.27 (3.70)	6.5	2.9	*Gadd45g*	growth arrest and DNA-damage-inducible 45 gamma	cell cycle, MAPKK activity, negative regulation of kinase activity, apoptosis
2.23	0.8	0.4	*Epha4*	Eph receptor A4	protein amino acid phosphorylation
2.18	0.8	0.4	*Zic3*	zinc finger protein of the cerebellum 3	transcription
2.14	0.8	0.4	*BB265744*	EST	
2.07	2.1	1.0	*Trib3*	tribbles homolog 3 (Drosophila)	
2.05	1.0	0.5	*Araf*	v-raf murine sarcoma 3611 viral oncogene homolog	cell cycle, protein amino acid phosphorylation, signal transduction
2.04	1.3	0.6	*B230117O15Rik*	RIKEN cDNA B230117O15 gene	
2.01	1.7	0.9	*Ppp1r2*	Protein phosphatase 1, regulatory (inhibitor) subunit 2 (Ppp1r2), mRNA	carbohydrate metabolism, glycogen metabolism
2.01	0.9	0.5	*Lhx1*	LIM homeobox protein 1	endoderm formation, regulation of transcription, gastrulation
2.01	1.6	0.8	*1500010G04Rik*	RIKEN cDNA 1500010G04 gene	

Table 3B

Ratio	Fold Change				
- - / + +	PS/Ctrl	PS/Ctrl			
Microarray (qRT-PCR)	-/-	+/+	Symbol	Description	Biological Process
0.52	0.8	1.5	*Ambp*	alpha 1 microglobulin/bikunin	transpor, protein-chromophore linkage, cell adhesion, pregnancy
0.51	1.0	2.0	*Suv39h2*	Suppressor of variegation 3-9 homolog 2 (Drosophila)	chromatin assembly or disassembly
0.51	0.6	1.2	*C030044M21Rik*	RIKEN cDNA C030044M21 gene	
0.51	0.6	1.2	*AV302409*	EST	
0.51	1.0	2.0	*Gpr30*	G protein-coupled receptor 30	signal transduction, G-protein coupled receptor protein signaling pathway
0.50	1.9	3.7	*Apol2*	apolipoprotein L, 2	lipid transport
0.49	0.8	1.5	*Smad3*	MAD homolog 3 (Drosophila)	negative regulation of transcription from RNA polymerase II promoter
0.49	0.8	1.7	*Lin7b*	lin 7 homolog b (C. elegans)	transport, exocytosis, intracellular signaling cascade, protein transport
0.48	1.2	2.5	*6430570G24*	hypothetical protein 6430570G24	
0.47	1.3	2.8	*B230215L15Rik*	RIKEN cDNA B230215L15 gene	
0.46	1.0	2.2	*Pmaip1*	phorbol-12-myristate-13-acetate-induced protein 1	release of cytochrome c, induction of apoptosis
0.45	0.7	1.6	*1810033B17Rik*	RIKEN cDNA 1810033B17 gene	
0.45	1.3	2.8	*1190002H23Rik*	RIKEN cDNA 1190002H23 gene	cell cycle
0.45	0.6	1.4	*Cox10*	COX10 homolog, cytochrome c oxidase assembly protein, heme A	heme biosynthesis, protein amino acid farnesylation
0.43	1.1	2.5	*BB147698*	EST	

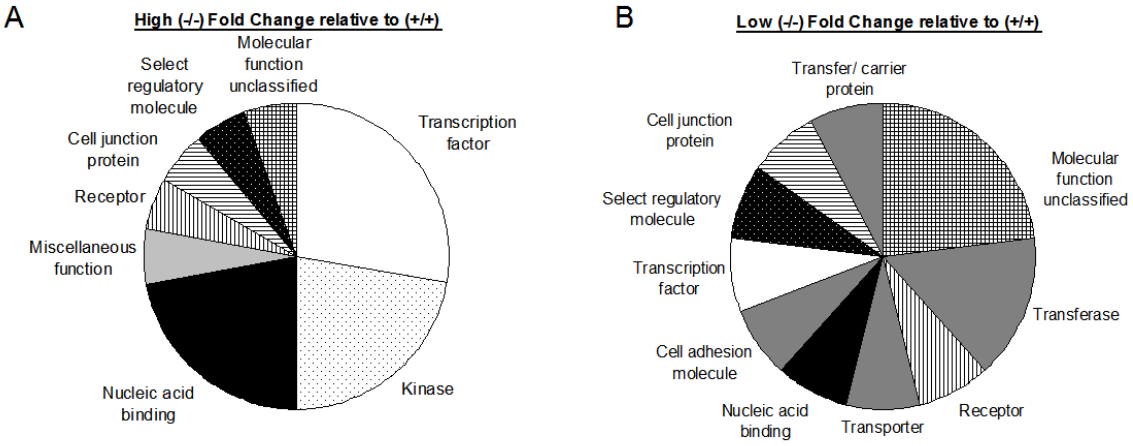

Figure 5.4 Diagram of molecular functions of genes with the most differential expression from Table 3A and 3B. that have a high ratio of expression between the two cell types. (A): Molecular function of the 15 genes with the highest ratio of fold change in MEF(-/-) cells after thermal preshock relative to MEF(+/+) cells as seen in Table 3A. (B): Molecular function of 15 genes with a lowest ratio of fold change in MEF(-/-) cells after thermal preshock relative to MEF(+/+) cells as seen in Table 3B. The genes were grouped according to their molecular function using Panther©.

5.4.4 Validation of Microarray Data Using qRT-PCR

In Figure 5.5, several genes from the microarray were selected for quantitative validation with qRT-PCR using the comparative C_T method with *Gapdh* as the reference gene.Six of these were chosen because they are known to be involved in the thermal response and are likely to be key interventional points in further studies e.g. *Hspa1b, Ddnaja4, Dnajb1, Hsp110, Hspb1, and Dnajb4* [21-25]. The other ones were chosen because they offer opportunities for further study.

QRT-PCR results confirmed that the *Hspa1b* message was absent in our MEF(-/-) cells despite the reported levels in the microarray signal that were due to detection of the substituted antibiotic resistance gene, neomycin. This is consistent with our negative Western blot findings for HSP70 protein in these cells (data not shown).

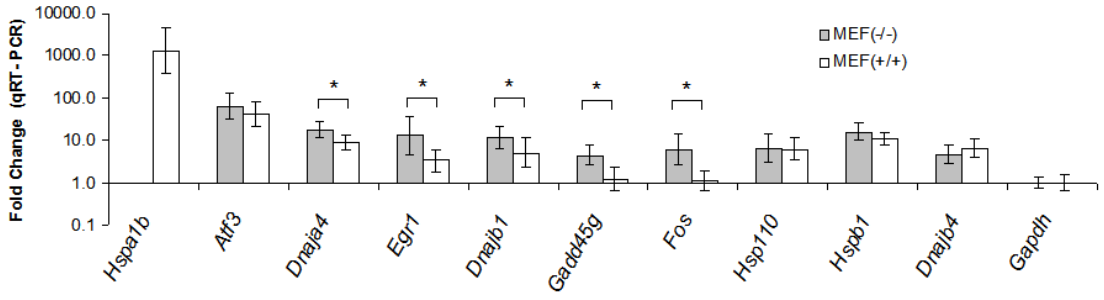

Figure 5.5 Gene expression in pretreated MEF(-/-) cells and MEF(+/+) cells as assessed through qRT-PCR. For validation of microarray experiments, selected genes were chosen for quantitative analysis to compare the fold changes in expression of heated relative to control samples using the comparative C_T method. The range represents the $2^{(-\Delta\Delta Ct \pm St.\ Dev.)}$. The symbol (*) represents genes that are differentially expressed between (-/-) and (+/+) cells to a statistically significance value of $p \leq 0.05$ using student's *t*-test.

In general, the qRT-PCR data showed higher fold inductions than the microarray data the trends and absolute values were the same as seen in Figure 5.5 and Table 5.2. The one discrepancy was the fold-change in *Hspa1b* in the MEF(+/+) cells. This gene showed a 99.5 fold change in microarray and a 1290.2 fold change in qRT-PCR. It is not clear why there is so much signal in the qRT-PCR but it is assumed to be related to the gene (*Hspa1b*) being one that was artificially reinserted in place of the original deletion site from the MEF(-/-) cells. This process may have affected the promoter site and the production of mRNA. From Western blot analysis, the levels of actual HSP70 protein are not consistent with this large of an increase in mRNA, but rather are similar to wild type cells (data not shown). Since *Hsp70* had no expression in MEF(-/-) cells, a statistical test was not performed. Other than *Hsp70*, there were five genes that showed statistically significant differences of $p \leq 0.05$ between the (-/-) and (+/+) cells: *Dnaja4, Egr1, Dnajb1, Gadd45g, and Fos*.

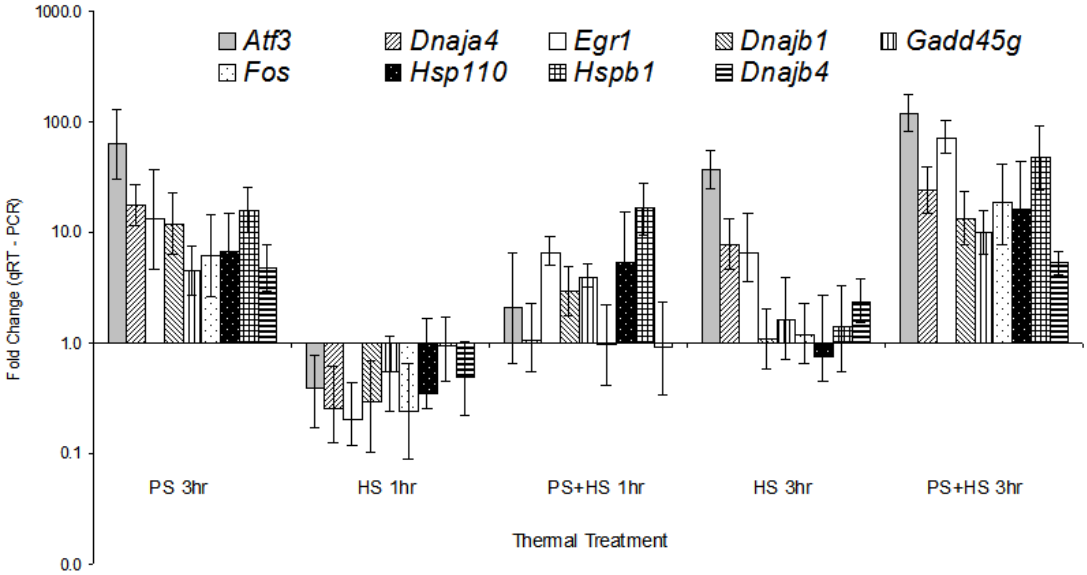

Figure 5.6 Gene expression of (-/-) cells after PS only, HS only, or PS+HS as assessed through qRT-PCR. Select genes were analyzed through the fold changes in expression of heated relative to unheated control samples using the comparative C_T method when normalized to *gapdh*. Cells were either preshocked only at 43° C for 30min (PS) and harvested at 3hrs later, heatshocked only at 45° C for 20min (HS) and harvested at 1 and 3 hours later or given a dual treatment of PS+HS and harvested at 1 and 3 hours later. The range represents the $2^{(-\Delta\Delta Ct \pm St.\ Dev.)}$.

5.4.5 QRT-PCR of Gene Expression From HS Only and PS+HS Treatment in (-/-) Cells

As a next step in characterizing the heat response of these genes from the qRT-PCR list, a second qRT-PCR analysis was done on MEF(-/-) samples that received severe heat shock only at 45°C for 20 min (HS) or severe heat shock with the mild pretreatment of 43°C for 30 min at four hours prior (PS+HS). The purpose of this experiment was to determine if thermally pretreating tissue would preserve mRNA levels within the cells after the severe heat shock. Presumably, this would provide insight into why these pretreated cells are able to survive better. The gene expression levels at 1 hour and 3 hours after the severe heating relative to unheated controls were normalized to *Gapdh* for each sample. The graph in Figure 5.6 shows the fold inductions of each gene with the error bars representing the range as

determined by the standard deviation of the $\Delta\Delta C_T$. The preshock only (PS) data was taken from Table 5.2 for comparison. The data shows that there are increased levels of mRNA in most of the conditions except for the 1 hour after HS Only samples. The HS 1hr sample actually shows a reduction in every mRNA level relative to unheated controls. This implies that the heat has destroyed the mRNA or that the cells were unable to synthesize new mRNA due to the heat stress. However, the expression does recover at the 3 hours after HS Only time point. For the pretreated samples with the secondary heat shock (PS+HS), there are low expression values at 1 hour but they recover to be highly upregulated at the 3 hour time.

5.5 Discussion

In order to more effectively understand the dynamics of various pretreatment modalities, it is necessary to investigate the specific cellular level response through an analysis of the proteins and molecular pathways that are activated or suppressed. Most commonly, the research involving pretreatment has only been able to observe one or two proteins at a time. With the advent of high throughput genomics of microarray analysis and subsequent qRT-PCR, it is now possible to screen the whole genome from a sample in order to elucidate all of the genes that may respond to a given stimulus.

A well-controlled model using water bath heat shock of cell cultures was chosen in anticipation of comparing the results to experiments with more complex variables such as laser irradiation or multi-cellular, organotypic skin cultures, or *in vivo* samples of tissue. Knowledge of the genetic patterns in this controlled case will permit a more tractable analysis of gene changes for subsequent experiments. Fibroblasts were chosen because they are the most abundant cell in the dermis and are important in almost all wound healing applications.

For these experiments we chose a time point of 3 hours after thermal pretreatment to harvest the RNA. We wanted to capture the expression profile at a time prior to the time that

the severe heat shock is usually given in the survival experiments seen in Figure 5.1. Ideally the mRNA at this 3 hr point would be representative of the proteins that are actually present in the cell at the 4 hr time point and beyond. A more extensive temporal analysis of the mRNA expression using qRT-PCR would be informative now that we have screened for significantly upregulated genes using the microarrays.

5.5.1 MEF(-/-) and MEF(+/+) Cells Show Similar Expression Profiles

One of the most salient features from the microarray experiments are the presence of genes that are upregulated in both MEF(-/-) and MEF(+/+). When these genes common to both cell types in the middle of Figure 5.2 are classified according to their molecular function (Figure 5.3) using Panther© [20], they show that the four most highly represented groups are: unclassified molecular function (21.1% of the total number of genes in the list that are classified), chaperones (15.8%), nucleic acid binding (15.8%), and transcription factors (13.2%). This is an expected distribution of genes - as any stimulus, such as heat, is likely to increase the upregulation of an assortment of genes which requires transcription factors and nucleic acid binding [26, 27]. The presence of chaperones is consistent with thermal stress within cells as they begin to repair damage with this class of proteins [21, 28]. When the molecular functions of the of the genes that are expressed in MEF(-/-) cells are grouped, they are: unclassified molecular function (25%), transcription factors (19.4%), and nucleic acid binding (16.7%). For the MEF(+/+) cells, the distribution is: unclassified molecular function (25%), receptors (10%), transcription factors (10%), nucleic acid binding (10%), and chaperones (5%). The higher abundance of transcription factors and nucleic acid binding genes in (-/-) cells implies that these cells are undergoing more stress than the (+/+) cells. Presumably, the MEF(-/-) cells are signaling the transcription and activation of proteins to rescue the damage from the pretreatment heat stress. However, this damage is sub-lethal

because viability assays of samples that have only been pretreated show no loss in viability compared to control cells. Consequently, these MEF(-/-) cells may be expending their resources in successfully repairing damage from the PS but are not able to withstand the subsequent stress of the HS. Also, the absence of HSP70 protein when the cells are being stressed may cause changes in the expression of various genes. Proteins are known to influence gene expression [29]. It is known that HSP70 can suppress the activation of apoptotic pathways. Likewise, the absence of HSP70 may allow the expression of gene products that are known to be part of the stress response (e.g. transcription factors and nucleic acid binding proteins) [26, 27, 30].

If the genes in Fig 5.2 that are in common between the two cell lines are grouped according to pathway (which requires more direct interaction amongst the components than the molecular function category), then the top four are: p53, apoptosis signaling, angiogenesis and the p38 MAPK pathways. The p53 pathway is an anti-tumorigenic pathway that works through a checkpoint system to prevent the accumulation of DNA damage by inducing apoptosis or cell cycle checkpoint control [31]. Consequently, it is important to cells that are undergoing changes, such as these heat shocked ones. Apoptosis signaling is expected to be upregulated in stressful situations as the cells determine their fate to survive or not depending on the state of their damage. The role of angiogenesis pathway after mild thermal stress has been documented previously and may be a response mechanism by cells to increase the transport of immune cells to the site of injury, a process resulting in a classic response to injury and granulation tissue [32]. The p38 MAPK pathway is responsible for signal transduction of environmental stress and plays a major role in the behavior of cells [33]. For the MEF(-/-) cells, the most highly represented pathway is the TGF-βeta signaling pathway (20%) with 15 other pathways also being represented. In the MEF(+/+) cells, apoptosis signaling was the pathway with the most genes but only 5 other pathways were

represented by the induced genes. It is not specified whether the apoptotic pathway is being activated or suppressed in these cells, but these pretreated cells do show equal viability to control cells, so they are not dying off (data not shown). It can be speculated that the lower number of pathways in the MEF(+/+) cells may be due to there being less damage in these cells due to the presence of HSP70. The MEF(-/-) cells may be turning on more pathways in an effort to respond to the thermal stress as best they can without the HSP70 protein.

When the twenty most highly induced genes from both cell types are listed in Table 5.1, it can be seen that there are many common genes between them. The greatest similarity between the cell types is the genes that are a part of the heat shock proteins category – also known as molecular chaperones (e.g. *Hspa1b*, *Hsp110*, *Hspb1, Dnaja4*, *Djanb1*, *Dnajb4*) - the last three of these are isoforms of HSP40. The most highly upregulated signal coming from *Hspa1b* (*Hsp70*) is consistent with the literature as being the most prominent responder to heat [34-36]. The most well known stimulus for *Hsp70* activation is unfolded protein within the cytosol and nucleus. Thermal stress unravels various proteins from their tertiary and quaternary structure, rendering them non-functional. As the constitutive heat shock proteins (e.g. HSP90, HSC70) within the cell recognize the exposed hydrophobic regions of these denatured proteins, they release sequestered HSF1 (heat shock factor 1) which is then free to trimerize and translocate to the nucleus for binding to the HSE (heat shock elements) which subsequently drives the transcription of the genes within the HSR [37, 38]. Only at this time is HSP70 able to take part in repairing damage to the cell because its basal levels are very low to non existent and there is no reservoir of protein within the cell to respond initially. The HSP70 pathway is not effective in protecting cells from a single thermal stress because it takes time to produce the protein despite the fact that both isoforms of *Hsp70* are intronless thus allowing rapid synthesis. Rather the strength of *Hsp70* lies in its protection from subsequent exposures. The contribution of inducible proteins to a single stress can also

be minimal if the stress is severe enough to preclude the synthesis of new proteins by damaging the machinery, e.g. ribosomes, that produces mRNA and protein, including HSP70 itself [39]. In Figure 5.6, the evidence of this stress can be seen in the HS Only samples at 1 hour and 3 hours. The damage induced by the severe thermal insult has prevented the cell from making the mRNA transcripts necessary for recovery.

Strategies of pretreatment to upregulate Hsp70 not only show the potential to reduce cellular level damage through the unfolded protein response and anti-apoptosis but also to improve wound healing at the tissue level by modulation of inflammation [40]. We did not see many inflammatory mediators being upregulated in our microarray data, but they would not be expected to be significant components in an *in vitro* model. Nevertheless, we have begun to investigate the functionality of HSP70 in wound healing through our animal studies of pretreatment wherein there is a positive correlation between *Hsp70* expression and increased tensile strength of full thickness scalpel wounds of the murine dorsum [41]. The concomitant upregulation of growth factors such as TGF-β by thermal means may be a contributing factor to this improved wound healing [42].

Of note from the qRT-PCR experiments in Figure 5.5 is that the expression of *Hspb1* was at 16 fold change in the MEF(-/-) cells while there was only a 1.2 fold change in MEF(+/+) cells. Consequently, HSPB1 may be particularly important when HSP70 is absent in cells. HSPB1 – also know as HSP25 – is a small heat shock protein that is activated by p38 which is part of the stress response mechanism of cells [33]. The p38 MAPK pathway is one of the pathways that was upregulated in both the MEF(-/-) and MEF(+/+) cells from Figure 5.2. HSPB1 has anti-apoptotic function that may be taking the place of the missing HSP70 in these cells [43].

In contrast, *Hsp110* does not show particularly disproportionate levels of qRT-PCR signal between MEF(-/-) and MEF(+/+) cells. This is expected since *Hsp110* is known to

have more of a role in high temperature stresses while the protocol that is used here is relatively mild at 43^{o} C [24].

Two of the *Hsp40* family of genes are also particularly upregulated in the qRT-PCR of the MEF(-/-) cells relative to the MEF(+/+) cells: *Dnaja4* (17.8 vs 9), *Dnajb1* (12 vs. 5.1), while one stays the same, *Dnajb4* (4.7 vs 6.5). HSP40 proteins have known interaction with HSP70 and they are dependent upon HSP70 for their ability to help refold heat inactivated proteins within the cytosol [23]. This result portrays HSP40 as an enhancer of the capacity of HSP70 to refold proteins because the presence of tetracycline induced HSP70 without HSP40 was able to rescue hamster fibroblast cells after thermal stress, however, to a lesser degree than thermally preshocked cells which included the HSP40 protein [10]. Consequently, HSP40 is considered a co-chaperone that works within the 'foldosome' (referring to the physical complex of proteins that assist in folding) to assist in substrate binding and release with HSP70 and HSP90 for refolding [25, 44]. It has been postulated that *Dnajb1* might be of particular importance for protection of functions within the nucleolus [25]. This form has been shown to localize to the nucleolus after heat shock while another form, *Dnaja1*, does not.

In contrast to the large increases in *Hsp40* induction, *Hsp90* does not show up as being greater than 2 fold-change on the microarray experiments. HSP90 is also responsible for helping repair denatured proteins through the 'foldosome' complex with HSP70, HSP40, p23, HIP and HOP [39]. Nevertheless, the inducible form of *Hsp90* (*Hsp90α*) does show a 50% increase in signal on the microarray after pretreatment in both cells types. The relative abundance (up to 2% of total protein content) in the cell of HSP90 under normal conditions may be a reason why it does not show large fold changes relative to the other genes on the list. HSP90 has constitutively required functions within the cell, such as steroid hormone signaling [21]. Furthermore, the activation of the refolding function for HSP90 may be more

through phosphorylation of the protein than through upregulation of synthesis, which is the mechanism for the highly inducible HSP70. So, in order to more fully characterize the role of *Hsp90*, phosphorylation assays and immunoprecipitation assays to probe molecular interactions with constitutive HSP90 protein would be beneficial.

In Figure 5.5, one of the most highly expressed genes is *Atf3* in both cell types. This gene has known function in DNA binding, protein dimerization, transcription factor activity, transcription repressor activity and is localized to the nucleus. While some of the literature notes a minor role in the unfolded protein response by *Atf3* [45], there is evidence of its role in regulating apoptosis through the JNK pathway (C-Jun N-terminal kinases) that may be contributing to the cell survival that we see in our pretreatment experiments [46].

P2rx7 is upregulated in both cell types as well and is a plasma membrane protein which is involved in cation and NADH transport, macrophage infiltration, collagen deposition and apoptosis [47, 48]. *Loricrin* and *Sprr1a* are proteins involved in the formation of the cornified envelope in epidermal cells [49, 50]. This layer serves as a barrier that protects the cell and organism from the environment which we speculate may be a beneficial effect in heat stressed tissues. While *Loricrin* is in both cell types, *Sprr1a* only shows up in the MEF(-/-) cells as being significantly upregulated in Table 5.2. *Loricrin* and *Sprr1a* make up 85% of epidermal protein content. However, the ratio of these two proteins can vary, which leads to changes in the flexible and toughness of the epidermis. *Sprr1a* acts as the minor crosslinking component that is mixed in with the major ground substance (*Loricrin*) [49]. Perhaps, the presence of significant expression of *Sprr1a* in the MEF(-/-) cells implies a preference of this phenotype for certain mechanical properties in the epidermis.

Egr1 shows a statistical difference in the expression in MEF(-/-) cells vs. the MEF(+/+) at (13.1 vs 3.4 fold) in the qRT-CPCR data which may allude to its role in thermal stress. *Egr1* is a nuclear protein involved in DNA binding and transcriptional activation. It

has been shown to be activated by TGF-βeta and it then subsequently activates the *Col1a2* gene which drives the production of type I procollagen [51]. The role of collagen stimulation by *Egr1* may be a component of the cellular wound healing response after thermal stress. Wound healing in the skin is known to bring about the production of new collagen to replace lost or damaged tissue [52].

Another gene preferentially upregulated in the MEF(-/-) cells with statistical significance was *Gadd45g*. This gene is known to respond to stress and it inhibits cell growth, acts as a cyclinB1 kinase inhibitor with a role in cell cycle checkpoint arrest, and it induces apoptosis [53, 54]. *Gadd45g* is ubiquitously expressed in all normal adult and fetal tissues, however, its transcriptional silencing and promoter hypermethylation were frequently detected in tumor cell lines [55]. The presence of this gene in (-/-) cells is most likely due to their inability to deal with the heat stress as they are shifting towards an apoptotic state.

Fos (also known as *c-fos*) was also statistically different between the two cell lines at 6.2 fold in MEF(-/-) vs 1.2 fold in the MEF(+/+) cells from the qRT-PCR data. This gene product is found in the nucleus and is responsible for regulation of transcription, DNA binding and protein dimerization. *Fos* coordinates with *c-Jun* to regulate *AP-1,* which is involved in cell cycle progression and cell proliferation [56].

5.5.2 Molecular Functions More Highly Upregulated in (-/-) Relative to (+/+) Cells

Table 5.3A and 5.3B was used to help discriminate the proteins that were particularly upregulated in one cell type over the other. Essentially, a ratio of the fold change gene expression levels relative to controls in each cell type was calculated. The high magnitude ratio values in Table 3A are genes that show relatively stronger induction in MEF(-/-) cells. In Table 5.3B, the lower magnitude ratio values are the genes more strongly induced in MEF(+/+) cells.

From Figure 5.4, the fact that transcription factors, nucleic acid binding proteins and kinases are the most highly induced group in the MEF(-/-) cells may indicate that these are under more stress than MEF(+/+) cells and require many transcriptional and signaling events to respond [57, 58]. Kinases are used for phosphorylation of proteins in many different instances and are an important part of signaling within the cell through activation and suppression of various pathways after stress [33]. In contrast to the distinct weightings of functions in the MEF(-/-) cells, the MEF (+/+) cells show a more evenly distributed profile of molecular functions which implies that the cells are more in homeostasis than in a damage repair mode. However, this damage in the MEF(-/-) cells is sub-lethal and does not manifest itself in viability assays of samples that have only been pretreated as they show no loss in viability compared to control cells (data not shown). The absence of the HSP70 protein may be driving the upregulation of the genes in these molecular functions for the MEF(-/-) cells. This data is consistent with the data in Figure 3 that showed the presence of some of the same molecular functions.

5.5.3 QRT-PCR of Gene Expression from HS Only and PS+HS Treatment in (-/-) Cells

The data in Figure 5.6 shows the changes in gene expression due to the different water bath thermal treatments. What is most readily evident is the presence of low expression values of all genes in the 1 hour post HS samples. It is not entirely clear if the heat stress destroys the mRNA within the cell or, alternatively, it prevents the synthesis of new mRNA. Most likely the effects seen here are a combination of these two phenomena: loss of existing mRNA and delay of synthesis of new mRNA. Message RNA is a labile molecule and it would be expected that if proteins are being denatured at this temperature (45^{o}C), then the mRNA would also be affected. By the 3 hour time point after HS only, the cells are able to recover and generate new mRNA.

In contrast to the severe HS, the PS only shows evidence as to why it is able to protect these cells from a secondary heat stress. The transcript levels are quite high at the 3 hour time point after PS alone, meaning that these cells are primed by the first, mild heatshock to withstand the secondary heat stress – either by having a protective mechanism for the mRNA already present within the cell or by preventing damage to the mRNA synthesis machinery. Presumably, there may be an interaction between some of the chaperone proteins of the HSR in shielding mRNA like they do for other proteins. Alternatively, the HSPs may be shielding the machinery that synthesizes mRNA (e.g. proteins such as: RNA polymerases and helicases). This would allow for the quick synthesis of new mRNA after the severe heat shock destroyed that which was present in the cell. The effects of having this protection already in the cell at the time of severe heat stress (HS) is seen in the PSHS 1 hour samples when contrasted to the HS 1 hour samples. The presence of the mRNA transcripts here means that they can then be used to make recovery proteins. At the 3 hour time point the thermotolerance afforded to the cells by the preshock can be seen as robust mRNA levels in the PS+HS samples which correlates to the increased survival seen in Figure 5.1. However, while the HS only samples at 3 hours have generally lower levels of mRNA, the exceptions are *Atf3, Dnaja4,* and *Egr1*. The transcript levels of these three genes are very high here which implies that they may be particularly important to recovery after severe heat stress if they are designed to be preferentially upregulated in a rapid fashion. It would be informative to extend this study to HSP70 competent cells as well as the presence of this protein may significantly alter the mRNA levels after thermal stress.

5.5.4 Applications

Knowledge of the pathways involved in pretreatment may lead to more effective therapy in a range of applications. In addition to thermal preconditioning, there exist a few

small molecule drugs that have been shown to upregulate or co-induce the heat shock response. One of the main benefits of these drugs over thermal methods is that they can activate the response without causing damage by denaturing proteins within the cell from a pretreatment heating. For clinical applications, these drugs may be easier to administer and may be more effective due to their targeted nature. Bimoclomol is a co-inducer of the HSR in that it facilitates the stabilization of HSF1 trimers [59-61]. These trimers then translocate to the nucleus to activate the HSE (heat shock elements) that drive transcription of heat shock genes. Bimoclomol can only work in conjunction with a thermal stimulus that will allow the trimers to form in the first place, but the thermal threshold is lowered. Geranyl geranyl acetone (GGA) upregulates the HSR response by attaching to proteins within the cell that bind HSF1[62, 63]. The HSF1 is then freed to trimerize and drive transcription of the HSR proteins. Potentially, these two candidates drugs may be able to mediate an effective pretreatment for laser wounds either separately or even in tandem. However the effects of these drugs need to be characterized relative to a standard thermal stress in order to fully understand their mechanisms and to preclude any deleterious interactions on the molecular level. An extension of this work would be to compare the genetic pathways of these pharmacological treatments next to thermal pretreatment.

While the data contained herein provides information as to which genes may be involved in thermotolerance in these cells, this is still a cell culture study. Therefore, it is lacking the interplay of signaling amongst many different cell types that would be found in a tissue model. In particular, there is not a systemic inflammatory response that has known functions in thermal stress and wound healing [33, 64-66]. In particular, HSP70 is know to downregulate the NF-κB pathway of inflammation [67]. However, this cell culture study will allow us to contrast the gene expression profiles of *in vitro* results to those of *in vivo* models in the future. In particular, the wound healing response of an *Hsp70* deficient mouse model

that is subjected to both thermal pretreatment and a severe thermal secondary burn injury would provide an insightful parallel to the *Hsp70* deficient cells.

5.6 Conclusions

In conclusion, this work provides a look into the genes responsible for rescuing cells from severe thermal stress. We have shown that when *Hsp70* is absent, cells can still benefit from a thermal preconditioning at 4 hours prior to a severe heat stress. The collection of genes between the cell types are varied but the MEF(-/-) cells show strong grouping in the nucleic acid binding and transcription factors which suggest more signaling is required to respond to the thermal stress. QRT-PCR validation of microarray data showed slightly higher levels of common genes in the MEF(+/+) cells. The most prevalently upregulated genes are those in the HSR (e.g. *Hsp40, Hsp110, Hsp25)*, however, *Atf3* also showed strong induction. Consequently, *Atf3* may be a potential candidate for the modulation of the survival of cells to thermal stress if it can be upregulated in advance of an insult to allow the cells to cope with the heat stress. Lastly, a comparison of gene levels by qRT-PCR after biphasic heating (PS+HS) versus HS Only showed a severe reduction in the capacity of cells to produce mRNA for the genes of interest after a single severe thermal stress. However, when pretreated, the cells were able to synthesize levels of mRNA greater than or similar to those of preshock (PS) alone. Ultimately, this work will contribute to the understanding of the molecular pathways that need to be manipulated in order to bring about better laser treatments through preconditioning methods.

5.7 Acknowledgements

All microarray experiments were performed in the Vanderbilt Microarray Shared Resource and analysis was carried out by Braden Boone. The Vanderbilt Microarray Shared Resource is supported by the Vanderbilt Ingram Cancer Center (P30 CA68485), the Vanderbilt Digestive Disease Center (P30 DK58404) and the Vanderbilt Vision Center (P30 EY08126).

QRT-PCR experiments were carried out in the Molecular Genetics Core of the Skin Disease Research Center at Vanderbilt with the help of Latha Raju.

The *Hsp70* deficient MEF(-/-) cells and the rescue MEF cells were a contribution from Dr. Clayton Hunt's lab at Washington University.

Dr. Prasad Shastri in the Department of Biomedical Engineering generously offered the use of the Synergy Biotek Fluorescence plate reader.

Evelyn Okediji assisted with cell culture work.

Funding Sources:

ASLMS (American Society for Laser Medicine & Surgery) Student Research Grant
ASLMS Research Grant
DOD/AFOSR award No. F49620-01-1-4029
Vanderbilt Medical Center Starbrite Grant

5.8 References

1. Rylander, M.N., et al., *Optimizing heat shock protein expression induced by prostate cancer laser therapy through predictive computational models.* J Biomed Opt, 2006. **11**(4): p. 041113.
2. Howard, J., et al., *Healing of laser incisions in rat dermis: comparisons of the carbon dioxide laser under manual and computer control and the scalpel.* Lasers Surg Med, 1997. **20**(1): p. 90-6.

3. Buell, B.R. and D.E. Schuller, *Comparison of tensile strength in CO2 laser and scalpel skin incisions.* Arch Otolaryngol, 1983. **109**(7): p. 465-7.
4. Ahcan, U., et al., *Port wine stain treatment with a dual-wavelength Nd:Yag laser and cryogen spray cooling: a pilot study.* Lasers Surg Med, 2004. **34**(2): p. 164-7.
5. Cao, Y., et al., *Impaired induction of heat shock protein implicated in decreased thermotolerance in a temperature-sensitive multinucleated cell line.* Pflugers Arch, 1998. **437**(1): p. 15-20.
6. Paithankar, D.Y., et al., *Subsurface skin renewal by treatment with a 1450-nm laser in combination with dynamic cooling.* J Biomed Opt, 2003. **8**(3): p. 545-51.
7. Pespeni, M., M. Hodnett, and J.F. Pittet, *In vivo stress preconditioning.* Methods, 2005. **35**(2): p. 158-64.
8. Murphy, P.J., et al., *Regulation of the dynamics of hsp90 action on the glucocorticoid receptor by acetylation/deacetylation of the chaperone.* J Biol Chem, 2005. **280**(40): p. 33792-9.
9. Huang, L., N.F. Mivechi, and D. Moskophidis, *Insights into regulation and function of the major stress-induced hsp70 molecular chaperone in vivo: analysis of mice with targeted gene disruption of the hsp70.1 or hsp70.3 gene.* Mol Cell Biol, 2001. **21**(24): p. 8575-91.
10. Nollen, E.A., et al., *In vivo chaperone activity of heat shock protein 70 and thermotolerance.* Mol Cell Biol, 1999. **19**(3): p. 2069-79.
11. Stankiewicz, A.R., et al., *Hsp70 inhibits heat-induced apoptosis upstream of mitochondria by preventing Bax translocation.* J Biol Chem, 2005. **280**(46): p. 38729-39.
12. Beckham, J. and E.D. Jansen. *HSP70 in Thermal Pretreatment of Murine Cell Culture*. in *Lasers in Modern Biology and Medicine: A Symposium honoring A.J. Welch*. 2008. Austin, TX: Landes Bioscience.
13. Beckham, J., et al., *Role of HSP70 In Cellular Thermotolerance.* In Submission.
14. Hunt, C.R., et al., *Genomic instability and enhanced radiosensitivity in Hsp70.1- and Hsp70.3-deficient mice.* Mol Cell Biol, 2004. **24**(2): p. 899-911.
15. Pandita, T.K., et al., *Regulation of telomere movement by telomere chromatin structure.* Cell Mol Life Sci, 2007. **64**(2): p. 131-8.
16. Zhang, B., S. Kirov, and J. Snoddy, *WebGestalt: an integrated system for exploring gene sets in various biological contexts.* Nucleic Acids Res, 2005. **33**(Web Server issue): p. W741-8.
17. Bio-Rad, *Real-Time PCR Applications Guide*.
18. AppliedBiosystems, *User Bulletin #2: ABI PRISM 7700 Sequence Detection System*. 2001.
19. Oliveros, J.C. *VENNY. An interactive tool for comparing lists with Venn Diagrams*. 2007 [cited; Available from: http://bioinfogp.cnb.csic.es/tools/venny/index.html.
20. Thomas, P.D., et al., *PANTHER: a library of protein families and subfamilies indexed by function.* Genome Res, 2003. **13**(9): p. 2129-41.
21. Frydman, J., *Folding of newly translated proteins in vivo: the role of molecular chaperones.* Annu Rev Biochem, 2001. **70**: p. 603-47.
22. Garrido, C., et al., *Heat shock proteins: endogenous modulators of apoptotic cell death.* Biochem Biophys Res Commun, 2001. **286**(3): p. 433-42.
23. Michels, A.A., et al., *Hsp70 and Hsp40 chaperone activities in the cytoplasm and the nucleus of mammalian cells.* J Biol Chem, 1997. **272**(52): p. 33283-9.
24. Oh, H.J., X. Chen, and J.R. Subjeck, *Hsp110 protects heat-denatured proteins and confers cellular thermoresistance.* J Biol Chem, 1997. **272**(50): p. 31636-40.

25. Uchiyama, Y., et al., *Heat shock protein 40/DjB1 is required for thermotolerance in early phase.* J Biochem, 2006. **140**(6): p. 805-12.
26. Feezor, R.J., et al., *Temporal patterns of gene expression in murine cutaneous burn wound healing.* Physiol Genomics, 2004. **16**(3): p. 341-8.
27. Sonna, L.A., et al., *Invited review: Effects of heat and cold stress on mammalian gene expression.* J Appl Physiol, 2002. **92**(4): p. 1725-42.
28. Morimoto, R.I., P.E. Kroeger, and J.J. Cotto, *The transcriptional regulation of heat shock genes: a plethora of heat shock factors and regulatory conditions.* Stress Inducible Cellular Responses, 1996. **77**: p. 139-63.
29. Alberts, B., *Molecular biology of the cell*. 4th ed. 2002, New York: Garland Science. xxxiv, [1548] p.
30. Bowman, P.D., et al., *Survival of human epidermal keratinocytes after short-duration high temperature: synthesis of HSP70 and IL-8.* Am J Physiol, 1997. **272**(6 Pt 1): p. C1988-94.
31. Riley, T., et al., *Transcriptional control of human p53-regulated genes.* Nat Rev Mol Cell Biol, 2008. **9**(5): p. 402-12.
32. Rattan, S.I., et al., *Stress-mediated hormetic modulation of aging, wound healing, and angiogenesis in human cells.* Ann N Y Acad Sci, 2007. **1119**: p. 112-21.
33. Cowan, K.J. and K.B. Storey, *Mitogen-activated protein kinases: new signaling pathways functioning in cellular responses to environmental stress.* J Exp Biol, 2003. **206**(Pt 7): p. 1107-15.
34. Beckham, J.T., et al., *Assessment of cellular response to thermal laser injury through bioluminescence imaging of heat shock protein 70.* Photochem Photobiol, 2004. **79**(1): p. 76-85.
35. OConnell Rodwell, C.E., et al., *A genetic reporter of thermal stress defines physiologic zones over a defined temperature range.* FASEB Journal, 2003. **18**(2).
36. Rylander, M.N., et al., *Correlation of HSP70 expression and cell viability following thermal stimulation of bovine aortic endothelial cells.* J Biomech Eng, 2005. **127**(5): p. 751-7.
37. Trinklein, N.D., et al., *Transcriptional regulation and binding of heat shock factor 1 and heat shock factor 2 to 32 human heat shock genes during thermal stress and differentiation.* Cell Stress Chaperones, 2004. **9**(1): p. 21-8.
38. Trinklein, N.D., et al., *The role of heat shock transcription factor 1 in the genome-wide regulation of the mammalian heat shock response.* Mol Biol Cell, 2004. **15**(3): p. 1254-61.
39. Duncan, R.F., *Inhibition of Hsp90 function delays and impairs recovery from heat shock.* Febs J, 2005. **272**(20): p. 5244-56.
40. Kovalchin, J.T., et al., *In vivo delivery of heat shock protein 70 accelerates wound healing by up-regulating macrophage-mediated phagocytosis.* Wound Repair Regen, 2006. **14**(2): p. 129-37.
41. Wilmink, G., et al., *Molecular Imaging-Assisted Optimization of Hsp70 Expression During Laser Preconditioning for Wound Repair Enhancement.* J Invest Dermatol, 2008. **In Press**.
42. Capon, A. and S. Mordon, *Can thermal lasers promote skin wound healing?* Am J Clin Dermatol, 2003. **4**(1): p. 1-12.
43. Pirkkala, L., P. Nykanen, and L. Sistonen, *Roles of the heat shock transcription factors in regulation of the heat shock response and beyond.* Faseb J, 2001. **15**(7): p. 1118-31.

44. Taylor, D.M., et al., *Characterizing the role of Hsp90 in production of heat shock proteins in motor neurons reveals a suppressive effect of wild-type Hsf1*. Cell Stress Chaperones, 2007. **12**(2): p. 151-62.
45. Whitmore, M.M., et al., *Negative regulation of TLR-signaling pathways by activating transcription factor-3.* J Immunol, 2007. **179**(6): p. 3622-30.
46. Katz, S. and A. Aronheim, *Differential targeting of the stress mitogen-activated protein kinases to the c-Jun dimerization protein 2.* Biochem J, 2002. **368**(Pt 3): p. 939-45.
47. Goncalves, R.G., et al., *The role of purinergic P2X7 receptors in the inflammation and fibrosis of unilateral ureteral obstruction in mice.* Kidney Int, 2006. **70**(9): p. 1599-606.
48. Ke, H.Z., *In vivo characterization of skeletal phenotype of genetically modified mice.* J Bone Miner Metab, 2005. **23 Suppl**: p. 84-9.
49. Candi, E., R. Schmidt, and G. Melino, *The cornified envelope: a model of cell death in the skin.* Nat Rev Mol Cell Biol, 2005. **6**(4): p. 328-40.
50. Candi, E., et al., *Transglutaminase cross-linking properties of the small proline-rich 1 family of cornified cell envelope proteins. Integration with loricrin.* J Biol Chem, 1999. **274**(11): p. 7226-37.
51. Chen, S.J., et al., *The early-immediate gene EGR-1 is induced by transforming growth factor-beta and mediates stimulation of collagen gene expression.* J Biol Chem, 2006. **281**(30): p. 21183-97.
52. Eming, S.A., T. Krieg, and J.M. Davidson, *Inflammation in wound repair: molecular and cellular mechanisms.* J Invest Dermatol, 2007. **127**(3): p. 514-25.
53. Mak, S.K. and D. Kultz, *Gadd45 proteins induce G2/M arrest and modulate apoptosis in kidney cells exposed to hyperosmotic stress.* J Biol Chem, 2004. **279**(37): p. 39075-84.
54. Vairapandi, M., et al., *GADD45b and GADD45g are cdc2/cyclinB1 kinase inhibitors with a role in S and G2/M cell cycle checkpoints induced by genotoxic stress.* J Cell Physiol, 2002. **192**(3): p. 327-38.
55. Ying, J., et al., *The stress-responsive gene GADD45G is a functional tumor suppressor, with its response to environmental stresses frequently disrupted epigenetically in multiple tumors.* Clin Cancer Res, 2005. **11**(18): p. 6442-9.
56. Monje, P., et al., *Regulation of the transcriptional activity of c-Fos by ERK. A novel role for the prolyl isomerase PIN1.* J Biol Chem, 2005. **280**(42): p. 35081-4.
57. Westerheide, S.D. and R.I. Morimoto, *Heat shock response modulators as therapeutic tools for diseases of protein conformation.* J Biol Chem, 2005. **280**(39): p. 33097-100.
58. Xu, D., L.P. Zalmas, and N.B. La Thangue, *A transcription cofactor required for the heat-shock response.* EMBO Rep, 2008.
59. Hargitai, J., et al., *Bimoclomol, a heat shock protein co-inducer, acts by the prolonged activation of heat shock factor-1.* Biochem Biophys Res Commun, 2003. **307**(3): p. 689-95.
60. Torok, Z., et al., *Heat shock protein coinducers with no effect on protein denaturation specifically modulate the membrane lipid phase.* Proc Natl Acad Sci U S A, 2003. **100**(6): p. 3131-6.
61. Lubbers, N.L., et al., *Oral bimoclomol elevates heat shock protein 70 and reduces myocardial infarct size in rats.* Eur J Pharmacol, 2002. **435**(1): p. 79-83.

62. Otaka, M., et al., *The induction mechanism of the molecular chaperone HSP70 in the gastric mucosa by Geranylgeranylacetone (HSP-inducer).* Biochem Biophys Res Commun, 2007. **353**(2): p. 399-404.
63. Suzuki, S., et al., *Geranylgeranylacetone ameliorates ischemic acute renal failure via induction of Hsp70.* Kidney Int, 2005. **67**(6): p. 2210-20.
64. Li, M., et al., *An essential role of the NF-kappa B/Toll-like receptor pathway in induction of inflammatory and tissue-repair gene expression by necrotic cells.* J Immunol, 2001. **166**(12): p. 7128-35.
65. Pockley, A.G., *Heat shock proteins, inflammation, and cardiovascular disease.* Circulation, 2002. **105**(8): p. 1012-7.
66. Malhotra, V. and H.R. Wong, *Interactions between the heat shock response and the nuclear factor-kappa B signaling pathway.* Crit Care Med, 2002. **30**(1 Suppl): p. S89-95.
67. Wong, H.R., et al., *Heat shock activates the I-kappaBalpha promoter and increases I-kappaBalpha mRNA expression.* Cell Stress Chaperones, 1999. **4**(1): p. 1-7.

CHAPTER VI

CONCLUSIONS AND FUTURE WORK

Josh T. Beckham

Department of Biomedical Engineering

Vanderbilt University

Nashville, TN 37235

6.1 Summary of Chapters

To summarize, this dissertation consisted of three manuscripts that outline the research investigating the cellular and molecular response to thermal stress. The three specific aims were addressed within the three chapters (III, IV, and V) through scientific methods of experimentation using three different cell types: a transgenic fibroblast line with a bioluminescent reporter, an *Hsp70* knockout fibroblast line and a control fibroblast line. Several different molecular approaches were used to ascertain the importance of HSP70 to thermal stress and which other proteins might be of interest for further study.

Specifically, the findings in Chapter III validated our bioluminescent reporter system, showed the response of *Hsp70* signaling to laser irradiation correlated to increases in damage, and utilized a novel implementation of the Arrhenius model to characterize gene promoter activity to heat stress. Typically, the Arrhenius analysis is applied to physical metrics of damage. In contrast, this work was important because it applied molecular and cellular level techniques to help understand the interaction of laser stress upon cells. Interventions that seek to reduce laser stress in human clinical applications could use this knowledge to effect changes on the genetic level. Specifically, promoter elements of genes can be silenced or activated through pharmacological means to modulate the production of heat responsive proteins. The advancement of medicine into the genetic sphere from a more traditional anti-body based approach requires more rigorous investigation into the genetic pathways and mechanisms. Bioluminescent reporter assays of gene promoter activity like the *Hsp70* system used herein are crucial to carrying out this work in an efficient manner due to its facile detection methods for determining the time course behavior to treatments.

Chapter IV describes work on pretreatment. First, pretreatment was shown to provide protection from heat stress and then the treatment parameters were optimized for fibroblast cells to bring about the most survival at 48 hrs. The effect of pretreatment was reported for four different severe temperature exposures. Then, the ability of pretreatment to protect cells against short duration, high temperature exposures was confirmed with a Ho:YAG laser. The causal relationship of HSP70 in this pretreatment response was proven by using an *Hsp70* deficient cell line that was compared to control cells. Another Arrhenius analysis was carried out that examined the damage in HSP70 deficient cells relative to control cells. This analysis was used to assess the damage response with and without pretreatment. We believe that this is the first time that the Arrhenius has been applied to pretreatment and it provides some interesting results that warrant further study concerning the threshold and rate of damage. Most salient, is the observation that the frequency factor increased with pretreatment. Perhaps this implies that the Arrhenius damage equation is not suitable for bi-phasic heating protocols. Essentially, a secondary term might need to be incorporated into the equation for this model to account for the inherent benefit to the pretreatment. This term would need to be opposite in sign to the standard integral because it serves to reduce damage and not increase it. Once a more complete model - that accurately predicts the thermal response in cells - is able to be formulated, then it can be used to help derive models for tissue that could provide guidance to clinicians for applying pretreatment strategies for their patients. In all, the work in this chapter contributes to the fundamental molecular level of knowledge for pretreatment that can be applied to tailoring thermal strategies in tissue studies.

In Chapter V, an analysis of gene expression after thermal stress was done. A microarray experiment was used to determine which genes out of 45,000 tested on the murine cDNA arrays might be responsible in the thermal stress response. While we knew the importance of *Hsp70*, the involvement of other pathways was less well understood. The data showed the presence of biological functions and pathways that were consistent with stress and highlighted a few genes with strong differential induction between *Hsp70*-deficient and control cells. From this work, future pretreatment strategies may be able to utilize these genes and pathways to bring about more effective therapies in tissue. Genes that prevent thermal damage from taking place could be activated in advance. However, if the damage is too severe then genes that stimulate the recovery and healing of tissue could be used as therapeutic targets after the thermal injury. The timing of the intervention would need to be more closely examined because stimulating the production of genes before heat stress may only serve to create a loading on the cell that made it less capable of surviving. There may be an optimal time after heat stress to provide a treatment that activates recovery and repair genes soon but with enough time for the cell to have effectively dealt with the initial stress. Ultimately, the work in this chapter sets a groundwork for defining those genes that could potentially be manipulated to bring about improved thermal damage responses in a clinical setting.

6.2 Future Work

There are many steps that need to be taken in order to further enhance and then translate this research into practical, clinical applications. First, further molecular analysis of some of the highly expressed genes in the microarray data would be desirable. *Atf3* and

Egr1 are two that look particularly interesting. Both of these genes were highly induced and *Egr1* showed significantly differential expression between the two cell lines. *Atf3* is implicated in apoptosis and may provide a mechanism to rescue cells from lethal thermal stress while *Egr1* has functionality in collagen production that may make it particularly applicable in dermal wound healing applications. Modification of the *Egr1* pathway might be most advantageous at some time after the thermal injury when tissue healing is taking place. In contrast, the interventional time for *Atf3* would most likely be before or immediately after a thermal injury in order to prevent the apoptotic signaling cascade from progressing too far. Studying the loss of function of these two genes through knockout cell lines or RNA interference techniques (RNAi) would yield some interesting data on their role in thermotolerance. Also, pharmacological inducers of the classical HSR need to be tested against thermal methods of pretreatment to determine how well they perform and what side effects they may have. These inducers may only provide partial benefits as compared to the complete HSR, but they also stand to produce fewer side effects due to their more isolated targets such as the HSE (heat shock element) that is the binding region of DNA for initiating the transcription of HSR genes.

This work focused on cell culture studies because, as a unicellular model, they are simplified in relation to a full *in vivo* system. Consequently, a study of the mechanisms involved can be more readily carried out without confounding variables. However, mouse models of pretreatment upon thermal burns should be carried out to more appropriately characterize the potential use of this strategy for alleviating damage in the skin. We have done some preliminary work on microarray analysis of pretreated tissue from FVB mice but did not get conclusive data. Also, we have obtained and bred a line of *Hsp70*

knockout mice of the C57/BL6 strain. These will be a logical extension to parallel the cell culture experiments. In initial studies we have shown no difference in skin tensile strength and no changes in scalpel wound strength when compared to wild type mice. One obstacle with using these mice might be their strain's inherent wound healing. The C57/BL6 mice heal relatively quickly compared to other strains. Consequently, it may be more difficult to probe changes in wound healing.

Ultimately, the ideal experiment to extend the current work would be able to show that HSP70 is the key mediator of thermal protection in an *in vivo* environment by using a thermal pretreatment followed by a severe thermal burn in an *Hsp70* knockout mouse. This experiment would parallel the *Hsp70* knockout cell studies nicely. However, the difficulty is being able to find a reproducible burn wound model that is not too severe. One option is a 2nd degree scalding wound with water [1]. Alternatively, we have a continuous wave diode laser that can be used for both pretreatment and the severe thermal injury.

6.3 Extensions of Research

There are many logical extensions of this work to the clinic. The most readily obvious are those in the field of cosmetic laser procedures (such as, laser skin resurfacing, wrinkle removal, skin tightening, port wine stain removal). The use of pretreatments could potentially reduce redness, swelling and inflammation at the site of irradiation. Patients would be able to more quickly return to work and have better aesthetic outcomes. There are already a few procedures that try to address this issue. Of note are cryogen spray cooling and cooled sapphire blocks. These reduce surface

temperatures and allow the clinician to target deeper skin tissue without killing or injuring the more superficial layers. Since these are performed at the same time as the laser procedure, they offer great convenience. However, pretreatments at several hours before could be used as a combination strategy with these other techniques to improve outcomes. Also, the surface cooling techniques may not be able to effectively protect tissue at the back side of the irradiation site that is deep within the tissue.

The use of topical pharmaceutical agents that incorporate the HSR inducers (e.g. Bimoclomal, geranyl geranyl acetone -GGA) would be an attractive solution because they could be applied by the patient before coming into the doctor's office. However, the ability to transport these drugs across the dermal barrier and maintain their efficacy has not been studied.

Another application where this work may benefit is if preconditioning is used to reduce damage from accidental thermal exposures. Often times in military applications, soldiers may be at a heightened risk of ocular damage from devices in the battlefield (either friend or foe)[2]. The effects upon the retinal cells to accidental exposure to laser sighting devices, retinal scanners or to weaponry may be mitigated if soldiers took a preconditioning agent before going into the field.

Another realm where thermal pretreatment has shown some promise is in neurological deficits. The fundamental basis for many neurological disorders is misfolded proteins and protein aggregates that lack functionality and act as toxins within the cells [3]. Consequently, there is work being done to stimulate the heat shock response in the brain to treat diseases such as Alzheimer's [4]. Also, amyotrophic lateral sclerosis (ALS/ Lou Gehrig's disease) manifests inadequate levels of heat shock response. This

deficiency implies an opportunity for therapy if there is simply a problem with signaling of the HSR. One group has shown efficacy in delivering exogenous HSP70 protein intraperitoneally injected three times weekly in delaying symptom onset and preserving motor function in ALS mice [5]. Perhaps a regimen of mild daily thermal stresses with a deep penetrating laser could stimulate HSPs enough to effect changes.

The extension of this work into cancer therapy stands to be a potentially medically beneficial application. Rylander has discussed the role of having less heat shock protein within a tumor that would reduce its ability to survive a thermal ablation procedure for prostate applications [6]. However, cancer cells usually have upregulated levels of heat shock proteins as they direct the proper folding of transcription factors, signaling molecules, kinases, and steroid hormones that are more prevalent in tumorigenic cells [3]. These extra heat shock proteins make the cancer cells more resistant to thermal stress than normal cells. A therapeutic strategy for removing tumors is targeted delivery of a lethal laser dose. In theory, a protocol that would precondition all of the tissue (normal and cancerous) would raise the thermotolerance level of the normal tissue to be closer to that of the tumor tissue. This might prevent damage to the surrounding healthy tissue and then a higher dose of laser therapy could be applied to the site to ensure tumor eradication.

To further tip the balance of thermotolerance away from the tumor cells in this scenario, a heat shock protein suppressor could be administered to the cancerous cells. There is a drug called, 17-AAG (a geldanamycin derivative), that selectively inhibits the action of HSP90 by binding to its nucleotide binding site and preventing its cycling with ATP to bind and release unfolded substrate proteins [7]. The key role of HSP90 in cancer

is the conformational maturation of oncogenic signaling proteins, including HER-2/ErbB2, Akt, Raf-1, Bcr-Abl and mutated p53 [7, 8]. Using this function of HSP90 as a target, 17-AAG has been used to suppress tumor growth and progression. Without HSP90's functionality, both the oncogenic signaling and thermotolerance would be reduced in these cells [9]. The key to the overall strategy is that 17-AAG has a 100-fold higher binding affinity to HSP90 derived from tumour cells than from normal cells [7]. Consequently, it handicaps the tumor cells more than the normal surrounding tissue from the standpoint of heat resistance. This would allow the thermal therapy to kill the tumor cells more effectively. If this drug was then combined with thermal pretreatment, the tumor would be subjected to a double edged sword. The pretreatment would raise the thermotolerance of the healthy tissue to the inherently high thermotolerance in the cancer cells and then the HSP90 inhibitor drug would lower the thermotolerance of the cancer cells for when they are subjected to the severe heat stress for ablation.

In summary, this dissertation has show the necessity of HSP70 for full thermotolerance while screening other proteins and pathways with potential involvement. Two unique analyses of thermal stress were performed using the Arrhenius damage model to characterize the behavior of *Hsp70* gene transcription and the effect of pretreatment on the activation energy and frequency factor. Furthermore, this work established that pretreatment strategies provide some of their thermotolerance by maintaining messenger RNA levels when a severe thermal insult is applied. These insights allows for a more fundamental understanding of the cellular stress response to heat and provides several opportunities for further study that could bring about therapeutic interventions to benefit society.

6.4 References

1. Feezor, R.J., et al., *Temporal patterns of gene expression in murine cutaneous burn wound healing.* Physiol Genomics, 2004. **16**(3): p. 341-8.
2. Bowman, P.D., et al., *Survival of human epidermal keratinocytes after short-duration high temperature: synthesis of HSP70 and IL-8.* Am J Physiol, 1997. **272**(6 Pt 1): p. C1988-94.
3. Westerheide, S.D. and R.I. Morimoto, *Heat shock response modulators as therapeutic tools for diseases of protein conformation.* J Biol Chem, 2005. **280**(39): p. 33097-100.
4. Wilhelmus, M.M., R.M. de Waal, and M.M. Verbeek, *Heat shock proteins and amateur chaperones in amyloid-Beta accumulation and clearance in Alzheimer's disease.* Mol Neurobiol, 2007. **35**(3): p. 203-16.
5. Gifondorwa, D.J., et al., *Exogenous delivery of heat shock protein 70 increases lifespan in a mouse model of amyotrophic lateral sclerosis.* J Neurosci, 2007. **27**(48): p. 13173-80.
6. Rylander, M.N., et al., *Optimizing heat shock protein expression induced by prostate cancer laser therapy through predictive computational models.* J Biomed Opt, 2006. **11**(4): p. 041113.
7. Kamal, A., et al., *A high-affinity conformation of Hsp90 confers tumour selectivity on Hsp90 inhibitors.* Nature, 2003. **425**(6956): p. 407-10.
8. Solit, D.B., et al., *Inhibition of heat shock protein 90 function down-regulates Akt kinase and sensitizes tumors to Taxol.* Cancer Res, 2003. **63**(9): p. 2139-44.
9. Duncan, R.F., *Inhibition of Hsp90 function delays and impairs recovery from heat shock.* Febs J, 2005. **272**(20): p. 5244-56.